ESC-TR-93-161(1)

MTR 92B0000027V1

Johnson-Gierhart Program Predictions of Excess Propagation Loss for Super-High Frequency Air-to-Ground Paths Volume 1: Theory and Numerical Results

By

M. M. Weiner
J. C. Herther

June 1993

Prepared for

Program Manager
CDSM Program
Electronic Systems Center
Air Force Materiel Command
United States Air Force
Hanscom Air Force Base, Massachusetts

Project No. 5010

Prepared by

The MITRE Corporation
Bedford, Massachusetts

Contract No. F19628-89-C-0001

REVIEW AND APPROVAL

This technical report has been reviewed and is approved for publication.

FOR THE COMMANDER

ROBERT E. WILSON, Major, USAF
Program Manager, CDSM Program

REPORT DOCUMENTATION PAGE

Form Approved
OMB No 0704-0188

1. AGENCY USE ONLY (Leave Blank)	2. REPORT DATE	3. REPORT TYPE AND DATES COVERED
	June 1993	Final

4. TITLE AND SUBTITLE
Johnson-Gierhart Program of Excess Propagation Loss for Super-High Frequency Air-to-Ground Paths
Volume 1: Theory and Numerical Results

5. FUNDING NUMBERS
F19628-89-C-0001
5010

6. AUTHOR(S)
Weiner, Melvin M.
Herther, John C.

7. PERFORMING ORGANIZATION NAME(S) AND ADDRESS(ES)
The MITRE Corporation
202 Burlington Road
Bedford, MA 01730-1420

8. PERFORMING ORGANIZATION REPORT NUMBER
MTR 92B0000027V1

9. SPONSORING/MONITORING AGENCY NAME(S) AND ADDRESS(ES)
Program Manager, CDSM Program (ESC/ICR)
Electronic Systems Center, AFMC
Hanscom AFB, MA 01731-5000

10. SPONSORING/MONITORING AGENCY REPORT NUMBER
ESC-TR-93-161(I)

11. SUPPLEMENTARY NOTES

12a. DISTRIBUTION/AVAILABILITY STATEMENT
Approved for public release; distribution unlimited.

12b. DISTRIBUTION CODE

13. ABSTRACT *(Maximum 200 words)*

The Johnson-Gierhart tropospheric propagation program of the Institute for Telecommunications Sciences is used to obtain predictions of excess propagation loss over that of free space for super-high frequency (SHF) air-to-ground paths within or on the radio horizon. The principal loss (gain) mechanisms considered are atmospheric absorption and refraction, surface multipath interferance, smooth spherical Earth diffraction, and single knife-edge diffraction caused by terrain roughness and/or a site-specified obstacle. The program uses a semi-empirical database to statistically weigh the losses from these mechanisms. The excess propagation loss increases with increasing range and can exceed 3 decibels at distances as close as halfway to the radio horizon.

14. SUBJECT TERMS
Air-to-Ground
Excess Propagation Loss
Johnson-Gierhart
Longley-Rice
Prediction Program

15. NUMBER OF PAGES
145

16 PRICE CODE

17. SECURITY CLASSIFICATION OF REPORT	18. SECURITY CLASSIFICATION OF THIS PAGE	19. SECURITY CLASSIFICATION OF ABSTRACT	20. LIMITATION OF ABSTRACT
Unclassified	Unclassified	Unclassified	SAR

EXECUTIVE SUMMARY

BACKGROUND

Free-space propagation is often assumed in the design of super-high frequency air-to-ground communication and radar systems with operating ranges within or on the radio horizon. This report demonstrates the inadequacy of this simplistic approach. Real-world propagation losses, quantified with the aid of an established propagation model, are presented as a function of altitude and range.

PURPOSE

A detailed discussion of the Johnson-Gierhart propagation program and its application to the estimation of propagation loss is presented. Various aircraft altitude and transmission ranges are compared. Environmental factors considered are climate, terrain roughness, and site-specified horizon limiting obstacles.

CONCLUSIONS

Free-space modeling of transmission loss of air-to-ground paths provides an adequate approximation for the combination of sufficiently short paths with sufficiently high altitudes of the air platform. For paths exceeding 75 nautical miles with air platforms below 20,000 feet, propagation losses in excess of free space cannot be ignored without jeopardizing the system design. The propagation loss distribution is shown to be log-normal for most of the scenarios of interest. Log-normally distributed propagation loss yields probabilities of detection that can be appreciably less than those predicted for signals with free-space propagation loss.

IMPLICATIONS

Statistical/semi-empirical propagation models, though not rigorously proven, remain useful tools with which to estimate performance because they are derived from a substantial database obtained from dedicated experiments over a period of years. The theory of probability of detection with log-normal statistics is maturing. The application of this theory to the design of long-range electronic systems should be the topic of a follow-on study.

ACKNOWLEDGMENTS

This document has been prepared by the MITRE Corporation under Project No. 5010, Contract No. F19628-89-C-0001. The contract is sponsored by the Electronic Systems Center, Air Force Materiel Command, United States Air Force, Hanscom Air Force Base, Massachusetts 01731-5000.

The investigation of excess propagation loss for the air-to-ground paths of this paper was suggested by James Lemon. Hilda Chow performed the initial Johnson-Gierhart computer program runs that showed the potentially large excess propagation loss over free space increasing as a function of range. Dima Seliverstov and Louis Gnerre performed additional runs for the variety of parameters analyzed. Nicholas Senio provided technical assistance and insight regarding atmospheric losses. Raul Blanche and Major Robert Wilson provided invaluable support in pursuing this investigation. Sandra Kunnel and Donna Silva typed the document, and Angeline Theodore provided editorial assistance.

TABLE OF CONTENTS

TABLE OF CONTENTS (CONCLUDED)

LIST OF FIGURES

LIST OF FIGURES (CONTINUED)

LIST OF FIGURES (CONTINUED)

LIST OF FIGURES (CONTINUED)

LIST OF FIGURES (CONTINUED)

LIST OF FIGURES (CONCLUDED)

LIST OF TABLES

SECTION 1

INTRODUCTION

Super-high frequency (SHF) (3 to 30 gigahertz (GHz)) air-to-ground and ground-to-air communication and radar systems are often designed to operate on or within the radio horizon. By reciprocity, the propagation loss is identical for paths in either direction. For many of these applications, the performance analysis must include propagation effects in excess of free space for the worst-case operational climate and terrain roughness. Allowance should also be made for differing site elevations and other horizon obstacles in delineating mission-based operational requirements since these factors significantly affect design characteristics. These operational parameters include altitude and transmission range that dictate type of aircraft and, ultimately, program practicality and cost. The cases of interest include typical altitudes of 22,000, 33,000, and 66,000 feet; operating ranges from 75 nautical miles (nmi) to greater than 200 nmi, and frequencies 2 to 18 GHz within the SHF band, since these parameters encompass mission performance requirements of most long-range radars, electronic support measures, and standoff support radar jammers.

The inadequacy of free-space propagation loss for medium- and long-distance air-ground transmission paths has been recognized from the earliest development of radio and radar. The presence of the Earth and the atmosphere introduce the following propagation loss (gain) mechanisms for paths within or on the radio horizon:

1. The Earth's surface reflects or scatters radiation and, in certain regions, produces an interference pattern.

2. The Earth and path obstructions casts a shadow and gives rise to diffraction phenomena.

3. The Earth's troposphere (the lower region of the atmosphere characterized by decreasing temperature with increasing altitude) is inhomogeneous and gives rise to refraction effects.

4. The Earth's atmosphere contains water vapor, oxygen vapor, and water droplets that absorb radiation.

The term "pattern-propagation factor" has been coined to encompass the one-way excess propagation field intensity over that of free space caused by these factors. The one-way free space propagation power loss plus the excess propagation power loss for loss-free isotropic transmitting and receiving antennas is called the "basic transmission loss."

The Longley-Rice [1 through 5] and Johnson-Gierhart [6 through 8] programs of the Institute for Telecommunications Sciences model the excess propagation loss by utilizing information based on a statistical/semi-empirical analysis of various terrain profiles and propagation measurements, primarily in the United States, in the frequency range of 0.02 to 20 GHz. The Longley-Rice program is for scenarios in which both the transmitter and receiver are at low altitudes. The Longley-Rice program is for propagation paths that are above referred to as "ground-to-ground." The Johnson-Gierhart program, which incorporates the 1977 extensions [8] into an IF-77 model, is for scenarios in which either the transmitter or receiver or both is at a high altitude. The Johnson-Gierhart program with the IF-77 model can accommodate air-to-air propagation paths and is therefore designated as the ATOA program. Prior to the 1977 extensions, the Johnson-Gierhart program was restricted to air-to-ground propagation paths [43].

These programs are restricted to frequencies above 20 megahertz (MHz) because "sky" and "ground" wave propagation paths, which can be dominant propagation paths at frequencies less than 20 MHz, are not included in these programs. These programs are restricted to frequencies less than 20 GHz because their predictions of absorption loss are not accurate near dipole moment resonances of the water and oxygen molecules in the troposphere.

These models are particularly useful in predicting propagation losses over irregular terrain for which knife-edge diffraction losses are significant. These programs use an empirical database to statistically weigh knife-edge diffraction losses with losses from multipath interference, smooth-spherical earth diffraction, and troposcatter modes of propagation.

Propagation paths over irregular terrain are commonly encountered in ground-to-ground, air-to-ground, and air-to-air tactical scenarios. In tactical scenarios, propagation paths of interest are usually for specified classes of paths and climates with location and time variabilities, rather than for a specific deterministic path. For example, one class of paths might be characterized as having rolling plains, average ground permittivity, random siting, and temperate climate. The propagation path loss for such environments are best characterized by statistical quantities which are semi-empirically determined. For this reason, the Longley-Rice and Johnson-Gierhart programs are well-suited for military tactical scenarios. Other statistical propagation programs such as EPM-73 [9] and TIREM [10] of the Department of Defense Electromagnetic Compatibility Analysis Center may be less complex. However, the modeling or validation of those programs usually relies on the empirical database of the Longley-Rice program.

For paths in which the terrain profile is specified, deterministic propagation programs may also be used. For example, MIT Lincoln Laboratory has recently developed deterministic propagation programs such as SEKE and performed measurements to validate these programs [11 through 14].

The theory, computer programs, and user's guides for the Longley-Rice and Johnson-Gierhart prediction models are given in references 1 through 8. The selection, utility, and comparison of these models, as well as their input parameter specification, are described in references 15 and 16. Extensive numerical results for various scenarios and ranges of input parameters, primarily for low altitude cases at Very High Frequency (VHF), are given in references 15 through 17.

The present paper presents extensive numerical results of basic transmission loss predicted by the Johnson-Gierhart program at frequencies of 2 to 15 GHz. The cases are for an airborne antenna at altitudes of 22,000 to 66,000 ft, a ground-based antenna at altitudes of 10 ft and 20 ft, and paths over irregular terrain with ranges extending to the smooth Earth radio horizon.

The Johnson-Gierhart prediction program differs from the Longley-Rice program principally in the following ways:

1. Only single-horizon diffraction (at the low-altitude site) rather than double-horizon diffraction is considered.

2. A standard exponential atmosphere rather than a uniform gradient atmosphere is assumed (the index of refraction decreases exponentially rather than linearly with increasing height).

3. An option exists for specifying whether the vertical lobing pattern from surface reflection multipath "determines the median level" (at a specific location of the lobing pattern) or "contributes to variability" (averaged over the lobing pattern) of the basic transmission loss.

4. An additional option exists for specifying whether terrain roughness and atmospheric inhomogeneities contribute to "instantaneous levels exceeded" or "hourly-median levels" of the basic transmission loss.

The excess propagation (loss or gain) at 2 to 15 GHz is more severe than at VHF frequencies for scenarios that are otherwise the same because:

1. Knife-edge diffraction by irregular terrain and obstacles is less effective at shorter wavelengths in transmitting energy into the optical shadow zone of the obstacles.

2. Multipath interference over smooth Earth has a lobing pattern with more frequent lobes.

3. Absorption loss by oxygen and water vapor is not negligible (0.019 decibels per kilometer (dB/km) at 10 GHz) for long ranges at 2 to 15 GHz.

4. Vegetative and urban area propagation loss is much more severe at shorter wavelengths.

5. Absorption by precipitation is more pronounced at the higher frequencies.

Section 2 discusses the characteristics of basic transmission loss in the SHF frequency band including such topics as time variability, location variability, and the increase in excess propagation loss with increasing range even for ranges as close as halfway to the radio horizon. Section 3 presents numerical results for various climates and various terrain-limited and obstacle-limited horizons. The applicability of basic transmission loss in determining probability of detection is discussed in section 4. The conclusions are given in section 5.

SECTION 2

BASIC TRANSMISSION LOSS

Excess propagation loss is equal to the difference between the quantities "basic transmission loss" and "free-space propagation loss." Free-space propagation loss is a deterministic quantity and is given by equation 2.3. Basic transmission loss is a stochastic quantity that is discussed in the remainder of this section under the following topics: definition, modes of propagation, suitability of the Johnson-Gierhart program, statistical characterization, long-term location variability database, long-term time variability database, antenna characterization, time availability options, surface reflection lobing options, atmospheric absorption, and examples of numerical results.

2.1 DEFINITION

Basic transmission loss $L_b(d)$ is a system margin parameter that is a stochastic function of the propagation range of great circle distance d between the transmitting and receiving antennas. More specifically, "the basic transmission loss (sometimes called path loss) of a radio circuit is the transmission loss expected between ideal, loss-free, isotropic, transmitting and receiving antennas at the same locations as the actual transmitting and receiving antennas" [18].

The basic transmission loss $L_b(d)$ (in decibels) may be expressed as

$$L_b(d) = L_{bo}(d) + U(d) + V(d) \tag{2.1}$$

where

$L_{bo}(d)$ = Local path propagation loss for a path with no buildings or significant vegetation in the immediate vicinity of the antennas (in dB)

$U(d)$ = Urban area propagation loss term resulting from buildings in the immediate vicinity of the antennas (in dB)

$V(d)$ = Vegetative propagation loss term resulting from significant vegetation in the immediate vicinity of the antennas (in dB)

The local path propagation loss $L_{bo}(d)$ in equation 2.1 may be expressed as

$$L_{bo}(d) = L_{bf}(d) + A(d) \tag{2.2}$$

where

$L_{bf}(d)$ = Free-space propagation loss (dB).

$$= 10\log_{10}\left(\frac{4\pi d}{\lambda}\right)^2 = 10\log_{10}\left(\frac{4\pi df}{c}\right)^2$$

$$= 32.447 + 20\log_{10} f_{MHz} + 20\log_{10} d_{km} \tag{2.3}$$

d_{km} = Great circle distance between transmitter and receiver antennas (km).

λ = RF carrier wavelength (in the same units as d).

f_{MHz} = RF carrier frequency (MHz).

c = Free space velocity of propagation = 0.29979 kilometers per microsecond (km/μs).

A(d) = Excess propagation loss over that of free space for a path with no buildings or significant vegetation in the immediate vicinity of the antennas (in dB). This term is usually modeled by semi-empirical methods.

The Johnson-Gierhart prediction program is concerned with estimating the excess propagation loss A(d) defined by equation 2.2. The urban loss U(d) and vegetative loss V(d) terms in equation 2.1 are not predicted by this program. These terms are usually much larger than A(d) for frequencies within the SHF band and for ranges within the smooth earth radio horizon. The propagation paths in the present paper are assumed to be devoid of appreciable vegetation or urban area clutter.

The excess propagation loss A(d) is a stochastic quantity because the scenarios of interest are generally not for deterministic propagation paths, but for specified classes of propagation paths with location and time variabilities. For example, the high altitude platform may be an aircraft whose oval racetrack flight pattern has its long legs normal to the direct-ray propagation path. The terrain profile underneath the direct-ray propagation path is constantly changing, thus introducing short-term location variability into the propagation path. The tropospheric index-of-refraction profile along the direct-ray propagation path is constantly changing, thus introducing short-term time variability. However, even if the platform were not moving, long-term location and time variabilities would be introduced into the propagation loss predictions because the terrain profile for a given interdecile roughness varies from site-to-site, and the tropospheric surface refractivity for a given climate varies from

hour-to-hour and season-to-season. Short-term location and time variabilities are included in the Johnson-Gierhart program by specifying the time availability option "instantaneous levels exceeded." Only the long-term location and time variabilities are included when specifying the time availability option "hourly median levels exceeded." Long-term location variability is determined by specifying the interdecile terrain roughness Δh. For $\Delta h = 0$, the long-term location variability is zero. Long-term time availability is determined by specifying one of eight different climates.

2.2 MODES OF PROPAGATION

Radio waves originating from the Earth generally may be propagated in three regions: (1) through or along the surface of the Earth (ground wave), (2) through the lower atmosphere of the Earth beneath the ionosphere (tropospheric propagation), or (3) by reflection or scatter in the upper atmosphere from natural reflectors such as the ionosphere or from artificial reflectors such as satellites (sky wave). At frequencies greater than 20 MHz, ground wave propagation losses (except for very short paths within the radio horizon and along the Earth's surface) and sky wave propagation losses (except for very long propagation paths beyond the radio horizon) are usually very much larger than tropospheric propagation losses. The dominant region of propagation is the one with the least propagation loss. The Johnson-Gierhart program considers only tropospheric propagation paths.

For tropospheric propagation over irregular terrain, the possible modes of propagation (see figure 2-1) may be categorized as follows:

1. Multipath interference (including atmospheric absorption and refraction)
2. Multipath-diffraction transition
3. Diffraction (smooth spherical earth and knife-edge)
4. Diffraction-tropospheric scatter transition
5. Tropospheric scatter

REGION	MODE
(1)	MULTIPATH INTERFERENCE
(2)	MULTIPATH – DIFFRACTION TRANSITION
(3)	DIFFRACTION (SMOOTH SPHERICAL EARTH AND KNIFE-EDGE)
(4)	DIFFRACTION – TROPOSPHERIC SCATTER TRANSITION
(5)	TROPOSPHERIC SCATTER

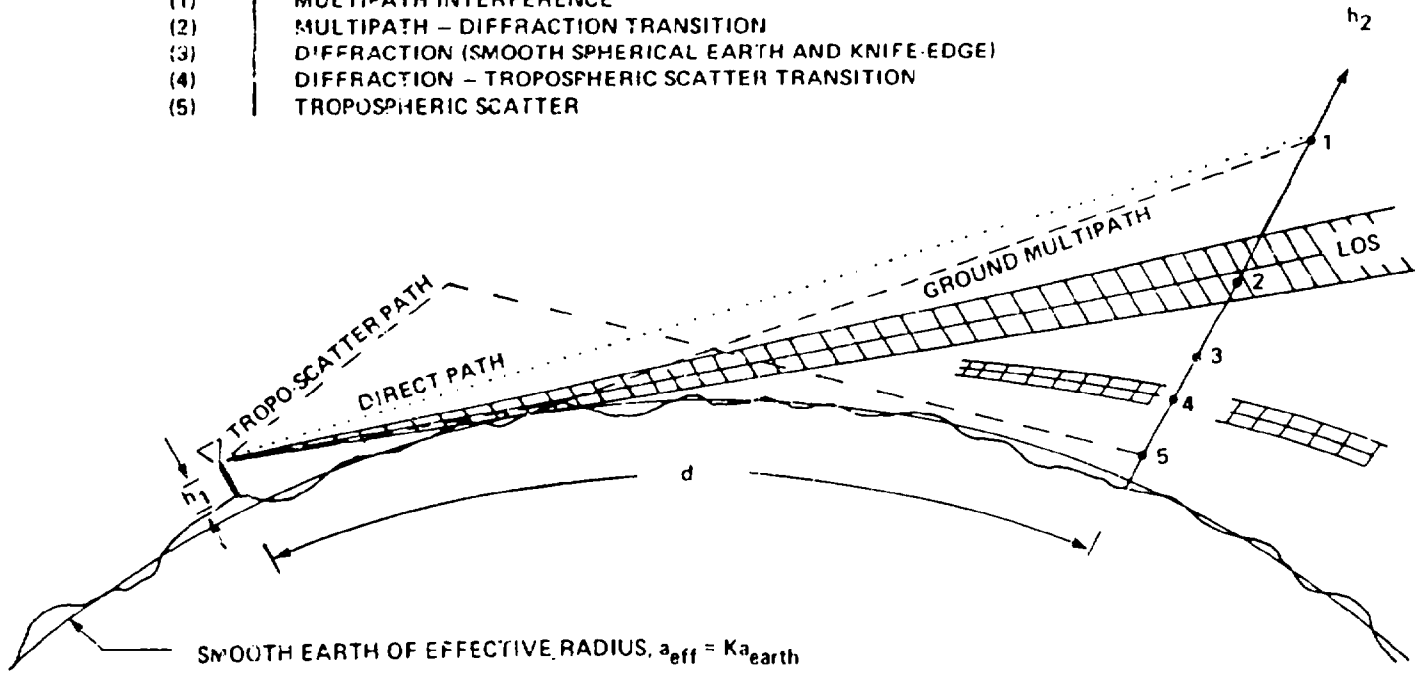

Figure 2-1. Various Tropospheric Propagation Modes Over Irregular Terrain

These propagation modes are for an earth of effective radius $a_{eff} = Ka_{earth}$ where a_{earth} is the physical radius of the earth and K is a scale factor allowing for refraction by the troposphere. When the effective earth's radius is utilized, the line-of-sight to the horizon is defined as the "radio line-of-sight." The radio line-of-sight path is electrically longer than the optical line-of-sight because at radio frequencies the scale factor K is generally greater than unity.

Mode 1 is the dominant mode of propagation for radio line-of-sight paths which clear the radio horizon by greater than approximately one-quarter of a Fresnel number, where the Fresnel number is the number of half-wavelengths of the path difference between the direct ray and the indirect ray specularly reflected from the ground [19]. Mode 2 occurs for radio line-of-sight propagation paths within one-quarter of a Fresnel number of the radio horizon. Mode 3 occurs for propagation paths beyond the radio horizon but more than one-quarter of a Fresnel number, but less than that for which tropospheric scatter starts to become significant. Mode 4 is a transition mode between diffraction and troposcatter modes. Mode 5 occurs for propagation paths sufficiently beyond the radio horizon where tropospheric scatter losses are less than diffraction losses. Except for mode 1 lobing, the excess propagation loss A(d) generally increases with decreasing height h_2 as the dominant mode of propagation progresses from 1 to 5. The direct-path, free-space propagation loss L_{bf}, given by equation 2.3, is plotted in figure 2-2 as a function of range and frequency.

Numerical results from the Johnson-Gierhart program of the basic transmission loss $L_b(d)$ and the corresponding excess propagation loss A(d) are summarized in tables 2-1 and 2-2, respectively for typical scenarios of interest. All of the propagation paths on smooth earth with no obstructing obstacle are well within the smooth earth radio horizon with a Fresnel zone clearance of more than one-quarter of a Fresnel number. Therefore, for unobstructed radio lines-of-sight, modes 1 and 2 are the dominant modes of tropospheric propagation. However, on irregular terrain or with nearby man-made obstacles, the radio line-of-sight will often be obstructed. Therefore, mode 3 may become dominant. Modes 4 and 5 are not dominant modes of propagation because the desired maximum operational range is too short in these scenarios. Generally speaking, in the case of *unobstructed* radio line-of-sight over smooth terrain, the principal mode of propagation is smooth-spherical earth diffraction

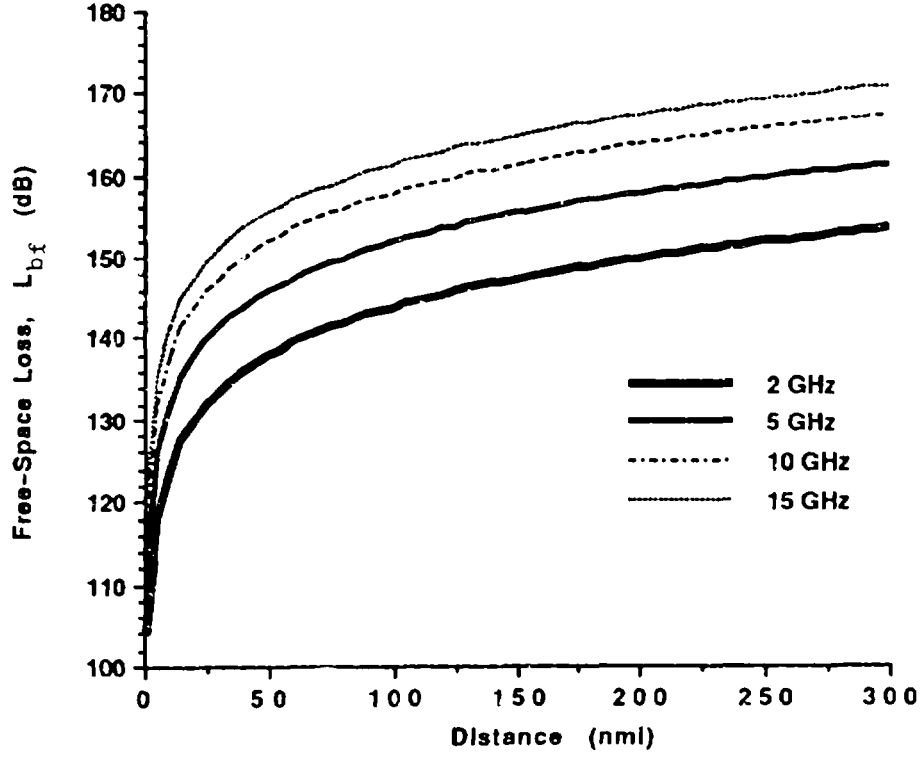

Figure 2-2. Free-Space Propagation Loss

Table 2-1. Basic Transmission Loss for Air-to-Ground Paths, f = 10 GHz

							Knife Edge Diffraction Determined by Terrain Δh			Knife Edge Diffraction Determined by Specified Obstacle			BASIC TRANSMISSION LOSS L_b(dB)				
Case	Frequency f (GHz)	Distance d (nmi)	Antenna Altitude above MSL h_2 (ft)	Antenna Height above MSL h_L (ft)	Grazing Angle of Specular Ray (mrad)	Path Length Difference of Specular and Direct Rays Fresnel Number (Half Wavelengths)	Terrain Roughness Interdecile Height Δh (ft)	Effective Obstacle Height (ft)	Effective Obstacle Distance to Facility Horizon (nmi)	Obstacle Height (ft)	Obstacle Distance to Facility Horizon (nmi)	Horizon Distance from Aircraft (nmi)	Free Space Loss L_{bf} (dB)	Expected Value $^{el}b^{e}$ (dB)	Standard Deviation $^{e}L_{b}$ (dB)	10% Confidence Level (dB)	90% Confidence Level (dB)
a	10	75	22000	20	40.1	38.2	0	0	5.4	-	-	170.3	155.4	157.8	6.5	152.0	166.1
a	10	75	22000	20	40.1	38.2	50	4	4.83	-	-	170.3	155.4	156.8	0.7	156.1	157.7
a	10	75	22000	20	40.1	38.2	50	-	-	50	0.6	170.3	155.4	156.8	0.7	156.1	157.7
b	10	125	22000	20	29.8	23.5	0	0	5.4	-	-	170.3	159.8	159.8	5.1	153.4	166.4
b	10	125	22000	20	29.8	23.5	50	4	4.83	-	-	170.3	159.8	163.4	4.2	158.5	168.3
b	10	125	22000	20	29.8	23.5	50	-	-	50	0.6	170.3	159.8	163.4	4.2	158.5	168.3
c	10	125	33000	20	43.3	35.3	0	0	5.4	-	-	210.6	159.8	162.7	5.2	156.6	168.8
c	10	125	33000	20	43.3	35.3	50	4	4.83	-	-	210.6	159.8	161.8	2.0	158.3	165.6
c	10	125	33000	20	43.3	35.3	50	-	-	50	0.6	210.6	159.8	161.8	2.0	158.3	165.6
d	10	200	33000	20	27.1	22.0	0	0	5.4	-	-	210.6	163.8	163.8	8.8	155.0	173.0
d	10	200	33000	20	27.1	22.0	50	4	4.83	-	-	210.6	163.8	169.1	6.0	161.4	176.5
d	10	200	33000	20	27.1	22.0	50	-	-	50	0.6	210.6	163.8	165.7	6.0	163.8	165.8
e	10	125	66000	20	86.8	78.6	0	0	5.4	-	-	310.5	159.8	161.8	4.3	156.7	167.7
e	10	125	66000	20	86.8	70.6	50	4	4.83	-	-	310.5	159.8	160.7	0.1	160.5	160.8
e	10	125	66000	20	86.8	78.6	50	-	-	50	0.6	310.5	159.8	160.7	0.1	160.5	160.8
f	10	200	66000	20	54.1	44.1	0	0	5.4	-	-	310.5	163.8	167.8	8.6	160.8	167.0
f	10	200	66000	20	54.1	44.1	50	4	4.83	-	-	310.5	163.8	169.6	3.5	167.3	171.3
f	10	200	66000	20	54.1	44.1	50	-	-	50	0.6	310.5	163.8	169.6	3.5	167.3	171.3

f= 10 GHz, Surface Reflection Lobing Determines Median Level, Instantaneous Levels Exceeded, Desert Climate, Poor Ground, 1.29 Earth Radius, Isotropic Antennas, Circular Polarization

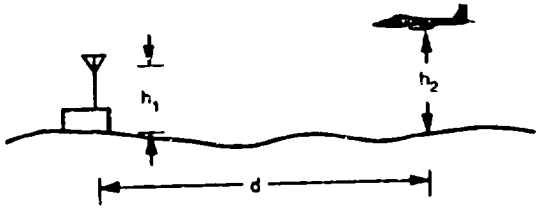

Table 2-2. Excess Propagation Loss for Air-to-Ground Paths, f = 10 GHz

Case	Frequency	Distance	Antenna Altitude above MSL	Antenna Height above MSL	Terrain Roughness Height	Effective Obstacle Height	Effective Obstacle Distance	Expected Value <A(d)>	10% Confidence Level	90% Confidence Level
	f	d	h_2	h_1	Δh	(ft.)	nmi			
	(GHz)	(nmi)	(ft.)	(ft.)	(ft)			(dB)	(dB)	(dB)
a	10	75	22000	20	0	0.0	5.4	2.4	-2.8	8.7
a	10	75	22000	20	50	4.0	4.8	[illegible].5	0.7	2.3
a	10	75	22000	20	50	50.0	0.6	1.5	0.7	2.3
b	10	125	22000	20	0	0.0	5.4	0.1	-6.4	6.6
b	10	125	22000	20	50	4.0	4.8	3.8	-1.3	9.5
b	10	125	22000	20	50	50.0	0.6	3.8	-1.3	9.5
c	10	125	33000	20	0	0.0	5.4	2.9	-3.2	10.0
c	10	125	33000	20	50	4.0	4.8	2.1	-1.5	5.8
c	10	125	33000	20	50	50.0	0.6	2.1	-1.5	5.8
d	10	200	33000	20	0	0.0	5.4	-0.2	-7.9	9.2
d	10	200	33000	20	50	4.0	4.8	5.3	-2.4	14.7
d	10	200	33000	20	50	50.0	0.6	21.9	0.0	32.0
e	10	125	66000	20	0	0.0	5.4	1.8	-3.1	7.9
e	10	125	66000	20	50	4.0	4.8	0.9	0.7	1.1
e	10	125	66000	20	50	50.0	0.6	0.9	0.7	1.1
f	10	200	66000	20	0	0.0	5.4	3.7	-3.0	3.1
f	10	200	66000	20	50	4.0	4.8	2.9	-1.6	7.4
f	10	200	66000	20	50	50.0	0.6	2.9	-1.6	7.4

f= 10 GHz, Surface Reflection Lobing Determines Median Level, Instantaneous Levels Exceeded, Desert Climate, Poor Ground, 1.29 Earth Radius, Isotropic Antennas, Circular Polarization

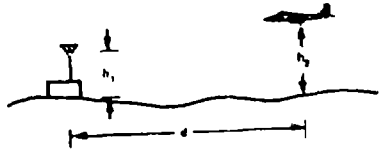

coupled with multipath interference between the direct and indirect signals reflected by the terrain to the receiver. In the case of an *obstructed* radio line-of-sight over irregular terrain, the principal mode of propagation is multipath interference and smooth-spherical earth diffraction coupled with knife-edge diffraction by the obstructing terrain.

In the multipath interference mode 1, the excess propagation loss of the nulls and peaks of the vertical lobing pattern increase with increasing range. The reason is that the Fresnel reflection coefficient R_o approaches -1 and the surface roughness reflection coefficient ρ_s approaches unity as the grazing angle approaches zero. (The amplitude of the specularly-reflected ray normalized to that of the incident ray is proportional to $R_o\rho_s$ [20].) The reflection coefficient ρ_s is given by equation 3.1 of section 3.

In the diffraction mode 3, the path loss increases exponentially with increasing distance of the transmitter or receiver into the shadow region of the obstructing terrain or obstacle. For a given distance into the shadow region, the sharpness of the obstructing terrain appreciably alters the path loss in a diffraction mode. Therefore, for a diffraction mode of propagation, slope and height distribution of the obstructing terrain affect the path loss.

In the Johnson-Gierhart program, the interdecile terrain roughness Δh affects the diffraction mode of propagation by altering the distance from the low-altitude antenna to its radio horizon. The program computes an effective obstacle height and effective obstacle distance to the low-altitude antenna facility as functions of the interdecile terrain roughness Δh, the atmosphere's surface refractivity N_S, and the height of the low-altitude antenna h_1. The excess propagation loss is increased in mode 3 and decreased in mode 1 with increasing values of Δh. A specific obstacle may also be introduced into the propagation path by specifying the obstacle height and distance from the low-altitude antenna facility.

For the scenarios of table 1, the Johnson-Gierhart statistical/semi-empirical program is particularly useful in modeling propagation loss over irregular terrain in the transition mode 2 of figure 2-1. The propagation loss for mode 2 is found from empirical data and from extrapolations between theoretical models for multipath interference and smooth-spherical earth diffraction.

2.3 SUITABILITY OF THE JOHNSON-GIERHART PROGRAM

The Johnson-Gierhart program is suitable to "high altitude" scenarios in which (1) the lower antenna is at a height above local ground greater than 0.5 m, (2) the higher antenna is at a sufficient height above local ground that the elevation angle at the lower antenna of the terrain-limited radio horizon is less than the elevation angle of the higher antenna, and (3) the terrain-limited radio horizon for the higher antenna is taken either as a common horizon with the lower antenna or as a smooth Earth horizon with the same elevation as the lower antenna effective reflecting plane. These altitude restrictions and the use of these programs are based on the following considerations.

1. Whereas two-ray multipath interference models are adequate for path clearances greater than 1/4 of a Fresnel number and whereas smooth earth spherical diffraction models are adequate for transhorizon paths well beyond the radio horizon, an extrapolation between these models, even for a smooth earth, is presently required for modeling of propagation paths near the radio horizon [19]. Reference 19 gives a deterministic computer program for such an extrapolation at low altitudes. However, for path loss averaged over random paths above irregular terrain, a semi-empirical, stochastic extrapolation is required. The empirical weighting accounts for knife-edge diffraction effects over a rough earth. The Johnson-Gierhart semi-empirical prediction program does such an extrapolation and allows for single horizon diffraction for both random terrain profiles and a specified obstacle.

2. Probabilistic predictions of path loss are possible because the database includes many samples for various locations, time of year, and experimental situations. Some of the database for the Johnson-Gierhart program is from 200 single horizon diffraction paths contained in the data of Longley, et al. [21]. Much of the database is from dedicated aircraft flights [22].

3. The Johnson-Gierhart prediction program is restricted to single-horizon diffraction which allows for ray tracing in standard atmospheres from the horizon back to the antenna site. Therefore, the Johnson-Gierhart program is applicable to paths at high elevations and steep elevation angles, but it is not applicable at low elevations where double-horizon diffraction may be significant.

4. The lower antenna is restricted to altitudes greater than 0.5 m because the ground wave is negligible at those altitudes for frequencies greater than 20 MHz.

In summary, the program is intended for use within the following ranges:

Parameter	Range
Frequency	100 to 20,000 MHz
Lower antenna height	$\geq$ 0.5 m
Higher antenna height	$\geq$ radio horizon height of lower antenna
Surface refractivity	200 to 400 N units
Elevation angle, of the irregular terrain radio horizon ray above the horizontal, at the lower antenna only	1 to 12 degrees
Distance, from the lower antenna to its terrain horizon, normalized to the corresponding smooth earth distance	0.1 to 3.0

The input parameter specifications for the program are given in references 7, 8, and 15 (table 8). In those references, an asterisk denotes the suggested numerical value for a parameter if the user does not specify a particular value. Unlike the Longley-Rice program, the asterisk values are not program-automatic default values, but must be specified by the programmer. The elevation angle of the horizon at the facility (lower antenna) and the distance from the lower antenna to its radio horizon are not program-input parameters, but are calculated internally by the program.

This program restricts the lower antenna site to locations for which the ratio of the distance to the terrain-limited (or obstacle-limited) radio horizon to that for a smooth-spherical earth is greater than 0.1 and less than 3.0. For example, this program would not be applicable to a scenario in which the ground site is at the bottom of a steeply rising hill (normalized distance < 0.1) or at the top of a mountain overlooking a valley (normalized distance > 3.0), because neither the empirical database nor the input parameters properly account for these severe geometries.

2.4 STATISTICAL CHARACTERIZATION

Consider now the basic transmission loss random variable $L_b(d)$ at a great circle distance d. The numeric value of the random variable $L_b(d)$ expressed in decibels is defined as the variate of $L_b(d)$ and is designated as "variate L_b." The cumulative distribution function, $q = \text{prob}\,[L_b < \text{variate } L_b\,]$, is tabulated in table 2-3 and plotted in figure 2-3 on normal probability paper for cases of tables 2-1 and 2-2 with the surface reflection lobing option "determines median level." In cases (a), (c), and (f), the cumulative distribution function q (which is the confidence level that the variate L_b is not exceeded) is well fitted by a straight line for confidence levels between 5 and 95 percent. The basic transmission loss L_b in decibels is thus approximately normally distributed for those cases. The basic transmission loss l_b expressed as a numeric is, therefore, approximately log-normally distributed. In

Table 2-3. Quantiles of Basic Transmission Loss for the Surface Reflection Lobing Option "Determines Median Level"

Case	Aircraft Altitude h_2 feet	Antenna Height h_1 feet	Distance d nmi	Free Space Loss L_{bf} dB	Estimated Quantiles of Transmission Loss $L_b(d,q)$(dB) Confidence Level, q in percent 5	10	20	30	40	50	60	70	80	90	95	$\langle L_b(d) \rangle$ Expected Value	σ_{L_b} Standard Deviation
a	22000	20	75	155.5	155.9	156.1	156.4	156.6	156.8	156.9	157.1	157.3	157.6	157.9	158.2	157.0	0.7
b	22000	20	125	159.8	158.0	158.5	159.2	160.0	161.4	162.6	163.9	165.2	166.8	169.2	171.5	163.4	4.2
c	33000	20	125	159.8	157.9	158.3	159.5	160.4	161.1	161.8	162.5	163.3	164.2	165.4	166.6	161.9	2.8
d	33000	20	200	163.8	160.6	161.4	162.5	163.2	165.5	167.7	169.7	171.9	174.4	178.5	182.1	169.1	6.8
e	66000	20	125	159.8	160.4	160.5	160.5	160.6	160.6	160.7	160.7	160.7	160.8	160.8	160.9	160.7	0.1
f	66000	20	200	163.9	161.4	162.2	163.8	165.0	166.0	166.9	167.7	168.6	169.7	171.2	172.5	166.8	3.5

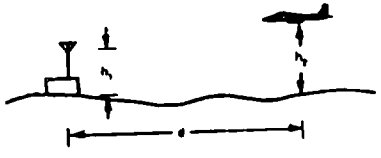

f = 10 GHz, Terrain Roughness Δh = 50 ft., Instantaneous Levels Exceeded
Desert Climate, Poor Ground, 1.29 Earth Radius, Isotropic Antennas, Circular Polarization

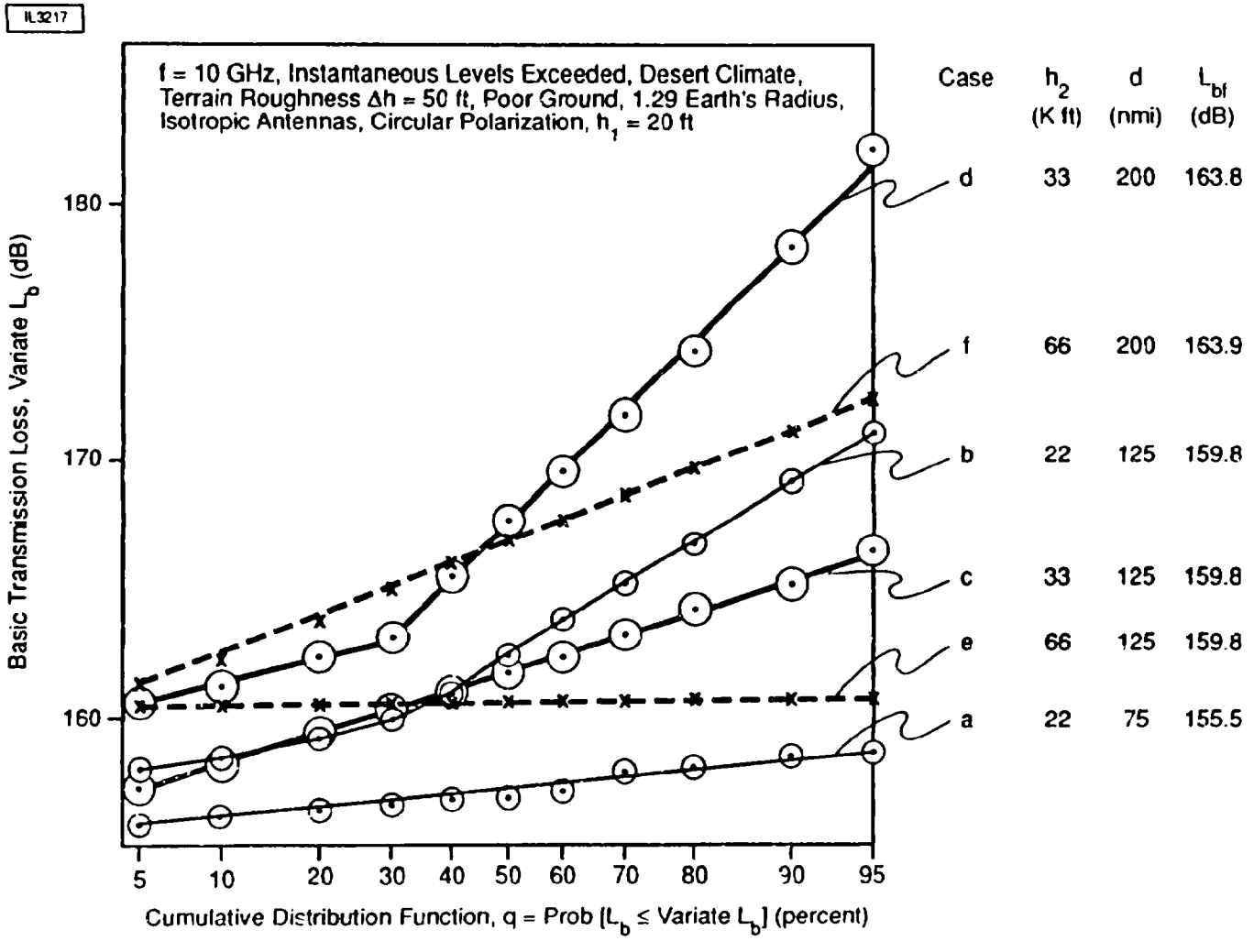

Figure 2-3. Cumulative Distribution Function of Basic Transmission Loss, Lobing Determines Median Level

cases (b) and (d), the basic transmission loss $L_b(d)$ is two-piecewise normally distributed with a breakpoint at q = 30 percent. In case (e), the horizontal straight line slope indicates that the basic transmission loss $L_b(d)$ is approximately equal to the free-space transmission loss $L_{bf}(d)$.

The variate $L_b(d)$ corresponding to a specified value q of the cumulative distribution function (confidence level in percent) is defined as the qth quantile of $L_b(d)$ and is designated as $L_b(d,q)$. Computer printouts of the basic transmission loss quantiles of table 2-3 are given in appendix C, run numbers 1 through 3. For a normal distribution of $L_b(d)$, the expected value $\langle L_b(d) \rangle$ and standard deviation $\sigma_{L_b(d)}$ are given by

$$< L_b(d) >= L_b(d,50) \tag{2.4}$$

$$\sigma_{L_b(d)} = L_b(d,84.1) - L_b(d,50) = L_b(d,50) - L_b(d,15.9) \tag{2.5}$$

For a basic transmission loss random variable $L_b(d)$ in decibels that is two-piecewise normally distributed with a breakpoint at the median value $L_b(d,50\ \text{percent})$, the expected value $\langle L_b(d) \rangle$ and standard deviation σ_{L_b} are given in references 15 and 16.

Location, time, and situation (model) uncertainties contribute to path loss variability in the Johnson-Gierhart program. The confidence level q, in which marginal probabilities of time, location, and situation are combined, is the only statistical service available in the Johnson-Gierhart program.

2.5 LONG-TERM LOCATION VARIABILITY DATABASE

Both the Longley-Rice and Johnson-Gierhart programs use information based on the same statistical/empirical study of various terrain profiles, primarily in the United States [23, 24]. In that study, each terrain profile is characterized by its interdecile height Δh. The interdecile height is the difference in heights corresponding to the 90 and 10 percent quantiles of the height deviation from the mean surface level. In the multipath mode of propagation, the interdecile height Δh is used to determine the surface roughness reflection coefficient ρ_s [23, 34]. In the diffraction mode of propagation, the interdecile height Δh (as well as the surface refractivity N_s and height h_1 of the lower antenna) is used to compute an effective knife-edge obstacle height and distance from the lower antenna facility.

2.6 LONG-TERM TIME VARIABILITY DATABASE

The distance from the higher antenna to the smooth-earth radio horizon increases monatomically with increasing index of refraction n_s of the troposphere at the Earth's surface. The surface refractivity N_s (in N-units) is defined as [25]

$$N_s = (n_s - 1) \times 10^6 \quad \text{(N-units)} \tag{2.6}$$

The Earth's effective radius a_{eff}, normalized to the earth's mean physical radius $a_{earth} = 6370$ km, is related to N_s by [25]

$$K = a_{eff} / a_{earth} = \left[1 - 0.04665 \exp\left(0.005577 N_s\right)\right]^{-1} \tag{2.7}$$

Equation 2.6 is an empirical formula that is valid for tropospheric paths near the Earth's surface where the conditions of a constant refractive index gradient and rectilinear propagation are approximately satisfied. The distances d_1 and d_2 to the radio horizon from the ground and aircraft antennas, respectively, are given by

$$d_{1,2} = (2\ K\ a_{earth}\ h_{1,2})^{1/2} \qquad (2.8)$$

where $h_{1,2}$ are the antenna heights of the ground and aircraft antenna heights above the mean surface level. The annual mean value $\overline{N_s}$ and its corresponding K factor are given in table 2-4 for ten different climates. The radio line-of-sight is greater than the optical line-of-sight because K is greater than 1. Climates 1 through 9 correspond to CCIR climates [26, 27], while climate 0 is a nominal continental all-year climate described in reference 6. The climate also determines the long-term time variability because the annual variation ΔN_s of the monthly mean is a function of the climate (see table 2-4). Desert climate is the most unfavorable climate for tropospheric propagation because it has the least value of $\overline{N_s}$ and has one of the largest values of ΔN_s. Conversely, equatorial climate is one of the best climates for minimizing tropospheric propagation loss because it has one of the largest values of $\overline{N_s}$ and the smallest value of ΔN_s. More detailed climate characteristics are given in reference 27. Statistical/empirical formulas for long-term time variability of basic transmission loss in the Longley-Rice and Johnson-Gierhart programs are given in reference 28. Long-term time availability may also be introduced into the Johnson-Gierhart program by specifying the season of the year and hourly block of the day instead of climate [27].

2.7 ANTENNA CHARACTERIZATION

The basic transmission loss defined in equation 2.1 is for loss-free isotropic transmitting and receiving antennas. Antenna ohmic losses are accounted for in the signal/noise equation by including the radiation efficiency of the transmitting antenna in its power gain and the radiation efficiency of the receiving antenna in the system operating noise factor [29, 30] rather than including the antenna ohmic losses in the excess propagation loss. Antennas with non-isotropic gain patterns may be treated as isotropic antennas in computing excess propagation loss provided that the directive gains of the antennas in the direction of the direct ray path is approximately the same as in the direction of the specularly-reflected ground multipath.

Table 2-4. Surface Refractivity for Various Climates

Climate		Surface Refractivity, N_s		
No.	Designation	Annual Mean, $\overline{N_s}$ (N-units)	(K factor)	Annual Variation ΔN_s of Monthly Mean (N-units)
0	Continental All-Year	301	1.33	–
1	Equatorial	360	1.53	0 to 30
2	Continental Subtropical	320	1.38	60 to 100
3	Maritime Subtropical	370	1.58	30 to 60
4	Desert	280	1.29	20 to 80
5*	Mediterranean	320	1.38	10 to 30
6	Continental Temperate	320	1.38	20 to 40
7	Maritime Temperate Overland	320	1.38	20 to 30
8	Maritime Temperate Oversea	320	1.38	20 to 30
9*	Polar	300	1.33	10 to 40

* Not used in the Johnson-Gierhart program.

For the scenarios of table 2-1, the grazing angle of the specularly-reflected multipath ray is less than two degrees. Therefore, for antennas with a 3-dB beamwidth greater than approximately two degrees, the basic transmission loss is generally suitable for estimating excess propagation loss except for multipath interference over smooth Earth. For such a case, the depth of the nulls is sensitive to the respective antenna gains in the directions of the direct and multipath rays. Non-isotropic gain patterns are accounted for in the signal/noise equation by restricting the parameters of transmitting antenna power gain and receiving antenna directive gain to be those in the direction of the direct ray path rather than in the directions of peak gains of the antennas [29, 30].

2.8 TIME AVAILABILITY OPTIONS

The user of the Johnson-Gierhart program must specify one of two time availability options, namely, "for instantaneous levels exceeded" or "for hourly median levels exceeded." As previously explained, the option "for instantaneous levels exceeded" includes both short-term and long-term variabilities of location and time, while the option "for hourly median levels exceeded" includes only long-term location and time variabilities in determining the quantiles of basic transmission loss. The short-term variabilities account for rapid signal fading that occurs when the terrain profile underneath the propagation path is constantly changing (because of a mobile transmitter or receiver) or the tropospheric index-of-refraction profile along the direct-ray propagation path is constantly changing. The 50 percent quantiles of basic transmission loss are identical for both time availability options. The time availability option affects how one specifies the system margin in the signal-to-noise equation. The system margin $M(d, r_i)$ in decibels is defined in equation 4.1 of section 4.

When the basic transmission loss $L_b(d)$ is used to determine either the signal S(d) or the noise N and the option "instantaneous levels exceeded" is chosen, then rapid fading of the system margin is included in S(d) or N and should not be included in the zero decibel margin signal-to-noise ratio $R(r_i)$ of equation 4.1. However, if the option "for hourly median levels exceeded" is selected, then rapid fading of the system margin should be included in the

quantity $R(r_i)$. In the present paper, numerical values of $L_b(d)$ are presented only for the option "instantaneous levels exceeded." When using these values to determine the system margin $M(d, r_i)$, one should use values of $R(r_i)$ that do *not* include rapid fading.

2.9 SURFACE REFLECTION LOBING OPTIONS

The user of the Johnson-Gierhart program must also specify one of two surface reflection lobing options: "contributes to variability" or "determines median level." In the option "contributes to variability," all of the quantiles of $L_b(d)$ are redistributed so that the variance is increased to account for the gain variation on the lobing pattern. That option does not show the lobing pattern as a function of distance d and apparently does not decrease the quantiles by the expected value of the lobing gain pattern averaged over the entire pattern. Quantiles of $L_b(d)$ for the lobing option "contributes to variability" at a given distance d for the cases of table 2-1 are tabulated in table 2-5 and plotted on normal probability paper in figure 2-4. Computer printouts of the basic transmission loss quantiles of table 2-5 are given in appendix C, run numbers 4 through 6. The quantiles of $L_b(d)$ in decibels are normally distributed for all of the cases.

In the lobing option "determines median level" all of the quantiles of basic transmission loss $L_b(d)$ are redistributed so that the 50 percent quantile includes the value of the lobing pattern at the specified distance d. The expected value of the lobing gain pattern averaged over the entire pattern is generally greater than 0 dB, because its peaks are broader than its nulls. Hence, the expected value of the lobing pattern loss in decibels is a negative quantity. For perfect surface reflection, the lobing pattern gain has a peak of 6 dB, a null of $-\infty$ decibels, and an expected value of 3 dB. The expected value of the lobing pattern gain decreases with decreasing modulus of the surface reflection coefficient. The plotting routine for the option "determines median level" prints out the lobing pattern as a function of distance d for the first ten lobes nearest the horizon. The quantiles of $L_b(d)$ (in decibels) for the lobing option "determines median level" at a given distance d are normally distributed and two-piecewise normally distributed for the cases of table 2-1 (see table 2-3 and figure 2-3).

Table 2-5. Quantiles of Basic Transmission Loss for the Surface Reflection Lobing Option "Contributes to Variability"

Case	Aircraft Altitude h_2 feet	Antenna Height h_1 feet	Distance d nm'	Free Space Loss L_{bf} dB	Estimated Quantiles of Transmission Loss $L_b(d,q)$(dB) Confidence Level, q in percent 5	10	20	30	40	50	60	70	80	90	95	$<L_b(d)>$ Expected Value	σ_{L_b} Standard Deviation
a	22000	20	75	155.5	155.9	156.1	156.4	156.6	156.8	156.9	157.1	157.3	157.6	157.9	158.2	157.0	0.7
b	22000	20	125	159.7	157.6	158.5	160.7	162.0	163.7	164.9	166.2	167.5	169.1	171.5	173.8	165.0	5.0
c	33000	20	125	156.7	157.3	158.3	159.5	160.4	161.1	161.8	162.5	163.3	164.2	165.4	166.6	161.9	2.8
d	33000	20	200	163.9	162.6	163.7	167.4	170.2	172.5	174.7	176.7	178.9	181.4	185.5	189.2	174.7	8.5
e	66000	20	125	159.8	160.4	160.5	160.5	160.6	160.6	160.7	160.7	160.7	160.8	160.8	160.9	160.7	0.1
f	66000	20	200	163.9	161.4	162.2	163.8	165.0	166.0	166.9	167.7	168.6	169.7	171.2	172.5	166.8	3.5

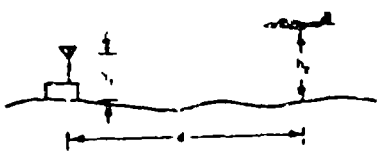

f = 10 GHz, Terrain Roughness Δh = 50 ft., Desert Climate, Poor Ground, Instantaneous Levels Exceeded Isotropic Antennas, 1.28 Earth Radius, Circular Polarization

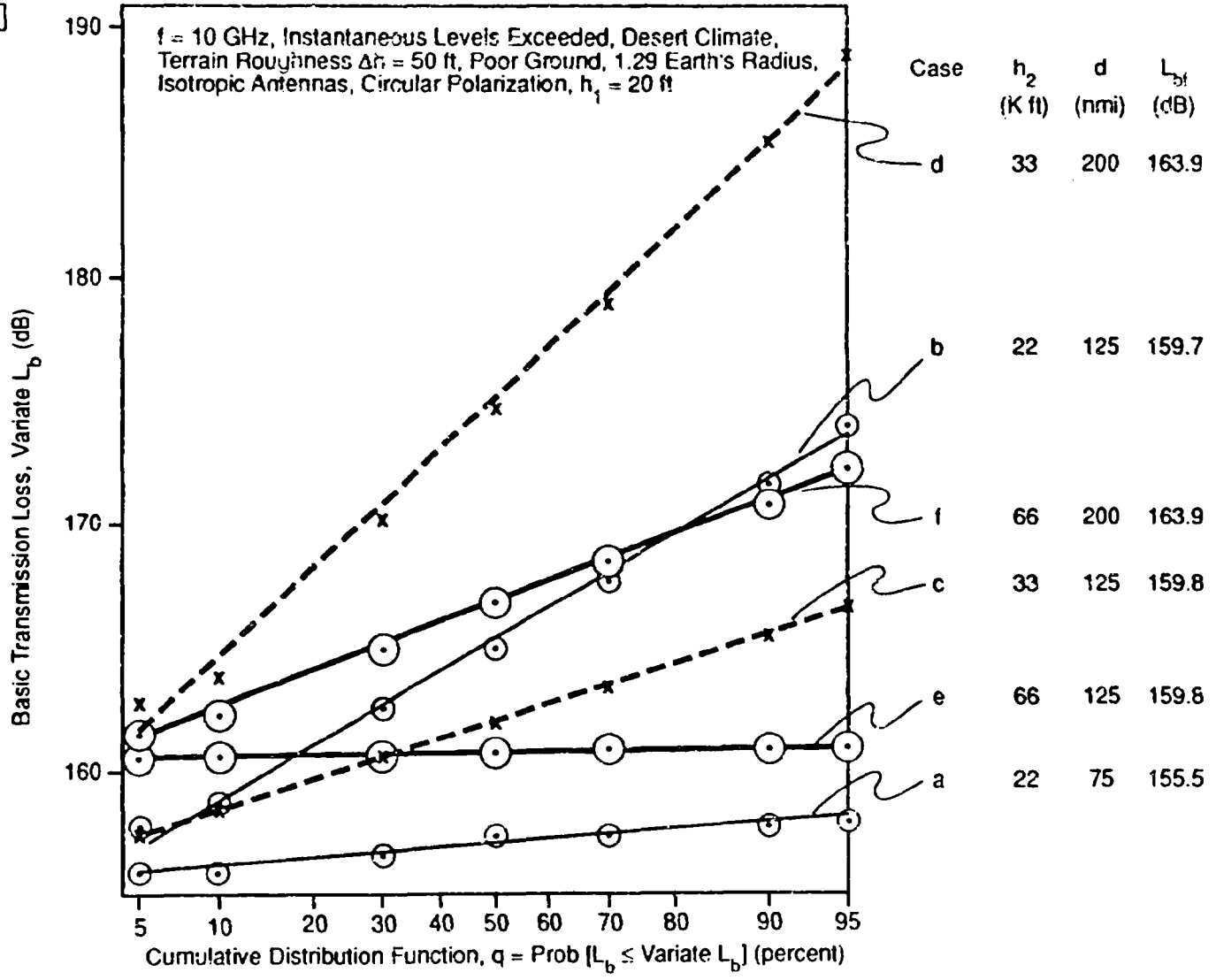

Figure 2-4. Cumulative Distribution Function of Basic Transmission Loss, Lobing Contributes to Variability

The expected values of the basic transmission loss $L_b(d)$ in table 2-3 are less than those in table 2-5 by the amounts 0, 1.6, 0, 5.6, 0, and 0 decibels for the corresponding cases (a), (b), (c), (d), (e), and (f), respectively. The standard deviations of the basic transmission loss $L_b(d)$ in table 2-5 are greater than those in table 2-3 by the amounts 0, 1.2, 0, 1.7, 0, and 0 decibels for the corresponding cases (a), (b), (c), (d), (e) and (f), respectively.

2.10 ATMOSPHERIC ABSORPTION

Oxygen and water vapor may absorb energy from a radio wave because the oxygen molecule has a permanent magnetic dipole moment with resonant peaks at 53 to 66 GHz and the water molecule has a permanent electric dipole moment with a resonant peak at 22.23 GHz [1] (see figure 2-5). For example, the atmospheric ... absorption coefficients for oxygen and water vapor are 0.015 dB/km and 0.004 dB/km, respectively, at 10 GHz. The corresponding transmission loss for a great-circle distance d = 100 nmi is 3.5 dB (= 100 nmi x 1.852 nmi/km x 0.019 dB/km). Therefore, the high altitude, air-to-ground slant paths of table 1 will have a transmission loss from atmospheric absorption alone of approximately 2 to 3 dB at distances less than one-half the distance to the radio horizon (d = 75 nmi) and 5 to 6 dB at distances near the radio horizon (d = 200 nmi), allowing for less absorption loss at the higher altitudes.

The attenuation of radio waves by precipitation (suspended water droplets and rain) often exceeds that from the combined oxygen and water vapor absorption [41]. The attenuation coefficient due to precipitation is a function of its intensity (see figure 2-6). For example, the rain attenuation coefficient at 10 GHz is 0.022 dB/km for a precipitation intensity of 2 millimeters per hour. Such a precipitation occurs in England approximately 50 times per year with a duration of 15 minutes to 2 hours.

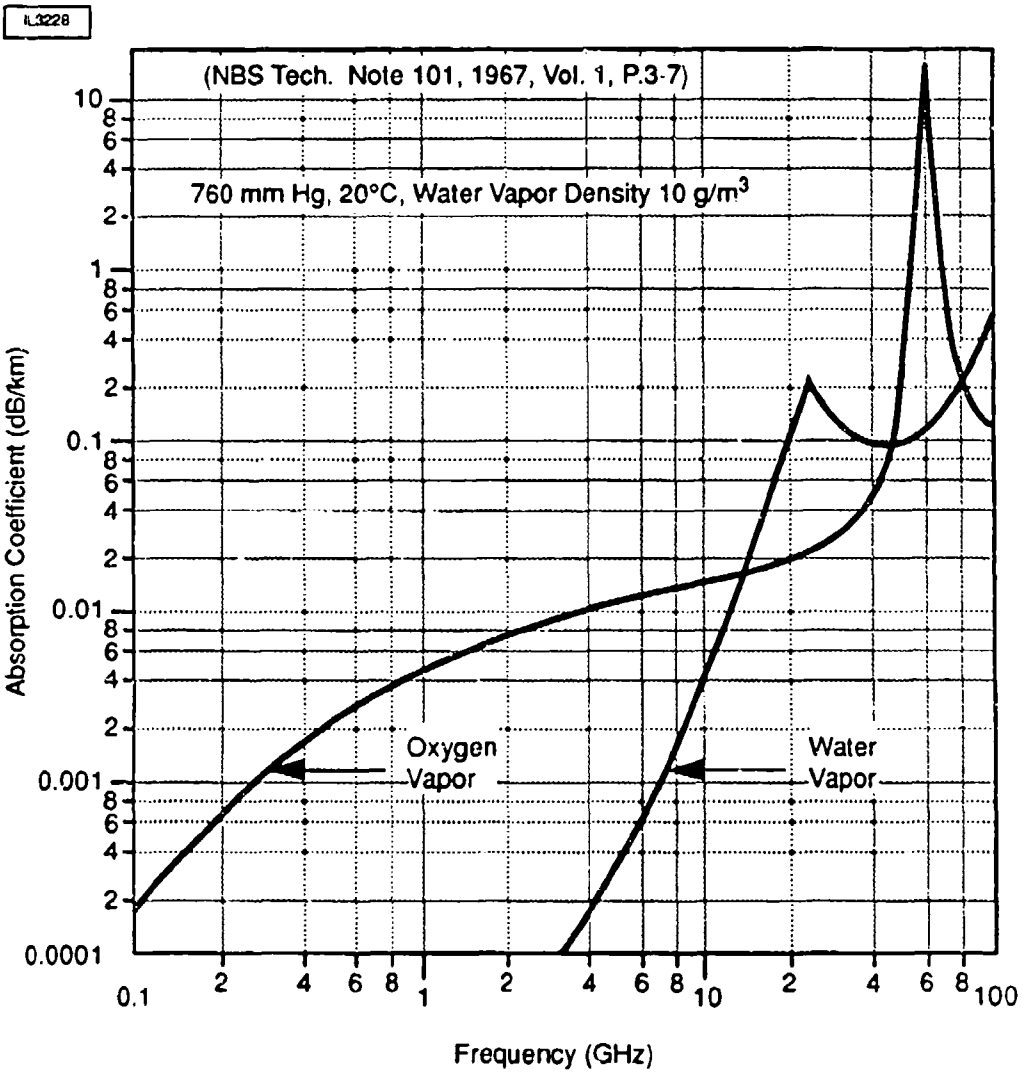

Figure 2-5. Atmospheric Surface Absorption Coefficients

IL3229

(CCIR, Report 233-3, 13th Plenary Assembly, Geneva, 1974)

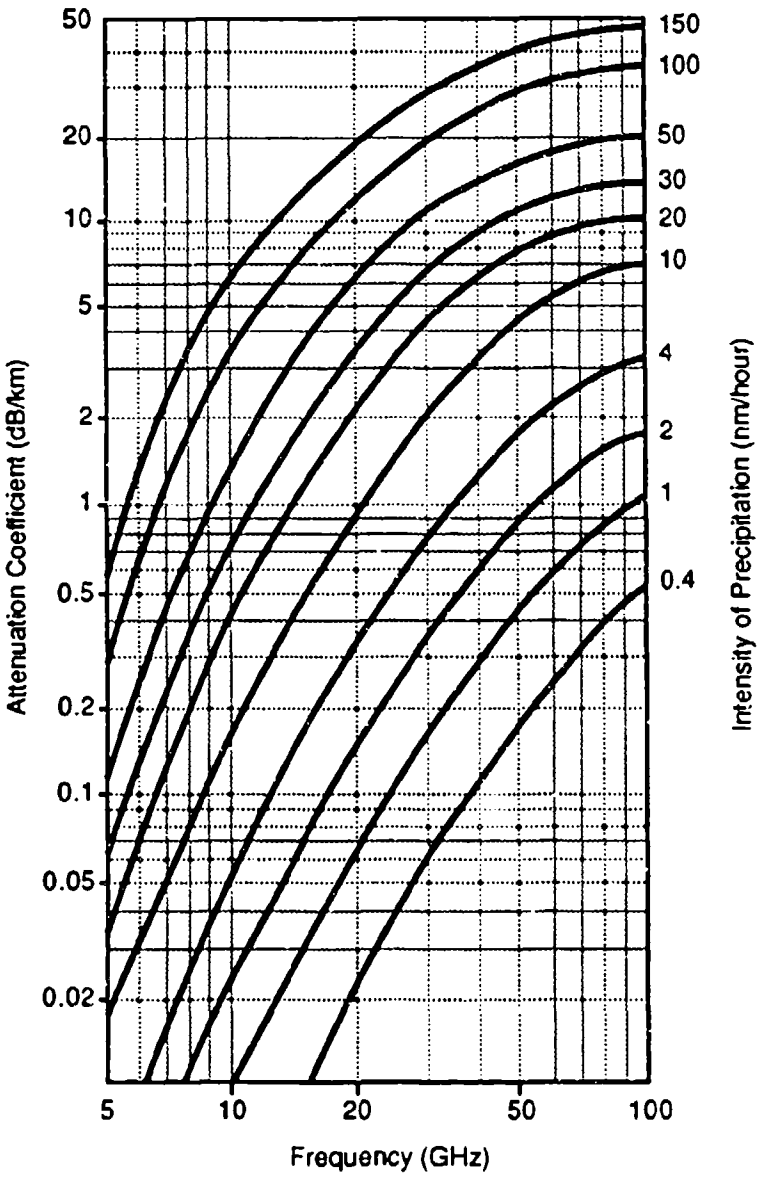

Figure 2-6. Rain Attenuation Coefficients

The Johnson-Gierhart program yields accurate predictions of atmospheric absorption for frequencies below 20 GHz and less accurate predictions above 20 GHz near resonant absorption peaks. Either the rain storm size or rain zone may be specified as an input parameter to the Johnson-Gierhart program. All of the numerical results of the present paper do not include precipitation.

2.11 EXAMPLES OF NUMERICAL RESULTS

The great-circle distance d for the air-to-ground paths of table 2-1 are well within the smooth spherical Earth radio horizon. The distance d for cases (a) through (f) are approximately 0.4, 0.7, 0.6, 0.9, 0.4, and 0.6 respectively, of the smooth earth radio horizon distances from the aircraft. The grazing angles of the indirect ray specularly reflected from a smooth spherical earth are 27 to 87 milliradians (0.5° to 1.5°). The corresponding path length differences of the specular and direct rays, expressed in half-wavelengths (sometimes referred to as the effective aperture Fresnel number) are 22 to 71. The principal mode of propagation for the smooth spherical Earth cases of table 2-1 is multipath interference including atmospheric absorption and refraction (mode 1 of figure 2-1) since the Fresnel number is greater than 0.25.

For the smooth spherical Earth ($\Delta h = 0$) cases of tables 2-1 and 2-2, the excess propagation loss has expected values $\langle A(d) \rangle$ = -0.2 to 3.7 dB, standard deviations $\sigma_{A(d)} = \sigma_{L_b}$ = 4.3 to 6.8 dB, ten percent quantiles A(d,10) = -7.9 dB to -2.8 dB, and ninety percent quantiles A(d,90) = 3.1 to 8.7 dB. The smooth Earth case for the smallest specular ray grazing angle (case d) has the smallest expected value of excess propagation loss (-0.2 dB), the largest standard deviation (6.8 dB), and the greatest difference between the 90 percent and 10 percent quantiles (17.1 dB). The reason for these results is that the lobing pattern is more pronounced (the Fresnel reflection coefficient R_o approaches -1) for small grazing angles. The smooth Earth case for the largest specular ray grazing angle (case e) has an excess propagation loss with an expected value 2 dB greater than that of case d, a standard deviation 2.5 dB less than that of case d, and a difference between the 90 percent and 10 percent quantiles that is 6.1 dB less than for case d. The 90 percent quantiles of excess propagation

loss for cases d and e are not appreciably different (9.2 dB for case d vs. 7.9 dB for case e). The above results, for air-to-ground propagation paths **well within the radio horizon and over a smooth spherical Earth**, indicate that the excess propagation loss is not necessarily larger for paths with smaller specular ray grazing angles. For paths with the smaller specular ray grazing angles, the excess propagation loss has smaller 10 percent quantile values, smaller expected values and slightly larger 90 percent quantile values. Air-to-ground paths with smaller grazing angles correspond to air platforms at longer ranges and lower altitudes.

The above conclusion, for air-to-ground paths well within the radio horizon and over a smooth spherical Earth is dramatically altered for the same propagation paths over rough Earth or Earth with obstacles. For rough Earth or Earth with obstacles, single knife-edge diffraction becomes the dominant mode of propagation at small grazing angles.

For the slightly rough Earth cases (Δh = 50 ft) of tables 2-1 and 2-2, the excess propagation loss A(d) has expected values $\langle A(d) \rangle$ = 0.9 to 5.3 dB, standard deviations $\sigma_{A(d)}$ = 0.1 to 6.8 dB, ten percent quantiles A(d,10) = 0.9 to 5.3 dB, and ninety percent quantiles A(d,90) = 1.1 to 14.7 dB. The case for the smallest specular ray grazing angle (case d) has the largest expected value of excess propagation loss (5.3 dB), the largest standard deviation (6.8 dB), and the largest difference between the 90 percent and 10 percent quantiles (17.1 dB). The case for the largest specular ray grazing angle (case e) has an excess propagation loss with an expected value 4.4 dB less than that of case d, a standard deviation 6.7 dB less than that of case d, and a difference between the 90 percent and 10 percent quantiles that is 16.7 dB less than for case d. Case e has the least variability in its propagation loss for paths over slightly rough Earth as is clearly illustrated by the nearly horizontal slope of its cumulative distribution function in figures 2-3 and 2-4. (A deterministic propagation loss, such as that of free space, would have a perfectly horizontal slope for all cumulative probability quantiles q, $0 \leq q \leq 1$.) The 90 percent quantiles of excess propagation loss for cases d and e are 14.7 dB and 1.1 dB, respectively. The above

results, for paths well within the radio horizon **but over slightly rough Earth**, indicate that the excess propagation loss is generally larger for paths with smaller specular ray grazing angles. For paths with the smaller grazing angles, the excess propagation loss has smaller 10 percent quantile values but larger expected values and larger 90 percent quantile values.

The excess propagation loss for paths well within the radio horizon and over slightly rough Earth becomes even more pronounced at the smaller grazing angles if an obstacle occurs near the ground antenna. For the specified obstacle cases (50-ft-tall obstacle at a distance of 0.6 nmi from the ground antenna on slightly rough Earth) of tables 2-1 and 2-2, the excess propagation loss A(d) has expected values $\langle A(d) \rangle$ = 0.9 to 21.9 dB, standard deviations $\sigma_{A(d)}$ = 0.1 to 8.0 dB, 10 percent quantiles A(d,10) = -7.9 dB to 0.7 dB, and 90 percent quantiles A(d,90) = 1.1 to 32.0 dB. The case for the smallest specular ray grazing angle (case d) has an excess propagation loss with the largest expected value (21.9 dB), the smallest standard deviation (0 dB), and the largest difference between the 90 percent and 10 percent quantiles (32 dB). The case for the largest specular ray grazing angle (case e) has an excess propagation loss with an expected value 21.0 dB less than that of case d, a standard deviation 7.9 dB less than that of case d, and a difference between the 90 percent and 10 percent quantiles that is 31.6 dB less than for case d. The 90 percent quantiles of excess propagation loss for cases d and e are 32.0 dB and 1.1 dB, respectively. The above results, for paths well within the radio horizon **but with an obstacle on slightly rough Earth** indicate that the excess propagation loss is much larger for paths with smaller specular ray grazing angles. For paths with the smaller grazing angles (cases b and d vs. cases a and e), the excess propagation loss has approximately the same 10 percent quantile values but much larger expected values and much larger 90 percent quantile values.

These examples of numerical results illustrate that the basic transmission loss for SHF air-to-ground propagation paths well within the (smooth Earth) radio horizon can be significantly larger than free-space loss. **The loss increases with decreasing grazing angle provided that the Earth is at least slightly rough (such as slightly rolling plains) or has obstacles on its surface near the ground antenna.**

SECTION 3

NUMERICAL RESULTS

The examples of numerical results in the previous section are restricted to a desert climate for propagation paths over smooth Earth, slightly rough (Δh = 50 ft) Earth, and slightly rough Earth with a 50-ft-tall obstacle at a distance of 0.6 nmi from the ground antenna. Extensive numerical results for other climates and obstructed paths are presented in sections 3.1 and 3.2, respectively.

3.1 CLIMATE RUNS

Basic transmission loss is a function of the index of refraction of the troposphere at the Earth's surface. The troposphere's surface refractivity N_S is a function of climate (see table 2-4 of section 2.6). In section 2.6, it was pointed out that desert climate is the most unfavorable climate for tropospheric propagation because the surface refractivity for desert climate has the least annual mean and one of the largest annual variations. Conversely, equatorial climate is one of the best climates for minimizing tropospheric propagation loss because the surface refractivity for equatorial climate has one of the largest annual means and the smallest annual variation. Quantitative results of the effect of climate on basic transmission loss are presented in this subsection. The computer printouts of basic transmission loss for all of the climate runs are presented in appendix D of volume 2. The climate runs are for a smooth spherical Earth ($\Delta h = 0$) and for a slightly rough Earth (Δh = 50 ft) with no additional obstruction.

All of the climate runs were performed for poor ground, circular polarization, and isotropic antennas at a frequency of 10 GHz with an aircraft antenna at height h_2 = 33,000 ft and a ground antenna at height h_1 = 10 ft. It should be noted that the ground antenna height is one-half that for the numerical examples of section 2. Therefore, knife-edge diffraction and smooth spherical Earth diffraction should be more pronounced for the climate runs of this subsection than for the numerical examples of section 2. The distance of the aircraft radio horizon varies from 220 nmi for a desert climate to 243 nmi for maritime subtropical climate.

The climate runs for a smooth spherical Earth (terrain $\Delta h = 0$) with surface reflection lobing options "determines median level" and "contributes to variability" are summarized in tables 3-1 and 3-2, respectively, at great circle distances d = 100 nmi, 150 nmi, 200 nmi, and 225 nmi. The principal mode of propagation is multipath interference at d = 100 nmi, smooth spherical Earth diffraction at d = 225 nmi, and multipath-diffraction transition at the intermediate distances d = 150 nmi and 200 nmi. The expected value, 90 percent quantile, and standard deviation of basic transmission loss are approximately independent of climate for d = 100 nmi (see tables 3-1 and 3-2). However, the basic transmission loss dependence upon climate becomes more pronounced for increasing value of d. For d = 225 nmi and "lobing determines median level," the expected value, 90 percent quantile, and standard deviation are approximately 38 dB, 41 dB, and 3 dB more, respectively, for desert (the least favorable) climate than for equatorial (the most favorable) climate. The basic transmission loss is approximately independent of the lobing options for the most favorable climate (equatorial) at the shortest path and for the most unfavorable climate (desert) at the shortest (d = 100 nmi) and longest (d = 225 nmi) paths.

The basic transmission loss for a smooth Earth ($\Delta h = 0$) is plotted in figures 3-1 through 3-8 as a function of distance for each of the various climates. In each figure, there are seven curves of basic transmission loss: free-space loss; 10%, expected value, and 90% confidence levels for "lobing determines median;" and 10%, expected value, and 90% confidence levels for "lobing contributes to variability." The basic transmission loss at each of the confidence levels for both of the lobing options is appreciably different from the free-space loss even at distances less than one-half the distance to the radio horizon. For example, at d = 100 nmi with "lobing contributes to variability," the 10% quantile, expected value, and 90% quantile are greater than the free-space values nominally by -3, 2, and 8 dB, respectively. At d = 200 nmi with "lobing contributes to variability," the respective quantiles are greater than the free-space values nominally by 0, 8, and 18 dB. The expected values of 2 dB and 8 dB excess propagation loss at d = 100 nmi and 200 nmi, respectively, result primarily from absorption by oxygen in the atmosphere. For lobing determines median, the ten lobes nearest the radio horizon have transmission loss minima (-2 to -8 dB) and maxima (14 to 40 dB) whose depths and peaks increase with increasing distance (because the modulus of the

Table 3-1. Basic Transmission Loss for Specified Climates; Terrain Roughness Δh = 0, Lobing Determines Median

CLIMATE	BASIC TRANSMISSION LOSS, L_b(d) (dB)															
	d = 100 nmi				d = 150 nmi				d = 200 nmi				d = 225 nmi			
	Free Sp	Exp Val	90%	Std Dev	Free Sp	Exp Val	90%	Std Dev	Free Sp	Exp Val	90%	Std Dev	Free Sp	Exp Val	90%	Std Dev
CONTINENTAL-ALL YEAR 0	157.9	160.1	166.4	4.5	161.4	171.8	176.6	3.8	163.5	174.0	183.1	7.0	164.9	193.3	203.2	7.7
EQUATORIAL 1	157.9	160.2	166.5	4.5	161.4	170.4	174.4	3.0	163.5	164.7	172.2	5.5	164.9	166.2	175.0	6.4
CONTINENTAL SUBTROPICAL 2	157.9	160.1	166.4	4.5	161.4	165.1	170.9	4.6	163.5	164.4	174	7.3	164.9	180.5	191.9	9.2
MARITIME SUBTROPICAL 3	157.9	160.1	166.3	4.5	161.4	166.5	174.2	5.8	163.5	174.1	184.4	8.1	164.9	180.5	191.9	9.2
DESERT 4	157.9	160.2	166.5	4.5	161.4	188.9	194.7	4.6	163.5	195.3	206.2	8.5	164.9	203.7	215.8	9.5
CONTINENTAL TEMPORATE 6	157.9	160.1	166.4	4.5	161.4	164.9	170.8	4.6	163.5	164.3	173.8	7.2	164.9	180.9	191.7	8.5
MARITIME TEMPORATE OVERLAND 7	157.9	160.1	166.4	4.5	161.4	165.8	170.4	3.5	163.5	165.3	174.0	6.5	164.9	184.2	193.9	7.3
MARITIME TEMPORATE OVERSEAS 8	157.9	160.1	166.4	4.5	161.4	165.0	170.3	4.1	163.5	163.9	173.9	7.5	164.9	180.3	192.3	8.7

f = 10 GHz, Instantaneous Levels Exceeded, Δh = 0 ft., Poor Ground,
Isotropic Antennas, Circular Polarization, Height h_1 = 33000 ft., Height h_2 = 10 ft.

Table 3-2. Basic Transmission Loss for Specified Climates; Terrain Roughness Δh = 0, Lobing Contributes to Variability

CLIMATE	BASIC TRANSMISSION LOSS, $L_b(d)$ (dB)															
	d = 100 nmi				d = 150 nmi				d = 200 nmi				d = 225 nmi			
	Free Sp	Exp Val	90%	Std Dev	Free Sp	Exp Val	90%	Std Dev	Free Sp	Exp Val	90%	Std Dev	Free Sp	Exp Val	90%	Std Dev
CONTINENTAL-ALL YEAR 0	157.6	160.1	166.3	4.5	161.4	165.5	172.8	5.5	163.9	172.2	181.3	7.0	164.9	193.3	203.2	..7
EQUATORIAL 1	157.6	160.2	166.4	4.5	161.4	165.2	172.1	5.0	163.9	169.3	177.4	5.9	164.9	172.3	181.1	6.4
CONTINENTAL SUBTROPICAL 2	157.6	160.1	166.3	4.5	161.4	166.6	174.2	5.8	163.9	174.1	184.4	8.1	164.9	180.5	191.9	9.2
MARITIME SUBTROPICAL 3	157.5	160.1	166.3	4.5	161.4	165.1	172.4	5.4	163.9	171.2	179.9	6.6	164.9	174.5	184.2	7.4
DESERT 4	157.6	160.2	166.4	4.5	161.4	166.9	175	6.1	163.9	174.8	185.7	8.6	164.9	203.7	215.8	9.5
CONTINENTAL TEMPORATE 6	157.6	160.1	166.3	4.5	161.4	166.7	174.3	5.8	163.9	173.4	183.3	7.7	164.9	182.6	193.4	8.5
MARITIME TEMPORATE OVERLAND 7	157.6	160.1	166.4	4.5	161.4	164.6	171.9	5.2	163.9	171.0	179.7	6.5	164.9	182.6	192.2	7.3
MARITIME TEMPORATE OVERSEAS 8	157.6	160.1	166.3	4.5	161.4	165.8	173.3	5.6	163.9	172.6	182.6	7.6	164.9	180.8	192.3	8.7

f = 10 GHz, Instantaneous Levels Exceeded, Δh = 0 ft., Poor Ground,
Isotropic Antennas, Circular Polarization, Height h = 33000 ft., Height h = 10 ft.

Johnson-Gierhart Program Run Data: Frequency: 10 GHz Climate: #0 Continental All-Year Terrain Delta h: 0 ft.
Refractivity: Effective Earth Radius: 4423 nmi Minimum Monthly Mean: See Legend N-Units Surface Type: Poor Ground
Aircraft Antenna Altitude: 33000 ft. above MSL Type: Isotropic Circular Polarization Time availability: For Instantaneous Levels Exceeded
Facility Antenna Height: 10 ft. above MSL Type: Isotropic Circular Polarization Horizon Obstacle Distance Determined
Surface Reflection Lobing: See Legend Confidence: See Legend Obst Distance: Determined at 4.5 nmi Obst Height: 0 feet

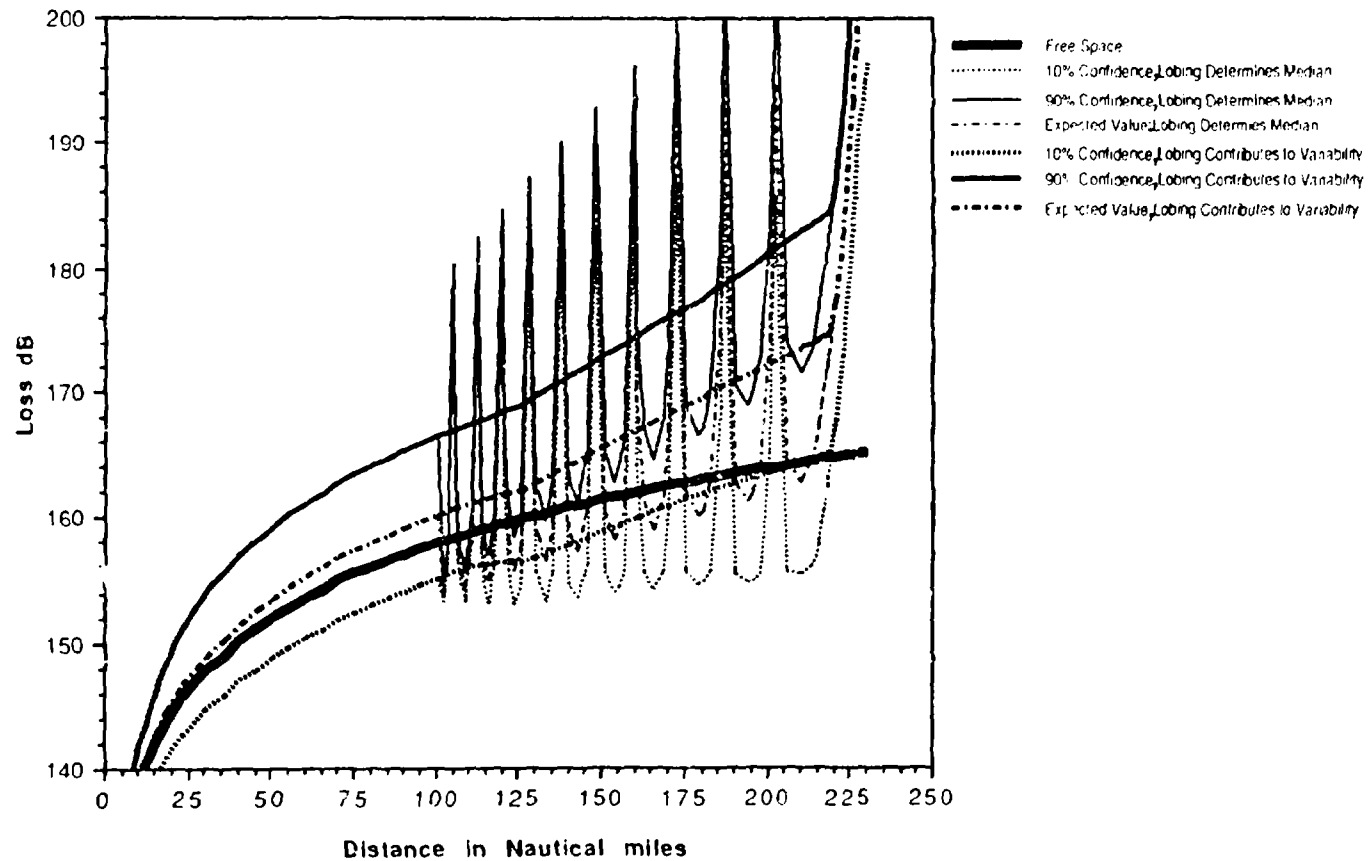

Figure 3-1. Basic Transmission Loss; Terrain Roughness Δh = 0, Continental All-Year Climate

Johnson-Gierhart Program Run Data: Frequency: 10 GHz Climate: #1 Equatorial Terrain Delta h: 0 ft.
Refractivity: Effective Earth Radius: 4423 nmi Minimum Monthly Mean: See Legend N-Units Surface Type: Poor Ground
Aircraft Antenna Altitude: 33000 ft. above MSL Type: Isotropic Circular Polarization Time availability: For Instantaneous Levels Exceeded
Facility Antenna Height: 10 ft. above MSL Type: Isotropic Circular Polarization Horizon Obstacle Distance Determined
Surface Reflection Lobing: See Legend Confidence: See Legend Obst Distance: Determined at 4.5 nmi Obst Height: 9 feet

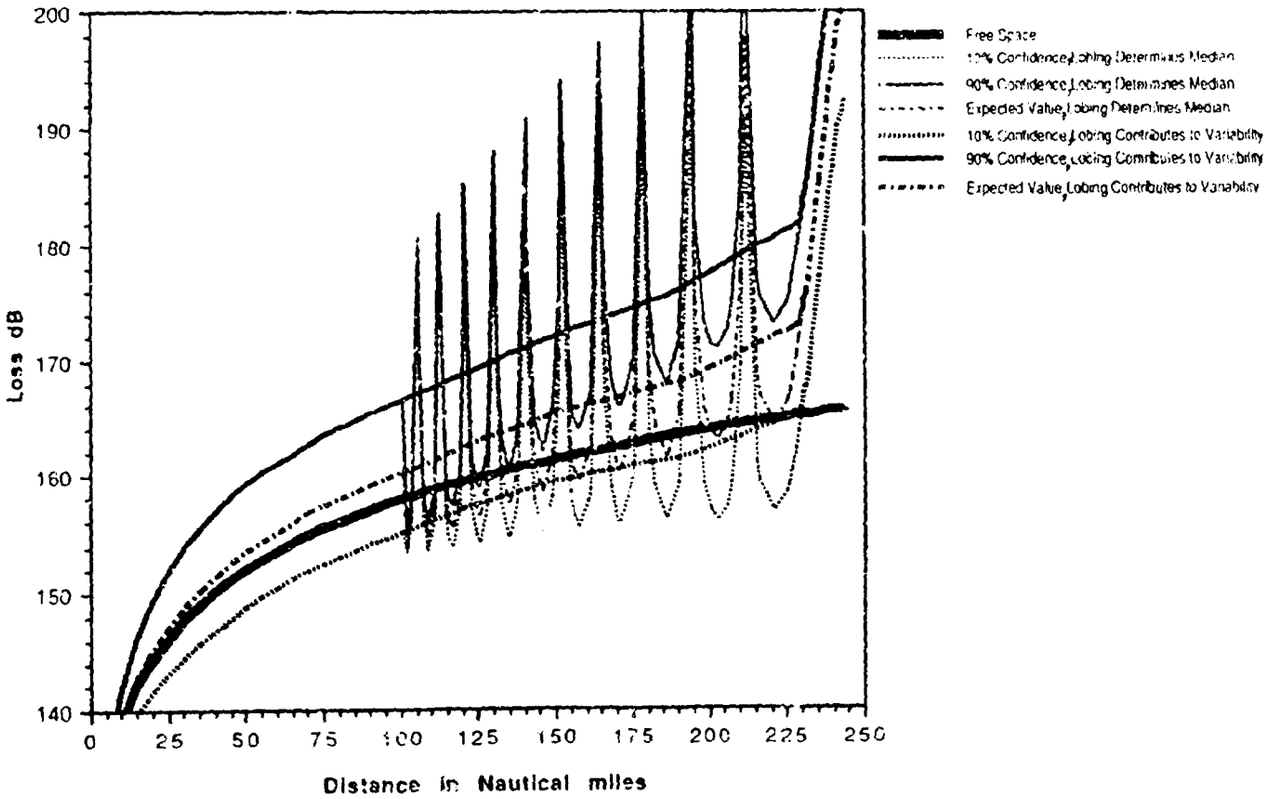

Figure 3-2. Basic Transmission Loss; Terrain Roughness Δh = 0, Equatorial Climate

Johnson-Gierhart Program Run Data: Frequency: 10 GHz Climate: #2 Continental Subtropical Terrain Delta h: 0 ft.
Refractivity: Effective Earth Radius: 4423 nmi Minimum Monthly Mean: See Legend N-Units Surface Type: Poor Ground
Aircraft Antenna Altitude: 33000 ft. above MSL Type: Isotropic Circular Polarization Time availability: For Instantaneous Levels Exceeded
Facility Antenna Height: 10 ft. above MSL Type: Isotropic Circular Polarization Horizon Obstacle Distance Determined
Surface Reflection Lobing: See Legend Confidence: See Legend Obst Distance: Determined at 4.5 nmi Obst Height: 0 feet

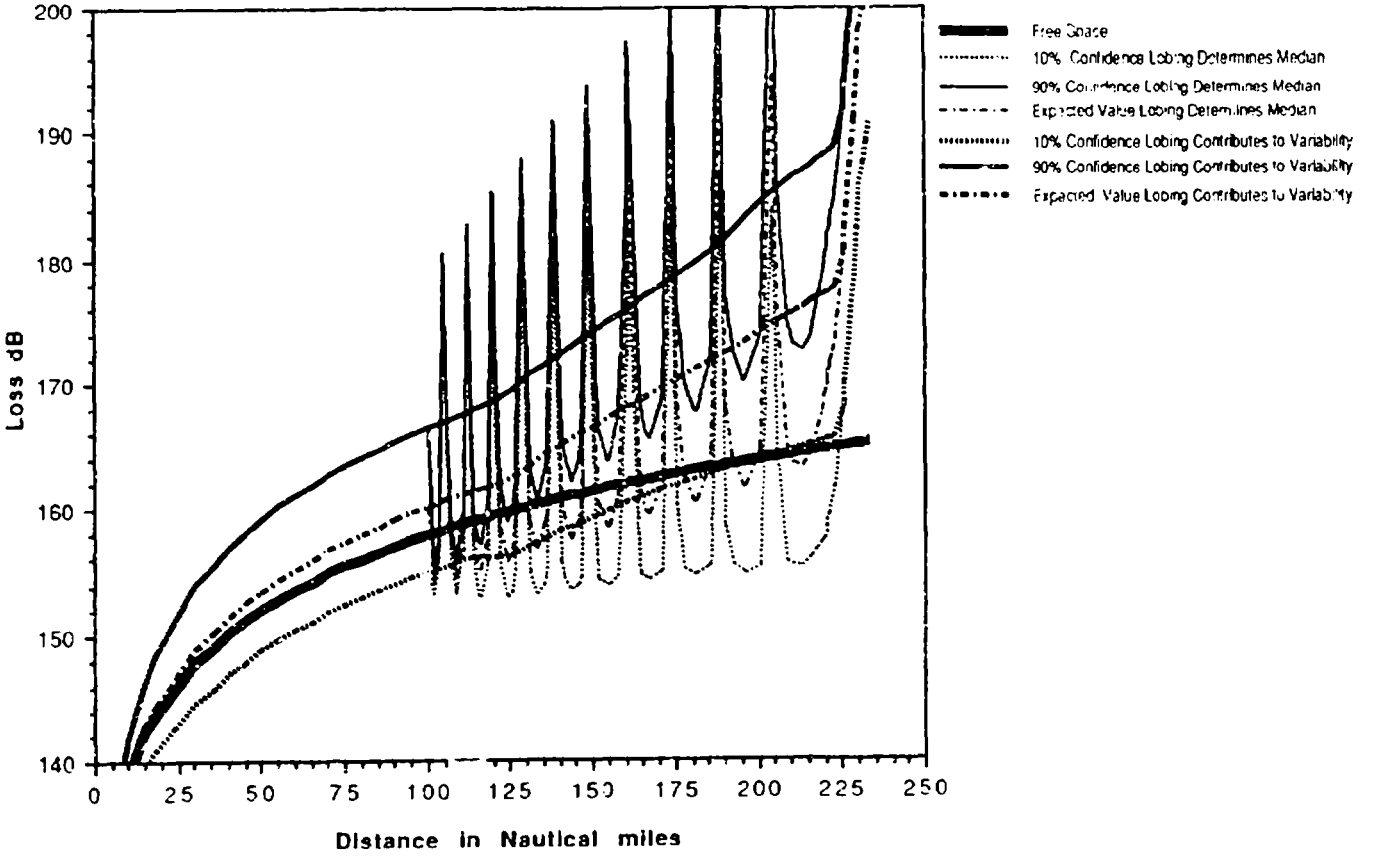

Figure 3-3. Basic Transmission Loss; Terrain Roughness Δh = 0, Continental Subtropical Climate

Johnson-Gierhart Program Run Data: Frequency: 10 GHz Climate: #3 Maritime Subtropical Terrain Delta h: 0 ft.
Refractivity: Effective Earth Radius: 4423 nmi Minimum Monthly Mean: See Legend N-Units Surface Type: Poor Ground
Aircraft Antenna Altitude: 33000 ft. above MSL Type: Isotropic Circular Polarization Time availability: For Instantaneous Levels Exceeded
Facility Antenna Height: 10 ft. above MSL Type: Isotropic Circular Polarization Horizon Obstacle Distance Determined
Surface Reflection Lobing: See Legend Confidence: See Legend Obst Distance: Determined at 4.5 nmi Obst Height: 0 feet

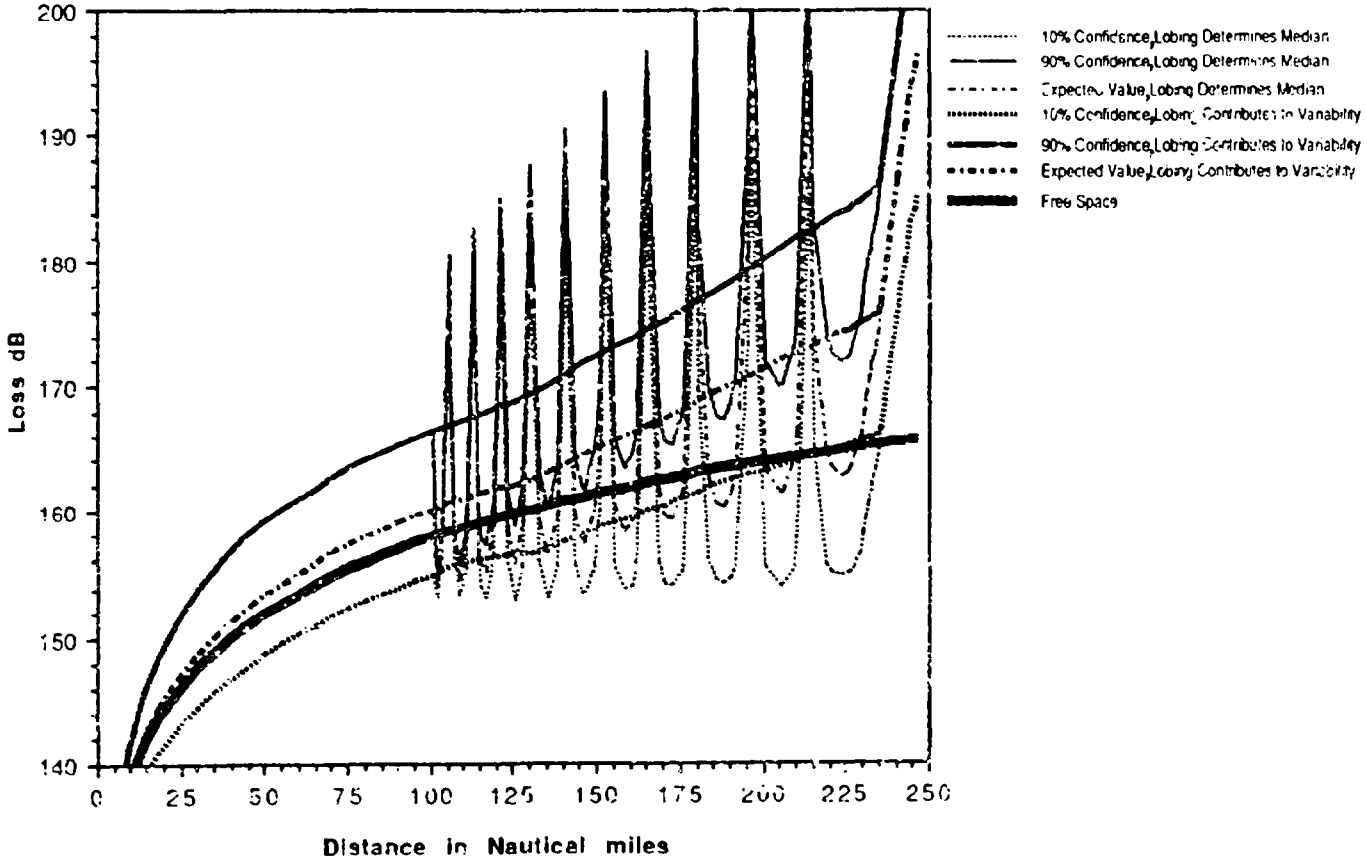

Figure 3-4. Basic Transmission Loss; Terrain Roughness Δh = 0, Maritime Subtropical Climate

Johnson-Gierhart Program Run Data: Frequency: 10 GHz Climate: #4 Desert Terrain Delta h: 0 ft.
Refractivity: Effective Earth Radius: 4423 nmi Minimum Monthly Mean: See Legend N-Units Surface Type: Poor Ground
Aircraft Antenna Altitude: 33000 ft. above MSL Type: Isotropic Circular Polarization Time availability: For Instantaneous Levels Exceeded
Facility Antenna Height: 10 ft. above MSL Type: Isotropic Circular Polarization Horizon Obstacle Distance Determined
Surface Reflection Lobing: See Legend Confidence: See Legend Obst Distance: Determined at 4.5 nmi Obst Height: 0 feet

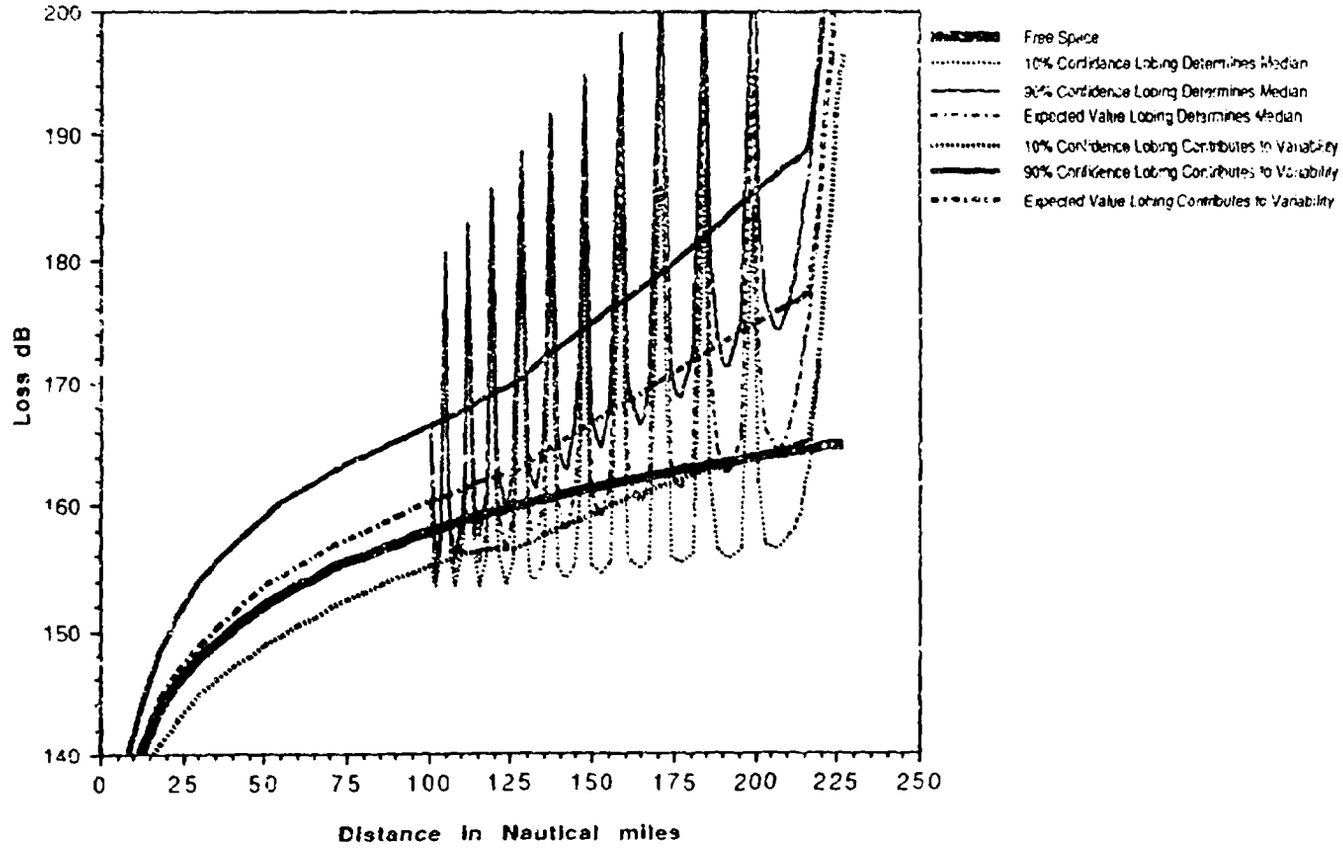

Figure 3-5. Basic Transmission Loss; Terrain Roughness Δh = 0, Desert Climate

Johnson-Gierhart Program Run Data: Frequency: 10 GHz Climate: #6 Continental Temperate Terrain Delta h: 0 ft.
Refractivity: Effective Earth Radius: 4423 nmi Minimum Monthly Mean: See Legend N-Units Surface Type: Poor Ground
Aircraft Antenna Altitude: 33000 ft. above MSL Type: Isotropic Circular Polarization Time availability: For Instantaneous Levels Exceeded
Facility Antenna Height: 10 ft. above MSL Type: Isotropic Circular Polarization Horiaon Obstacle Distance Determined
Surface Reflection Lobing: See Legend Confidence: See Legend Obst Distance: Determined at 4.5 nmi Obst Height: 0 feet

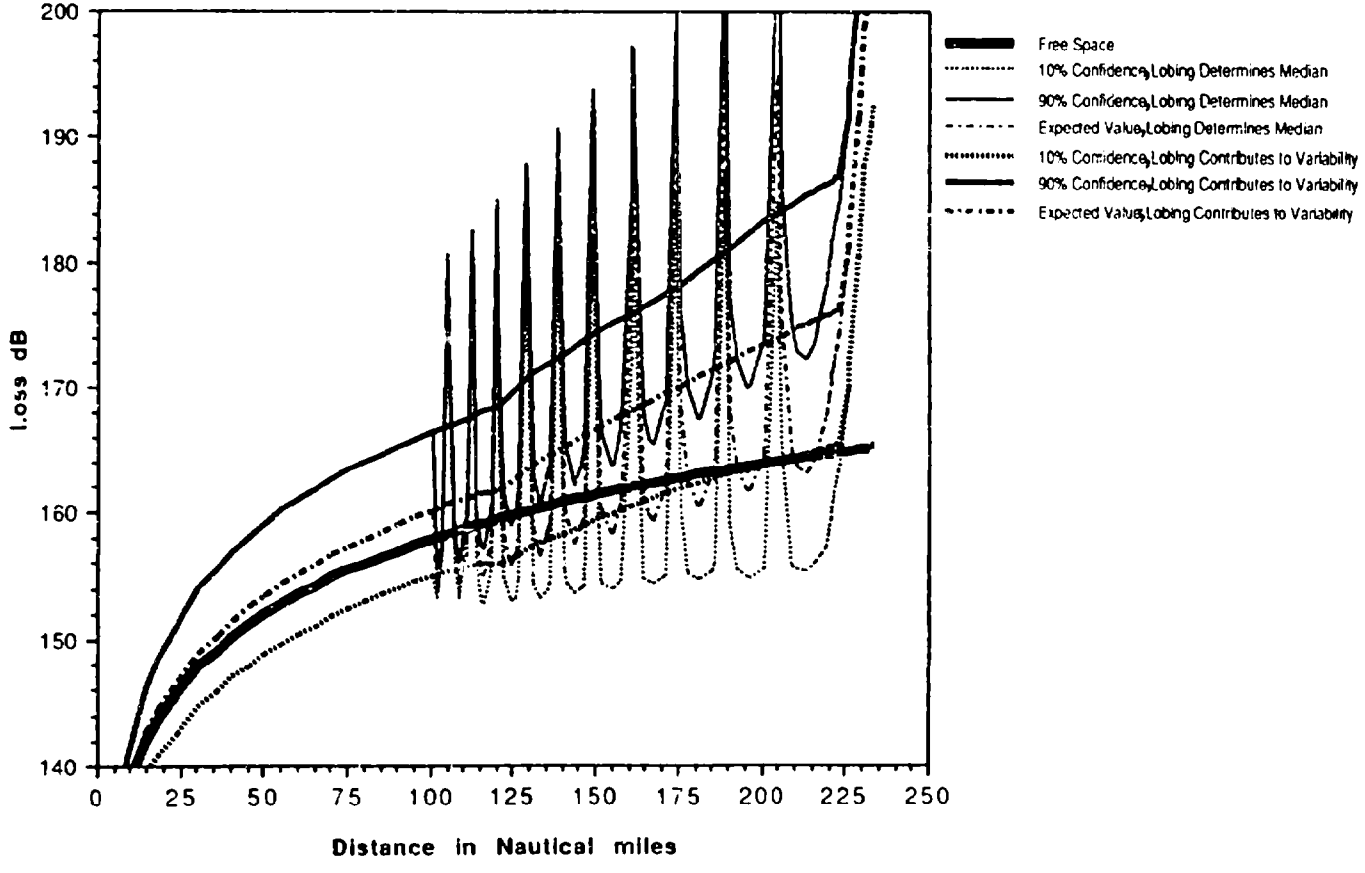

Figure 3-6. Basic Transmission Loss; Terrain Roughness Δh = 0, Continental Temperate Climate

Johnson-Gierhart Program Run Data: Frequency: **10 GHz** Climate: **#7 Maritime Temperate Overland** Terrain Delta h: **0 ft.**
Refractivity: Effective Earth Radius: **4423** nmi Minimum Monthly Mean: **See Legend** N-Units Surface Type: Poor Ground
Aircraft Antenna Altitude: **33000** ft. above MSL Type: Isotropic Circular Polarization Time availability: For Instantaneous Levels Exceeded
Facility Antenna Height: **10** ft. above MSL Type: Isotropic Circular Polarization Horiaon Obstacle Distance **Determined**
Surface Reflection Lobing: **See Legend** Confidence: **See Legend** Obst Distance: **Determined at 4.5** nmi Obst Height: **0** feet

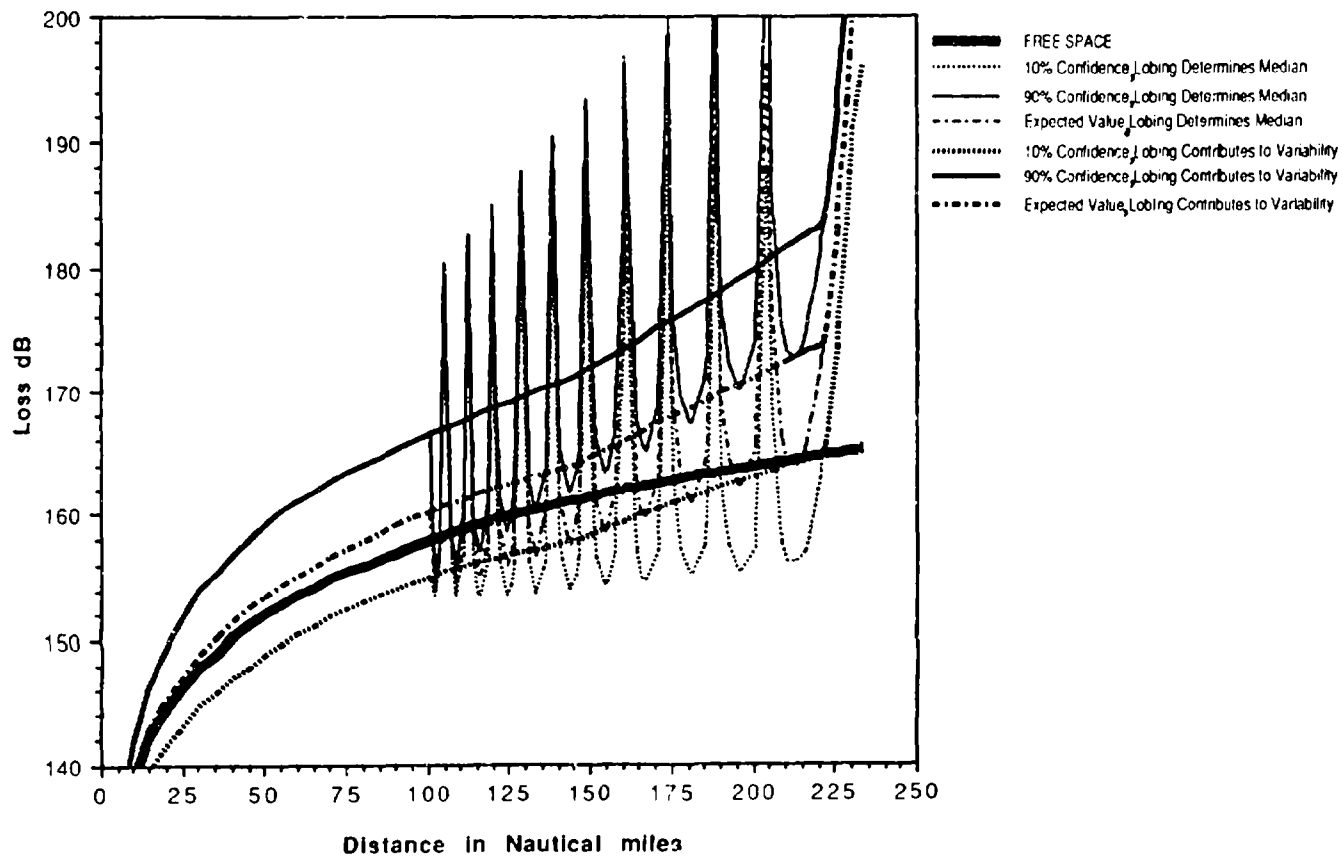

Figure 3-7. Basic Transmission Loss; Terrain Roughness Δh = 0, Maritime Temperate Overland Climate

Johnson-Gierhart Program Run Data: Frequency: 10 GHz Climate: #8 Maritime Temperate Oversea Terrain Delta h: 0 ft.
Refractivity: Effective Earth Radius: 4423 nmi Minimum Monthly Mean: See Legend N-Units Surface Type: Poor Ground
Aircraft Antenna Altitude: 33000 ft. above MSL Type: Isotropic Circular Polarization Time availability: For Instantaneous Levels Exceeded
Facility Antenna Height: 10 ft. above MSL Type: Isotropic Circular Polarization Horizon Obstacle Distance Determined
Surface Reflection Lobing: See Legend Confidence: See Legend Obst Distance: Determined at 4.5 nmi Obst Height: 0 feet

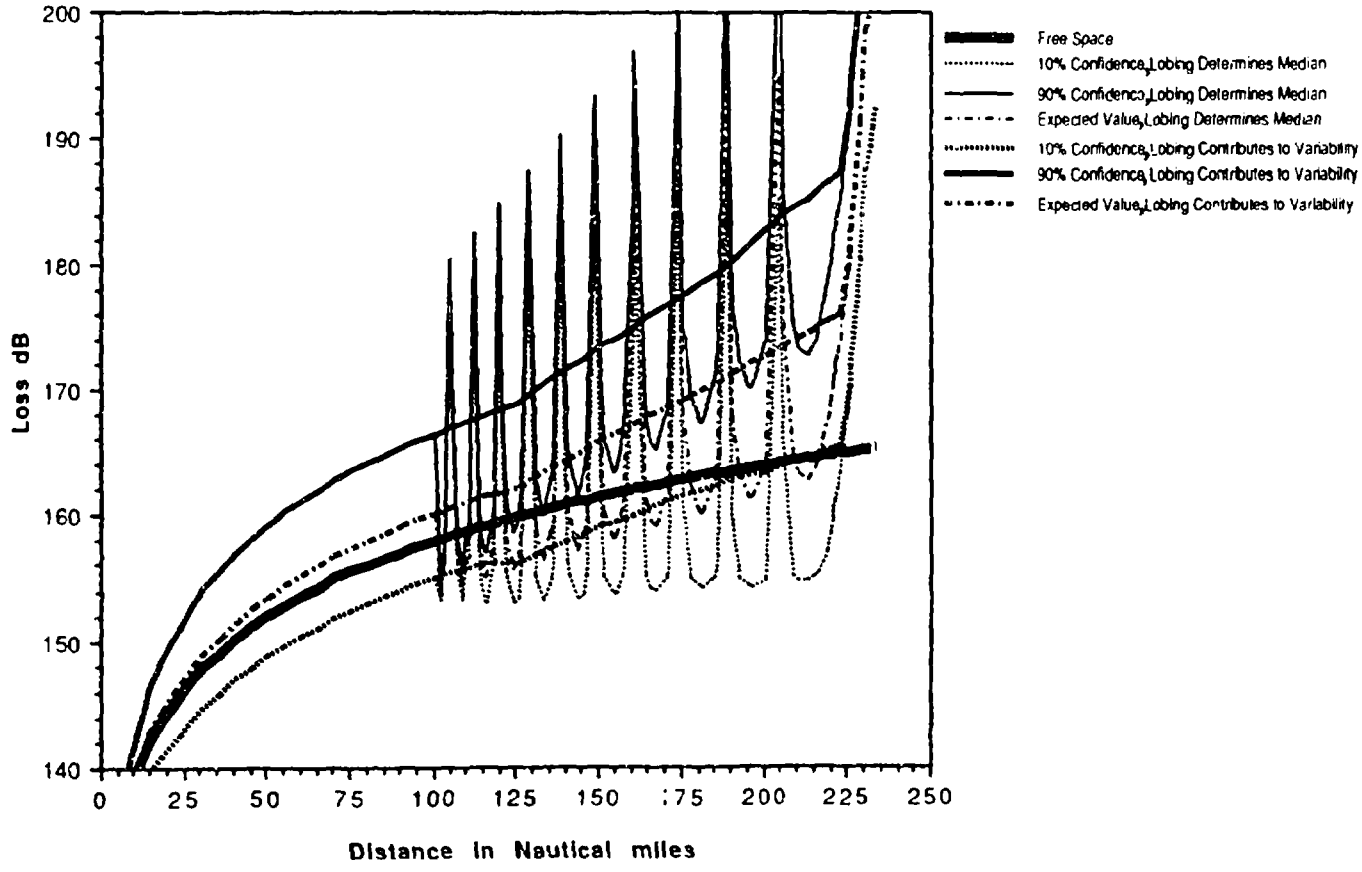

Figure 3-8. Basic Transmission Loss; Terrain Roughness Δh = 0, Maritime Temperate Oversea Climate

Fresnel reflection coefficient approaches unity with increasing distance). The locations of the minima and maxima vary with the type of climate. The discontinuity in slope of the "lobing contributes to variability" curves in figures 3-1 through 3-8 is caused by Johnson-Gierhart modeling of a breakpoint within the multipath interference mode of propagation (including atmospheric absorption and refraction). The reason for the breakpoint is not clear. It appears that the breakpoint results from an adjustment factor to the Longley-Rice long-term variability distribution so that air-to-air and air-to-ground paths have a long-term variability that agrees with the empirical data base. In figure 3-1 the breakpoint is at d = 125 nmi.

The excess propagation loss for various climates is compared in figures 3-9 through 3-12 for paths and smooth spherical Earth at distances d = 100, 150, 200, and 225 nmi. At d = 100 nmi, the excess propagation loss is approximately independent of the climate. At d = 225 nmi, the excess propagation loss has nominal expected values of 39 dB for desert climate and less than 8 dB for equatorial climate; 90 percent confidence levels of 50 dB for desert climate and less than 16 dB for equatorial climate.

The climate runs for the same cases as in tables 3-1 and 3-2; but for a slightly rough Earth (terrain (Δh = 50 ft) instead of a smooth Earth, summaries are found in tables 3-3 and 3-4. The trends are similar to those of tables 3-1 and 3-2 except that the transmission losses are 1 to 8 dB larger. At d = 225 nmi and lobing "determines the median level," the expected value, 90 percent quantile, and standard deviation of the transmission loss are approximately 36, 41, and 3 dB, respectively; more for desert climate than for equatorial climate. These loss differences between climates are not appreciably larger than those for $\Delta h = 0$.

For paths over slightly rough Earth (Δh = 50 ft) and "lobing determines median," the basic transmission loss and excess propagation loss for various climates are compared in figures 3-13 through 3-16. The expected values and 90 percent confidence levels of excess propagation loss do not vary appreciably with climate for distances as large as 200 nmi.

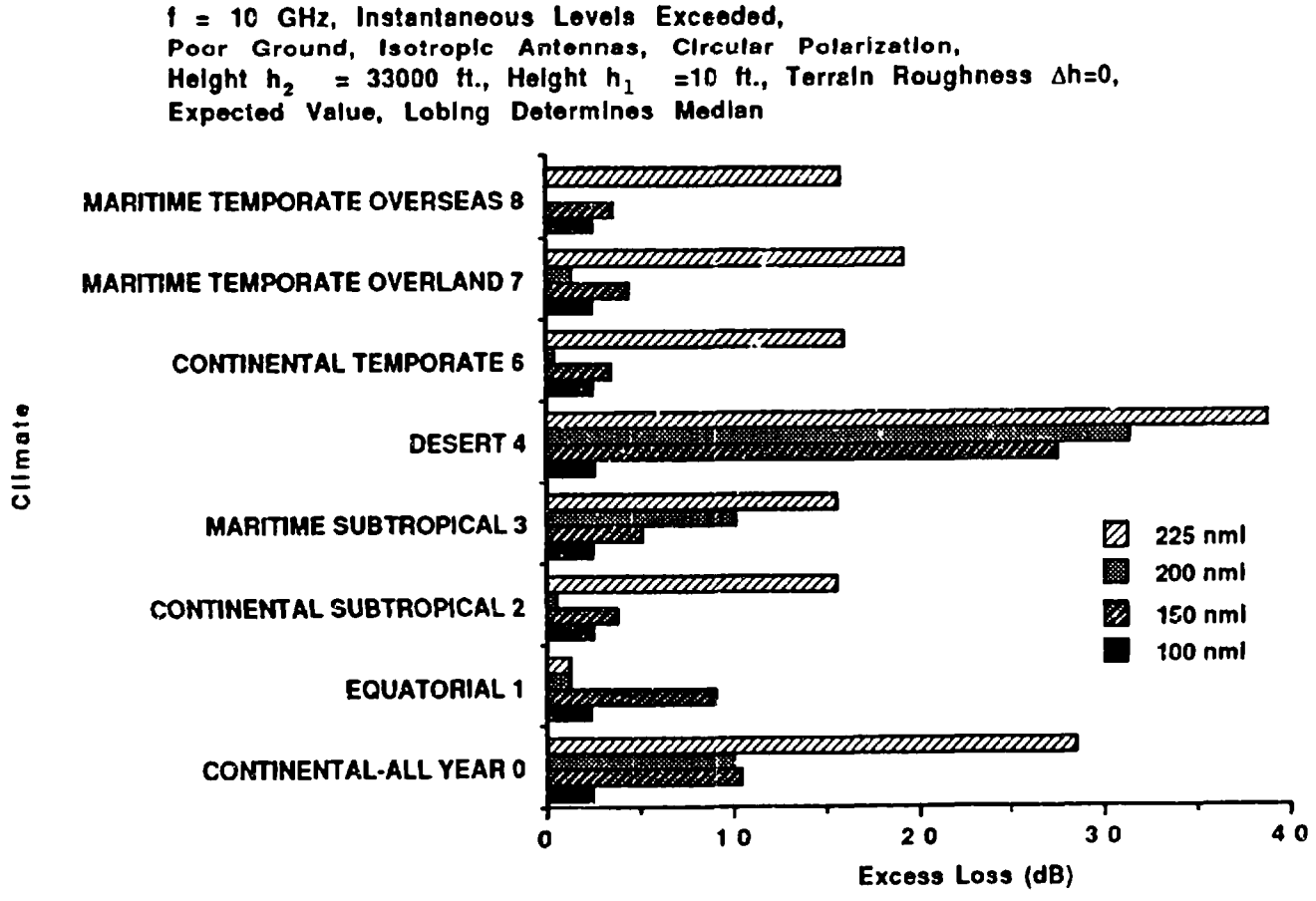

Figure 3-9. Comparison of Expected Values of Excess Propagation Loss for Various Climates; Terrain Roughness Δh = 0, Lobing Determines Median

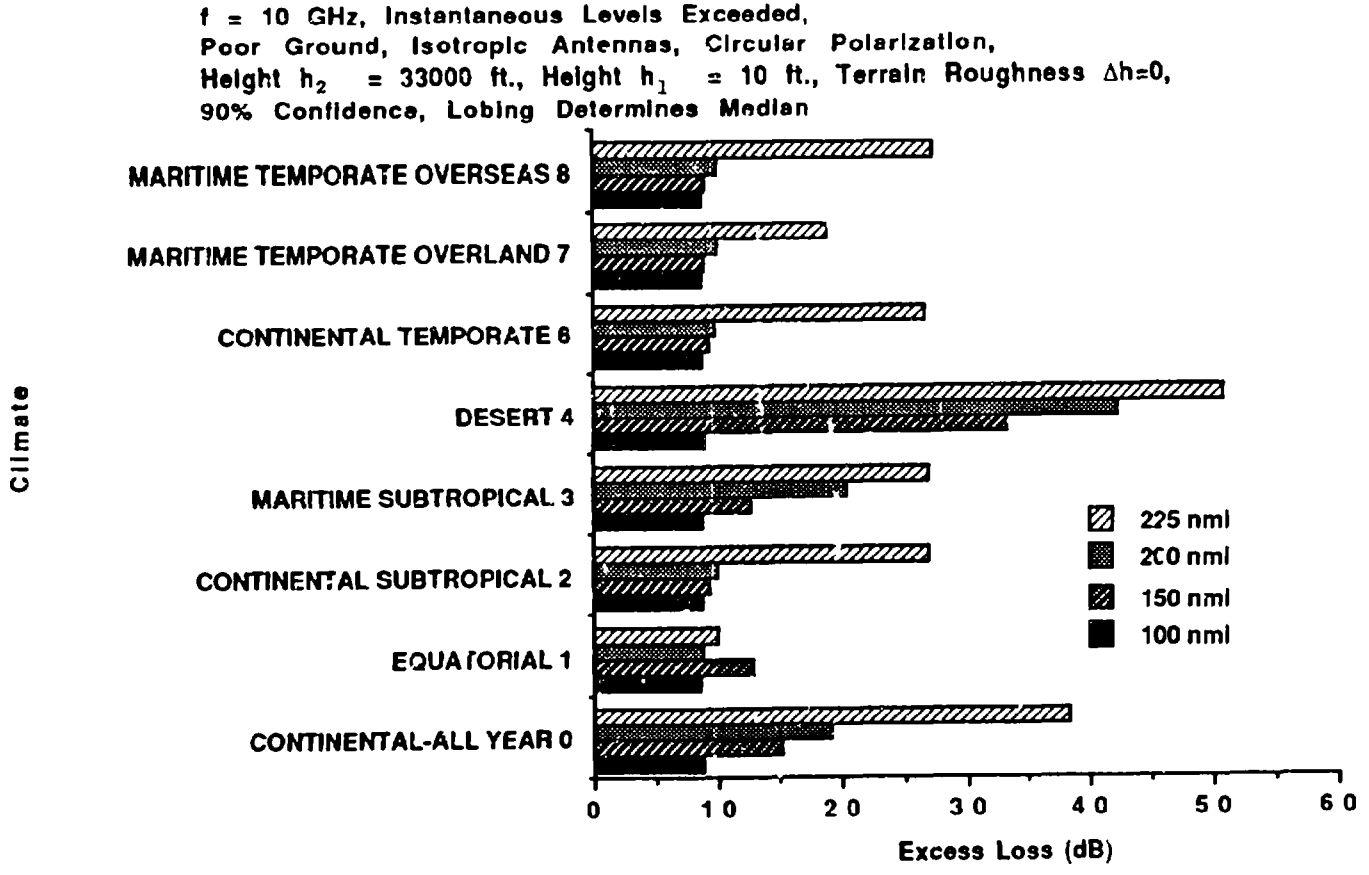

Figure 3-10. Comparison of 90 Percent Confidence Levels of Excess Propagation Loss for Various Climates; Terrain Roughness Δh = 0, Lobing Determines Median

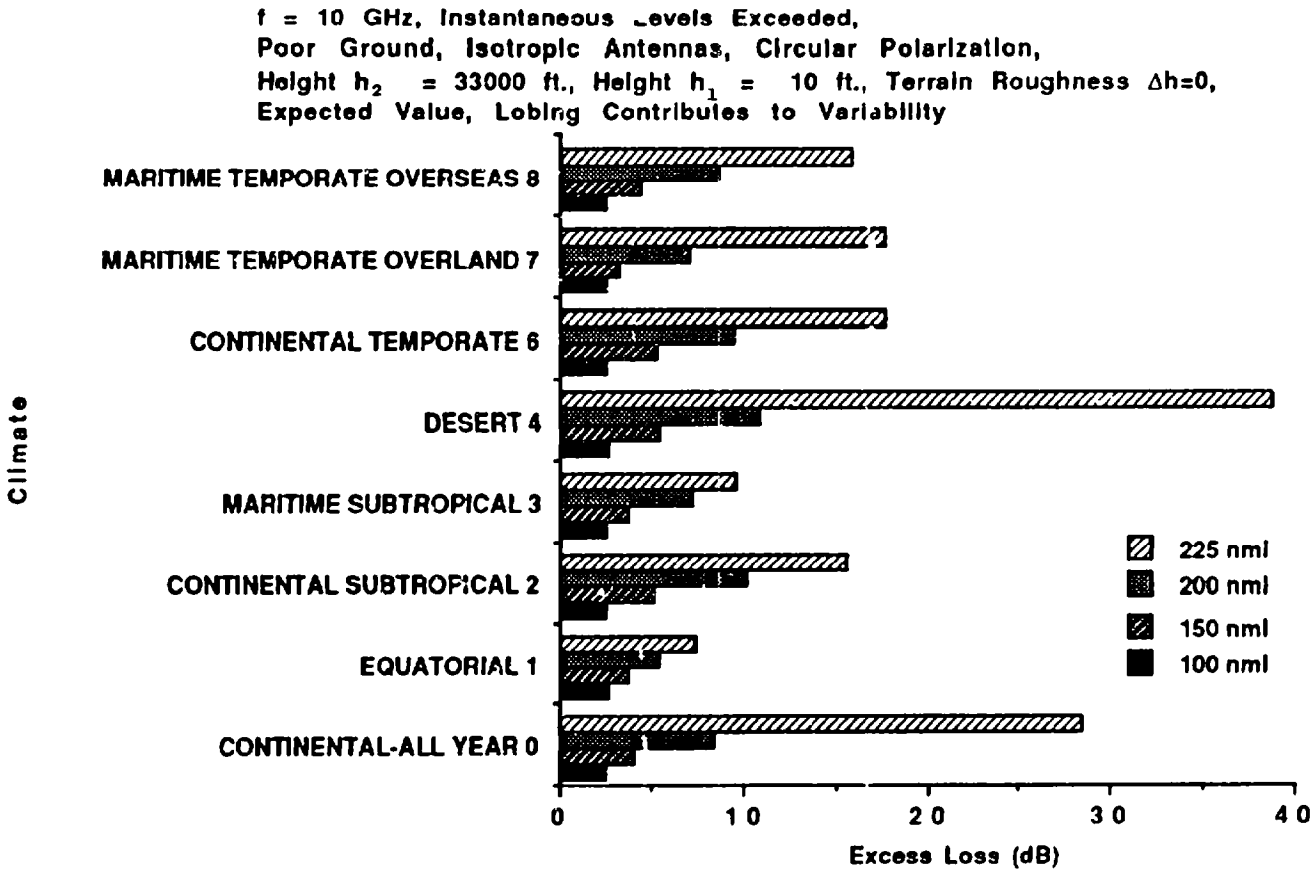

Figure 3-11. Comparison of Expected Values of Excess Propagation Loss for Various Climates; Terrain Roughness Δh = 0, Lobing Contributes to Variability

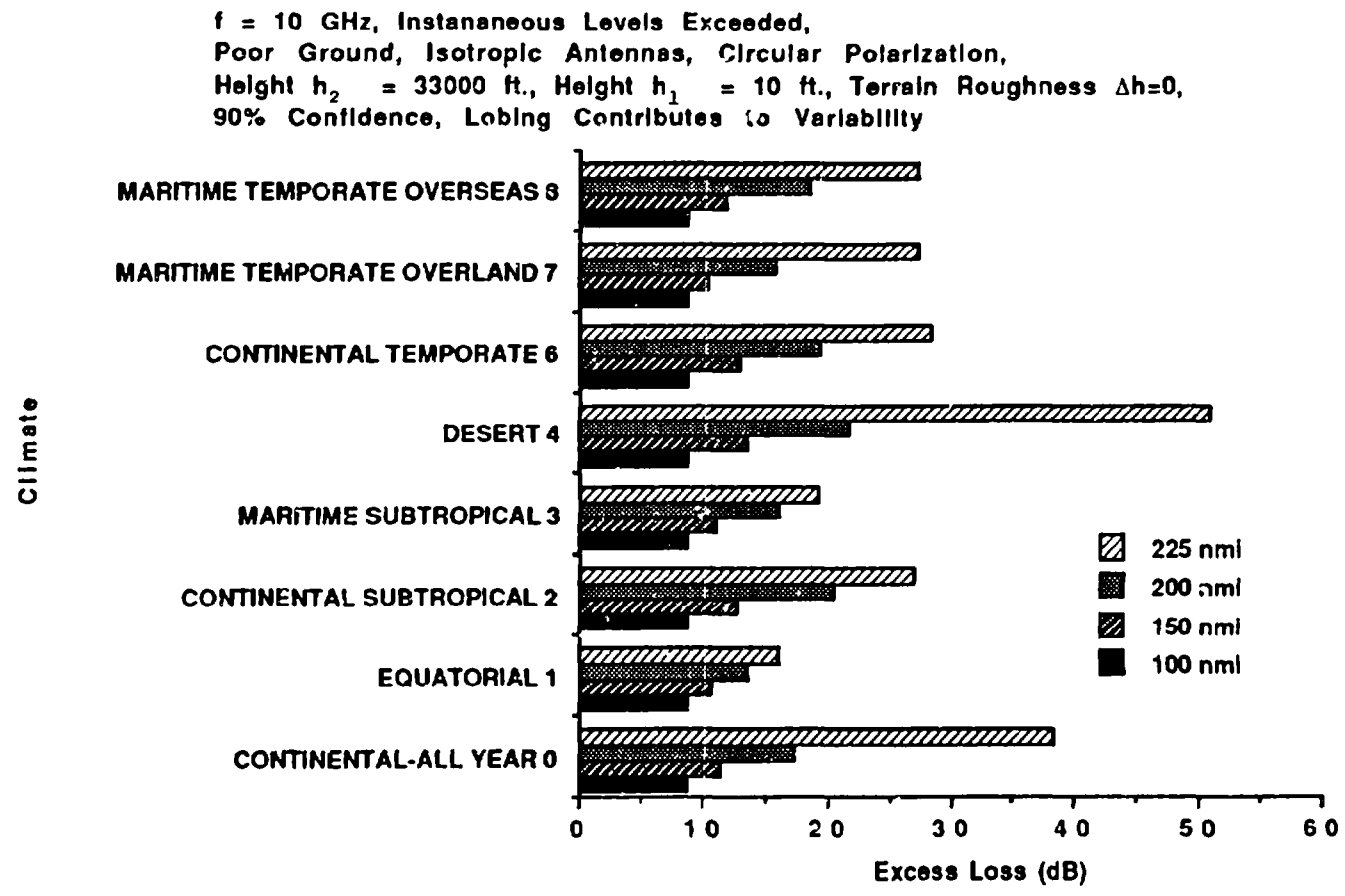

Figure 3-12. Comparison of 90 Percent Confidence Levels of Excess Propagation Loss for Various Climates; Terrain Roughness Δh = 0, Lobing Contributes to Variability

Table 3-3. Basic Transmission Loss for Specified Climates; Terrain Roughness Δh = 50 ft, Lobing Determines Median

CLIMATE	BASIC TRANSMISSION LOSS, $L_b(d)$ (dB)															
	d = 100 nmi				d = 150 nmi				d = 200 nmi				d = 225 nmi			
	Free Sp	Exp Val	90%	Std Dev	Free Sp	Exp Val	90%	Std Dev	Free Sp	Exp Val	90%	Std Dev	Free Sp	Exp Val	90%	Std Dev
CONTINENTAL-ALL YEAR 0	157.6	160.1	166.3	4.5	161.4	165.5	172.6	5.5	163.9	172.2	181.3	7.0	164.9	193.3	203.2	7.7
EQUATORIAL 1	157.6	160.2	166.4	4.5	161.4	165.2	172.1	5.0	163.9	169.3	177.4	5.9	164.9	172.3	181.1	6.4
CONTINENTAL SUBTROPICAL 2	157.6	160.1	166.3	4.5	161.4	166.5	174.2	5.8	163.9	174.1	184.4	8.1	164.9	180.5	191.9	9.2
MARITIME SUBTROPICAL 3	157.6	160.1	166.3	4.5	161.4	165.1	172.4	5.4	163.9	171.2	179.9	6.6	164.9	174.5	184.2	7.4
DESERT 4	157.6	160.2	166.4	4.5	161.4	166.9	175	6.1	163.9	174.8	185.7	8.6	164.9	203.7	215.8	9.5
CONTINENTAL TEMPORATE 5	157.6	160.1	166.3	4.5	161.4	166.7	174.3	5.8	163.9	173.4	183.3	7.7	164.9	182.6	193.4	8.5
MARITIME TEMPORATE OVERLAND 7	157.6	160.1	166.4	4.5	161.4	164.6	171.9	5.2	163.9	171.0	179.7	6.5	164.9	182.6	192.2	7.3
MARITIME TEMPORATE OVERSEAS 8	157.6	160.1	166.3	4.5	161.4	165.8	173.3	5.6	163.9	172.6	182.6	7.6	164.9	180.8	192.3	8.7

f = 10 GHz, Instantaneous Levels Exceeded, Δh = 0 ft., Poor Ground,
Isotropic Antennas, Circular Polarization, Height h = 33000 ft., Height h = 10 ft.

Table 3-4. Basic Transmission Loss for Specified Climates; Terrain Roughness Δh = 50 ft, Lobing Contributes to Variability

CLIMATE	BASIC TRANSMISSION LOSS, $L_t(d)$ (dB)															
	100 nmi				150 nmi				200 nmi				225 nmi			
	Free Sp	Exp Val	90%	Std Dev	Free Sp	Exp Val	90%	Std Dev	Free Sp	Exp Val	90%	Std Dev	Free Sp	Exp Val	90%	Std Dev
CONTINENTAL-ALL YEAR 0	157.9	159.2	159.6	0.4	161.4	164.9	169.8	3.8	163.9	172.2	181.3	7.0	164.9	192.1	202.0	7.7
EQUATORIAL 1	157.9	159.3	159.8	0.4	161.4	164.6	168.6	3.0	163.9	169.2	176.8	5.6	164.9	172.3	181.1	6.4
CONTINENTAL SUBTROPICAL 2	157.9	159.2	159.7	0.8	161.4	166	171.6	4.6	163.9	174.1	184.4	8.1	164.9	181.9	193.3	9.2
MARITIME SUBTROPICAL 3	157.9	159.2	159.7	0.4	161.4	164.5	169.3	3.7	163.9	171.2	179.6	6.4	164.9	174.3	184.0	7.4
DESERT 4	157.9	159.3	159.8	0.4	161.4	166.4	172.5	4.8	163.9	174.8	185.7	8.6	164.9	206.4	218.5	9.5
CONTINENTAL TEMPORATE 6	157.9	159.1	159.7	0.4	161.4	166.2	172.0	4.6	163.9	173.4	183.3	7.7	164.9	182.3	193.1	8.4
MARITIME TEMPORATE OVERLAND 7	157.9	159.2	159.7	0.4	161.4	164.0	168.7	3.5	163.9	170.9	179.6	6.5	164.9	184.0	193.7	7.3
MARITIME TEMPORATE OVERSEAS 8	157.9	159.1	159.6	0.4	161.4	165.2	170.5	4.1	163.9	172.6	182.6	7.5	164.9	182.2	193.7	8.7

f = 10 GHz, Instantaneous Levels Exceeded, Poor Ground,
Isotropic Antennas, Circular Polarization, Height h_1 = 33000 ft., Height h_2 = 10 ft.

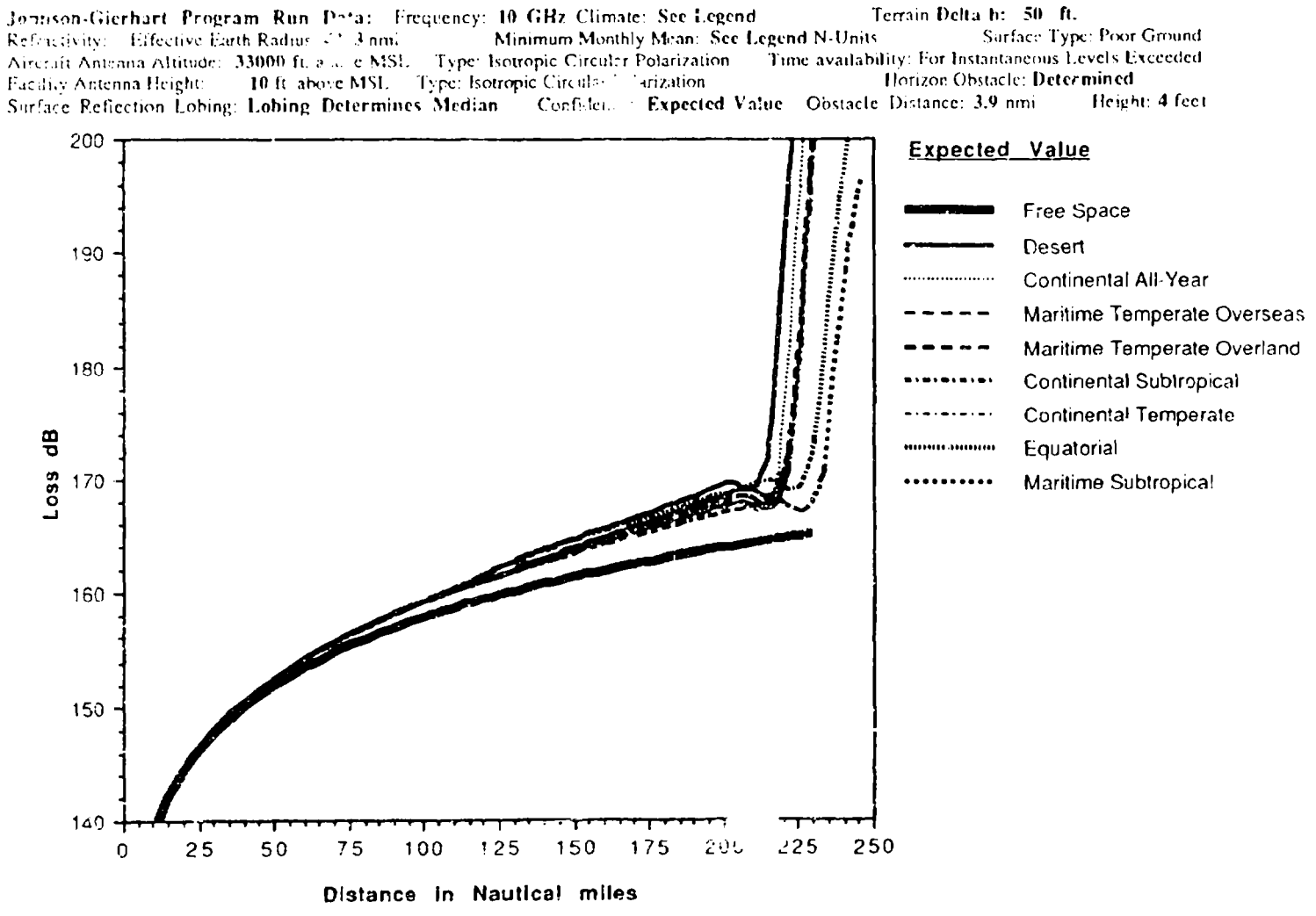

Figure 3-13. Comparison of Expected Values of Basic Transmission Loss for Various Climates; Terrain Roughness Δh = 50 ft, Lobing Determines Median

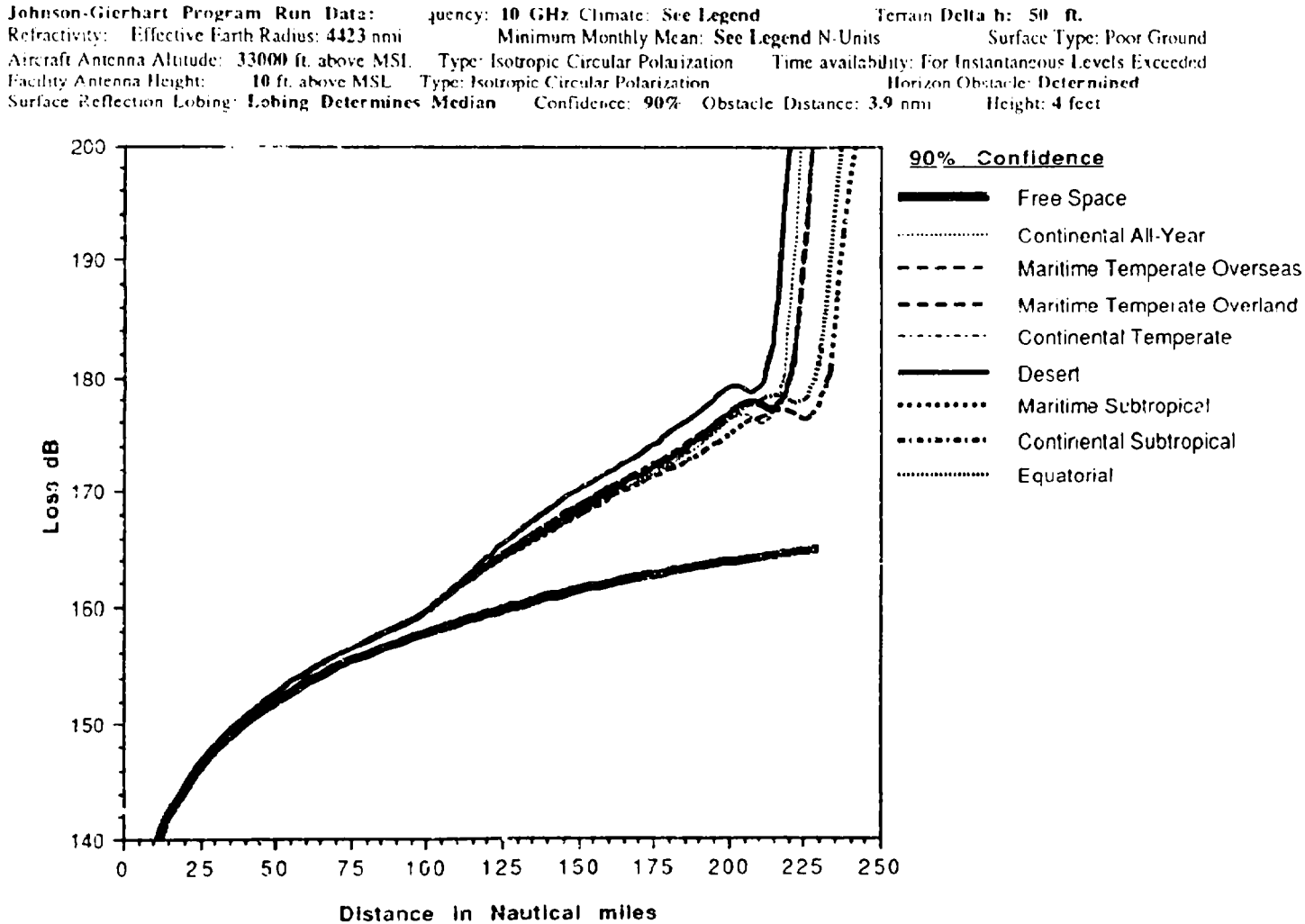

Figure 3-14. Comparison of 90 Percent Confidence Levels of Basic Transmission Loss for Various Climates; Terrain Roughness Δh = 50 ft, Lobing Determines Median

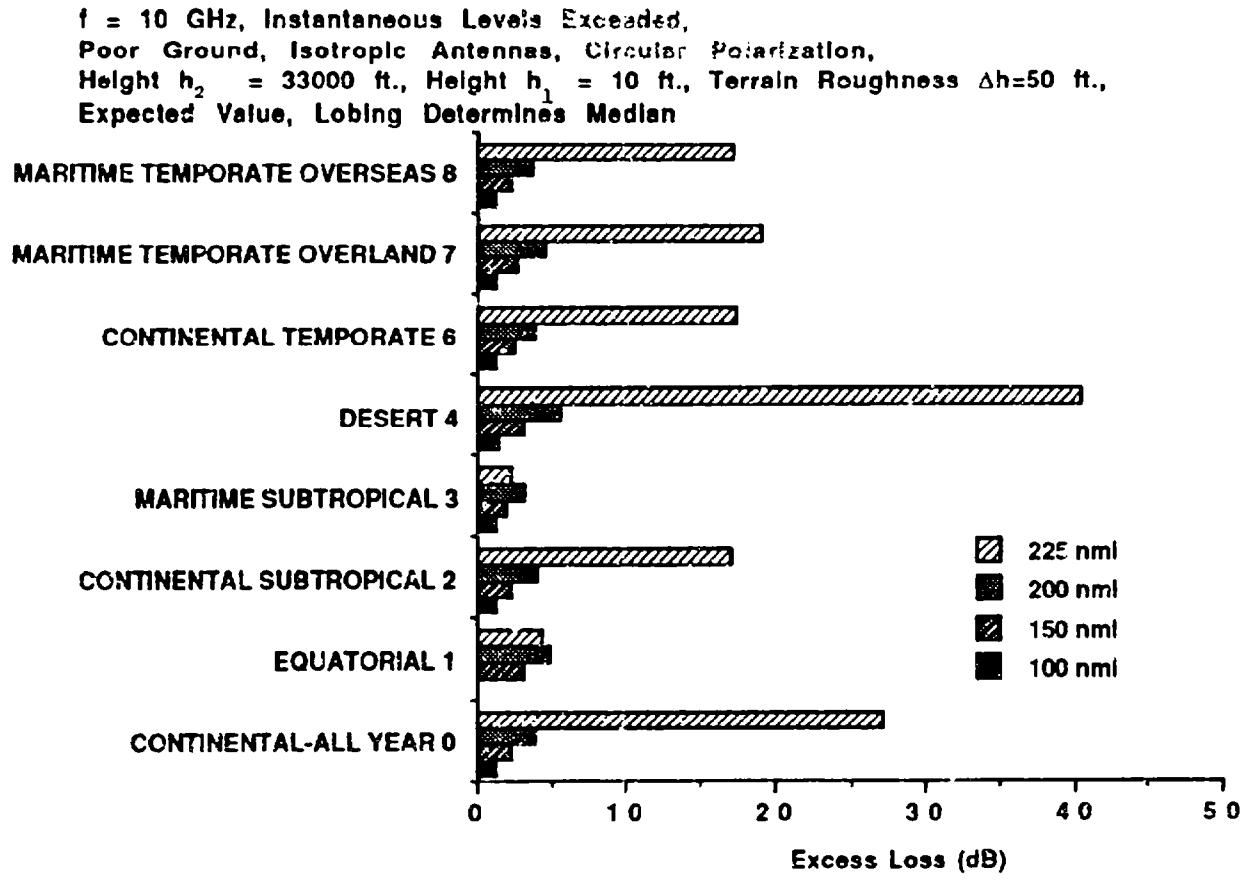

Figure 3-15. Comparison of Expected Values of Excess Propagation Loss for Various Climates; Terrain Roughness Δh = 50 ft, Lobing Determines Median

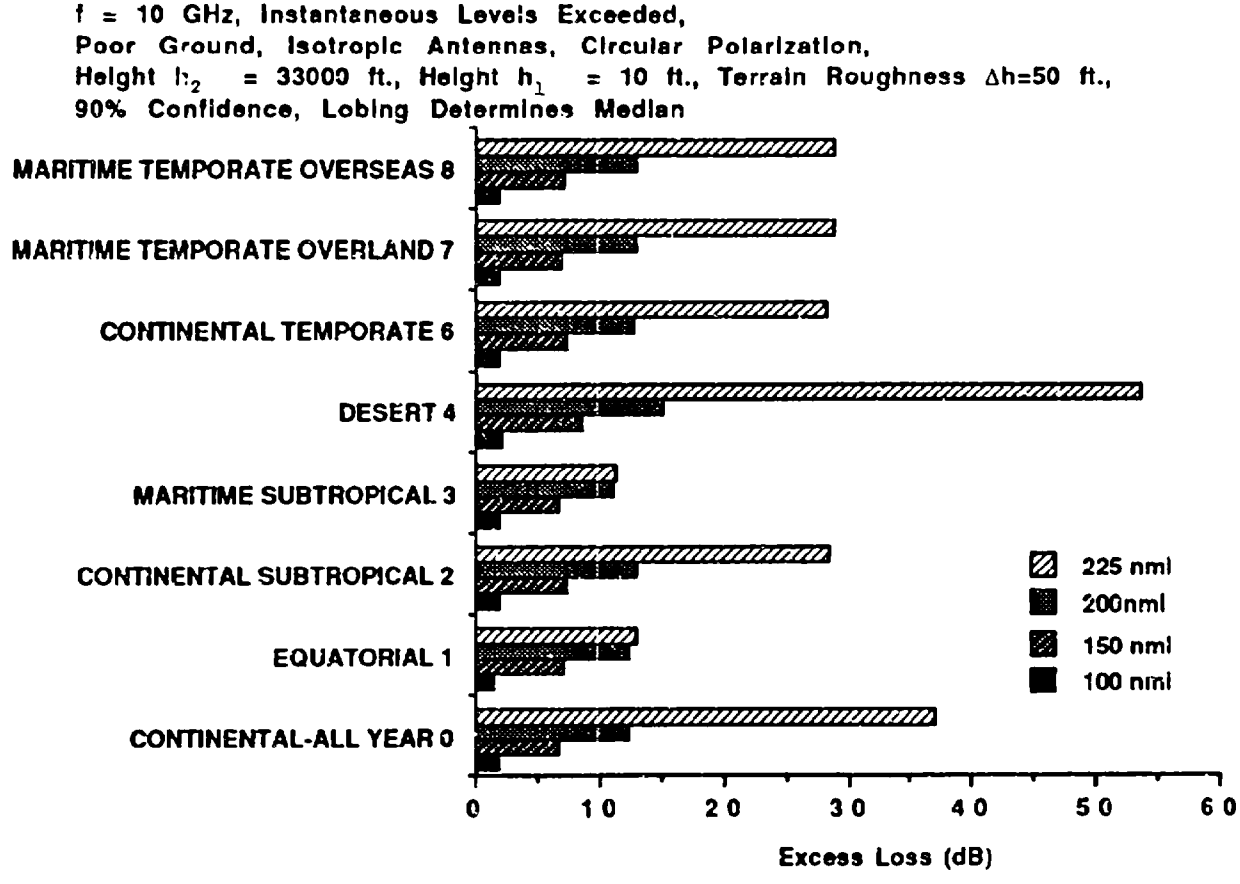

Figure 3-16. Comparison of 90 Percent Confidence Levels of Basic Transmission Loss for Various Climates; Terrain Roughness Δh = 50 ft, Lobing Determines Median

For "lobing contributes to variability" and $\Delta h = 50$ ft, the basic transmission loss and excess propagation loss are compared for various climates in figures 3-17 through 3-20. The most remarkable feature of figures 3-17 and 3-18 is the absence of a pronounced lobing pattern for $\Delta h = 50$ ft, unlike the distinct lobing patterns of figures 3-1 through 3-8 for $\Delta h = 0$.

The lobing pattern is less pronounced for rough surfaces because the surface reflection coefficient ρ_s approaches zero as Δh becomes increasingly large. The surface reflection coefficient ρ_s is given by (reference 40)

$$\rho_s = \begin{cases} \exp(-g/2), & \text{normally-distributed surface height random variable} \\ \exp(-g^{1/2}/2), & \text{Longley-Rice and Johnson-Gierhart semi-empirical formula} \end{cases} \tag{3.1}$$

where

$g^{1/2}$ = surface roughness Rayleigh parameter $= (2\pi/\lambda)(2\sin\psi)\sigma_H$

ψ = grazing angle of specular ray

σ_H = standard deviation of the surface height random variable H with respect to the mean surface level

The surface height standard deviation σ_H is related to the interdecile terrain roughness Δh in the Longley-Rice and Johnson-Gierhart programs by [24]

$$\sigma_H = \begin{cases} 0.39\,\Delta h, & \Delta h \le 12\,\text{ft} \\ 0.78\,\Delta h \exp\left[-0.5\,(\Delta h)^{1/4}\right], & \Delta h > 12\ \text{ft} \end{cases} \tag{3.2}$$

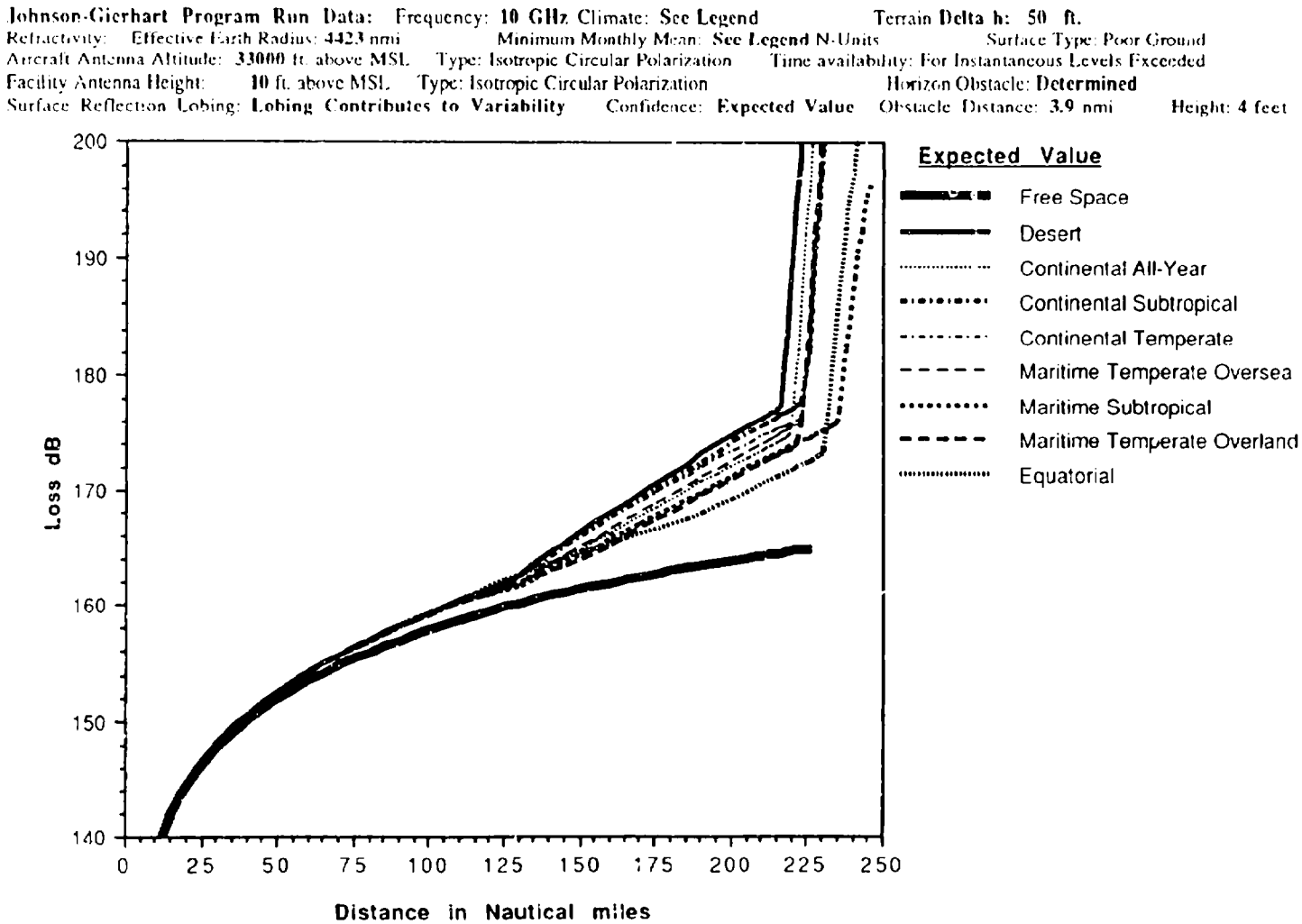

Figure 3-17. Comparison of Expected Values of Basic Transmission Loss for Various Climates; Terrain Roughness Δh = 50 ft, Lobing Contributes to Variability

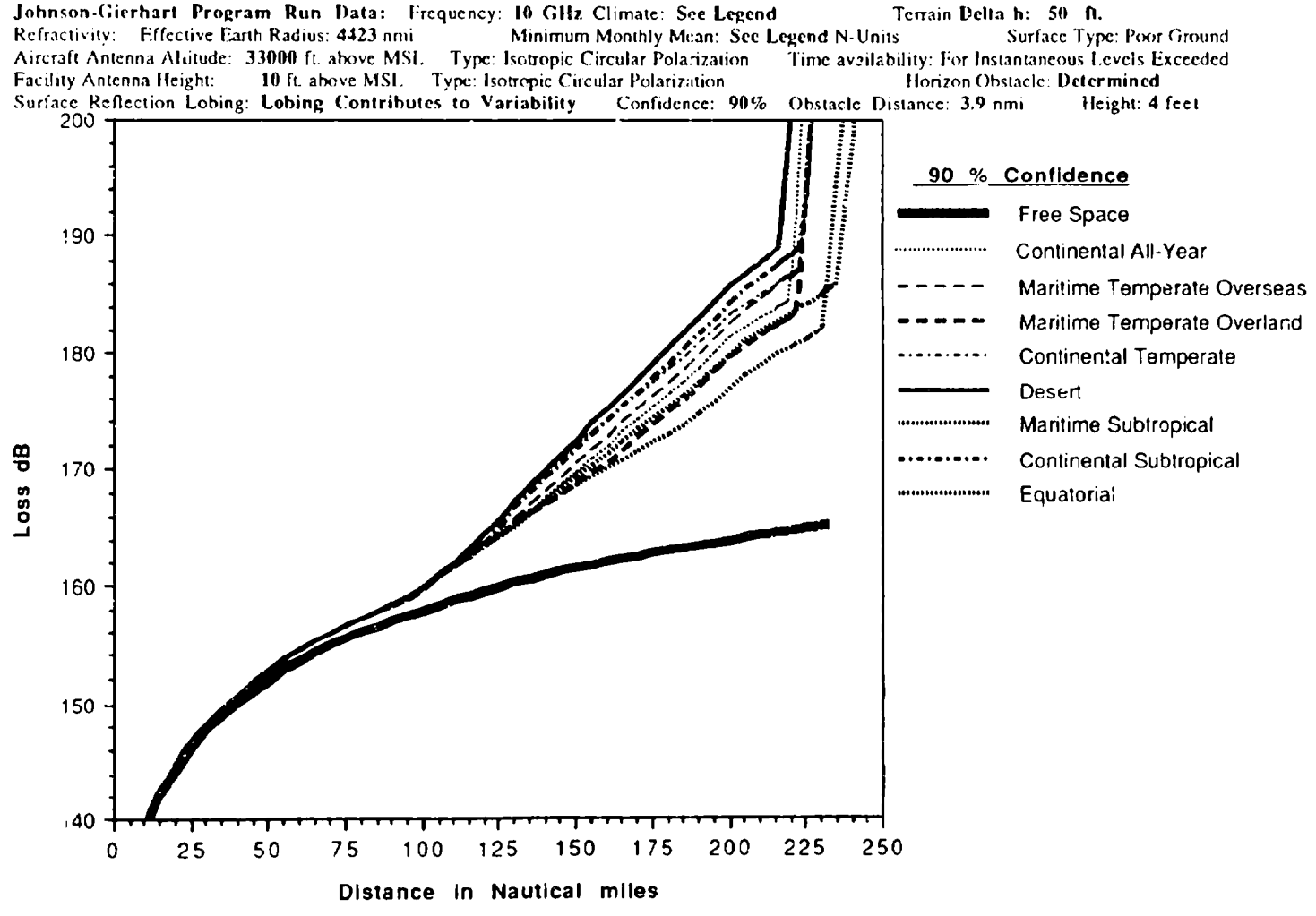

Figure 3-18. Comparison of 90 Percent Confidence Levels of Basic Transmission Loss for Various Climates; Terrain Roughness Δh = 50 ft, Lobing Contributes to Variability

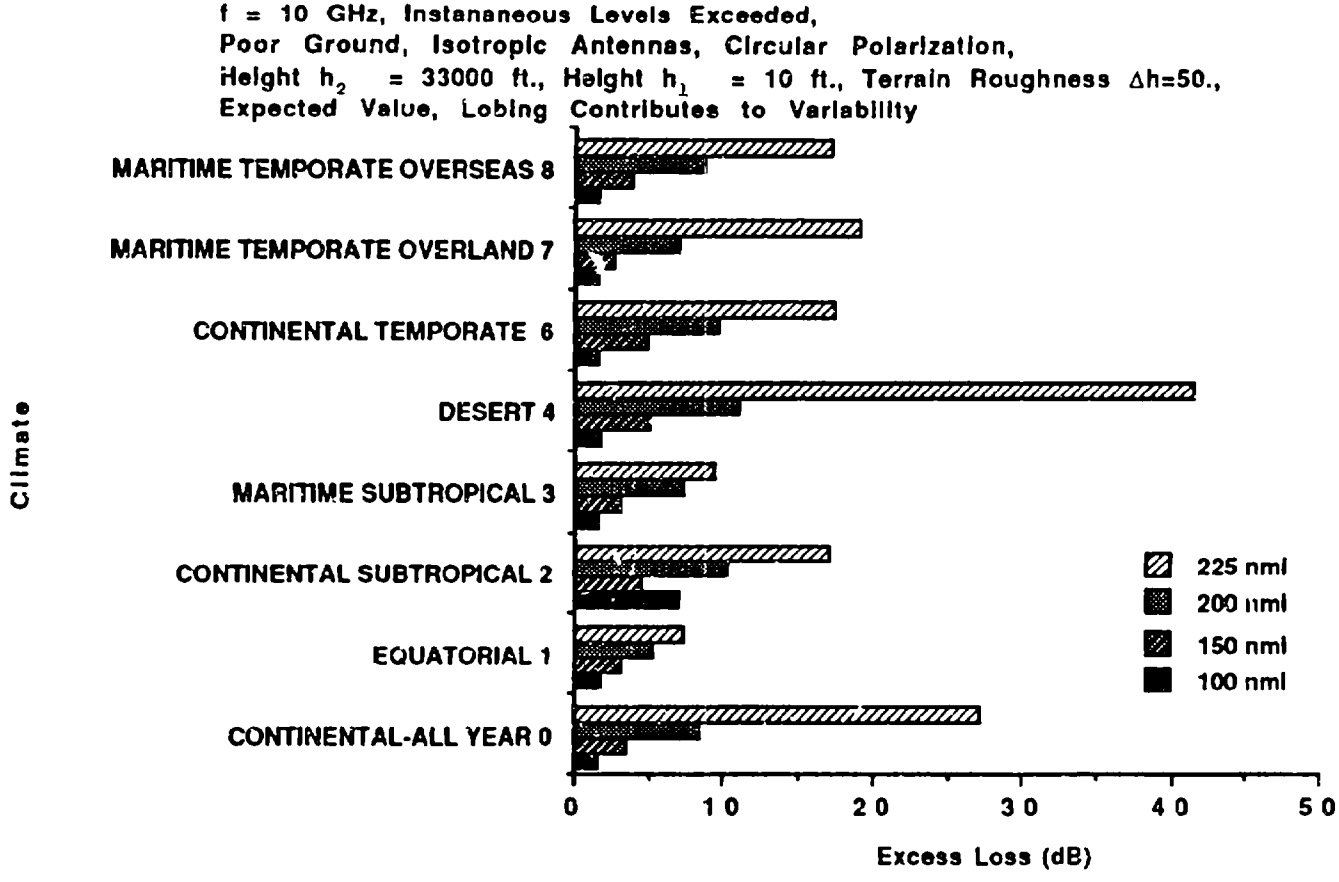

Figure 3-19. Comparison of Expected Values of Excess Propagation Loss for Various Climates; Terrain Roughness Δh = 50 ft, Lobing Contributes to Variability

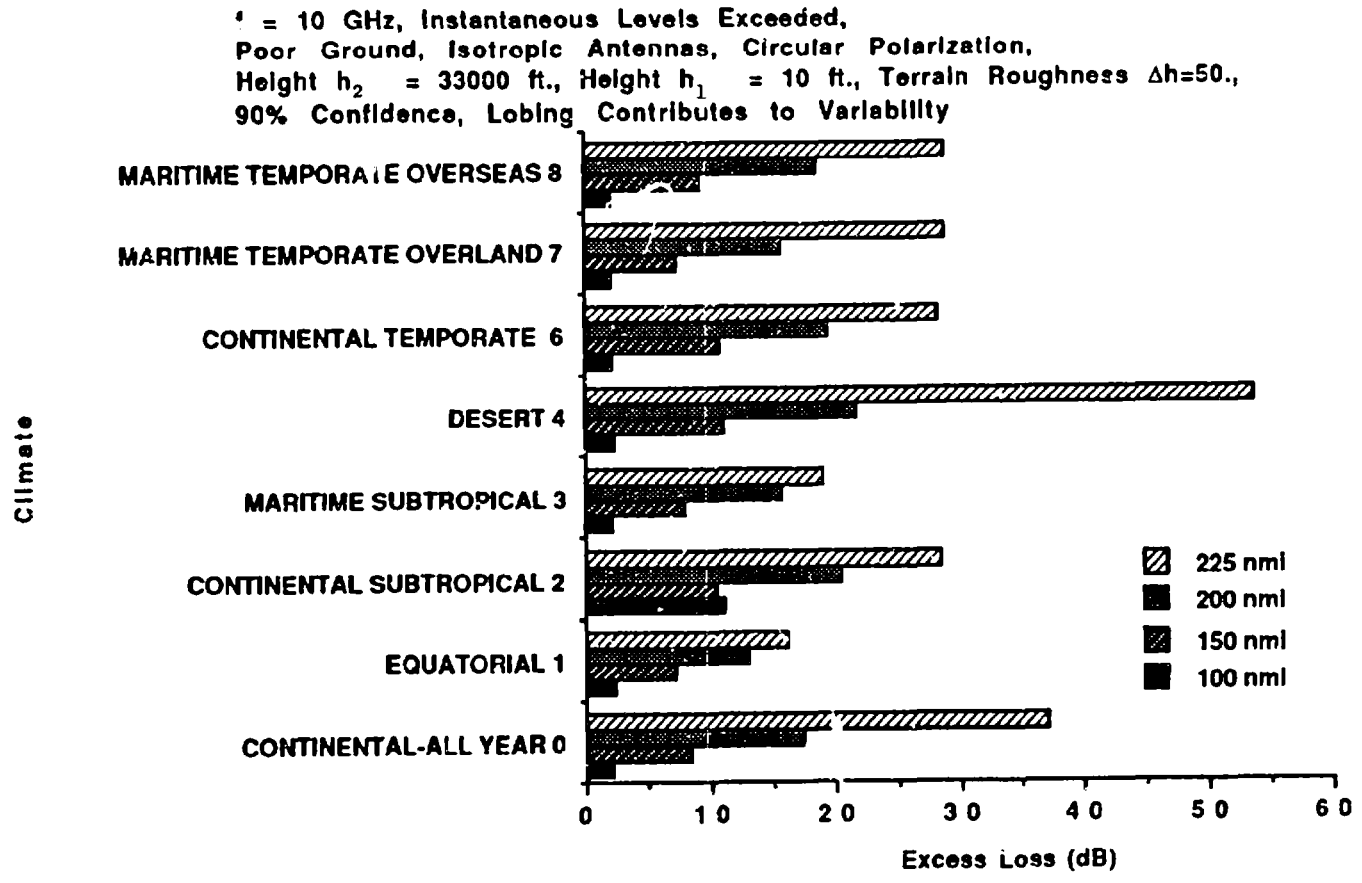

Figure 3-20. Comparison of 90 Percent Confidence Levels of Basic Transmission Loss for Various Climates; Terrain Roughness Δh = 50 ft, Lobing Contributes to Variability

The lobing pattern predicted by the Johnson-Gierhart program for slightly rough surfaces is probably less pronounced than actual patterns because the semi-empirical formula for the surface reflection coefficient ρ_s (see equation 3-1) does not have zero slope at $g^{1/2} = 0$ [40]. Propagation paths over slightly rolling plains or rough Earth ($\Delta h \leq 15$ ft) have lobing patterns that are much less distinct than for the same paths over water or over very smooth plains but perhaps more distinct than that predicted by the Johnson-Gierhart program.

3.2 OBSTRUCTED PATH RUNS

Single knife-edge diffraction becomes an increasingly dominant mode of propagation with increasing obstruction of the propagation path. In the Johnson-Gierhart program, the height and location of the limiting knife-edge is determined by the terrain roughness and any site-specified obstacle. The site-specified obstacle might be vegetation, a building, or a terrain ridge. Quantitative results of the effect of path obstructions on basic transmission loss are presented in this subsection. The computer printouts of basic transmission loss for all of the obstructed path runs are presented in appendix E of volume 2. All of the obstructed path runs were performed for poor ground, circular polarization, isotropic antennas, and a desert climate.

The obstructed path runs are for a ground antenna at a height $h_1 = 20$ ft with the exception of two runs for which $h_1 = 3$ ft. The runs, at frequencies of 2, 5, 10, and 15 GHz, are for aircraft antenna altitudes $h_2 = 22{,}000$ ft, 33,000 ft, and 66,000 ft.

The expected values and 90 percent confidence levels of basic transmission loss for the obstructed path runs with the surface reflection lobing option "determines median level" are summarized in tables 3-5 and 3-6, respectively. In case d (the case with the smallest grazing angle of incidence), the expected value and 90 percent confidence level of excess propagation loss exceed those for $\Delta h = 0$ by more than 10 dB and 15 dB, respectively; for $\Delta h = 50$ ft and by more than 20 dB and 30 dB, respectively; for $\Delta h = 50$ ft with a 50-ft obstacle. In cases a, b, c, e, and f (corresponding to larger grazing angles of incidence), the excess propagation loss is not increased significantly by diffraction in the obstructed path. Similar results are obtained with the lobing option "contributes to variability" (see tables 3-7 and 3-8).

Table 3-5. Expected Values of Transmission Loss for Various Obstructions, Lobing Determines Median

Case	Aircraft Antenna Height feet	Ground Antenna Height feet	Distance nmi	Frequency GHz	BASIC TRANSMISSION LOSS, $L_b(d)$ AND EXCESS PROPAGATION LOSS, A(d)									
					Free Space L_{bf} (dB)	Basic $\langle L_b \rangle$ (dB)	Excess $\langle A \rangle$ (dB)	Basic $\langle L_b \rangle$ (dB)	Excess $\langle A \rangle$ (dB)	Basic $\langle L_b \rangle$ (dB)	Excess $\langle A \rangle$ (dB)	Basic $\langle L_b \rangle$ (dB)	Excess $\langle A \rangle$ (dB)	Basic $\langle L_b \rangle$ (dB)	Excess $\langle A \rangle$ (dB)
						Δhs 0 ft. Determines Obstacle		Δhs 50 ft. Determines Obstacle		Δhs 50 ft. 50 ft. Obstacle at 0.6 nmi		Δhs 150 ft. Determines Obstacle		Δhs 250 ft. Determines Obstacle	
a	22000	20	75	5	142.4	147.8	-1.6	150.4	1.0	150.4	1.0				
				10	155.4	157.8	2.4	158.9	1.5	158.9	1.5				
				15	158.9	162.1	3.2	161.2	2.3	161.2	2.3				
b	22000	20	125	5	153.8	155.6	1.8	156.5	2.7	156.5	2.7				
				10	159.8	159.9	0.1	163.4	3.6	163.4	3.6				
				15	163.3	162.5	-0.8	168.3	5.0	168.3	5.0				
c	33000	20	125	2	145.8	144.0	-1.8	147.3	1.5	147.3	1.5				
				5	153.8	150.1	-3.7	155.7	1.9	155.7	1.9				
				10	159.8	162.7	2.9	161.9	2.1	161.9	2.1	162.0	2.2	162.0	2.2
				15	163.3	167.2	3.9	166.5	3.2	166.5	3.2				
	33000	3	125	2	145.9	142.6	-3.3	147.4	1.5						
d	33000	20	200	2	149.9	149.1	-0.8	159.3	9.4	171.7	21.8				
				5	157.8	158.4	0.6	161.5	3.7	177.6	19.9				
				10	163.8	163.6	-0.2	159.1	5.3	185.7	21.9	169.4	5.6	180.0	16.2
				15	167.4	171.8	4.4	174.8	7.4	192.5	25.1				
	33000	3	200	2	149.9	162.8	12.9	157.0	7.1						
e	66000	20	125	10	159.8	161.6	1.8	160.7	0.9	160.7	0.9				
f	66000	20	200	10	163.9	167.6	3.7	166.8	2.9	166.8	2.9				

Surface Lobing Determines Median, Excess Loss = Expected Value - Free Space,
Desert Climate, Poor Ground, Isotropic Antennas, Circular Polarization

Table 3-6. 90 Percent Confidence Levels of Transmission Loss for Various Obstructions, Lobing Determines Median

Case	Aircraft Antenna Height feet	Ground Antenna Height feet	Distance nmi	Frequency GHz	Free Space L_{bf} (dB)	Basic L_b Δhx 0 ft. Determines (dB)	Excess A Obstacle (dB)	Basic L_b Δhx 50 ft. Determines (dB)	Excess A Obstacle (dB)	Basic L_b 50 ft. at (dB)	Excess A 50 ft. Obstacle 0.8 nmi (dB)	Basic L_b Δhx 150 ft. Determines (dB)	Excess A Obstacle (dB)	Basic L_b Δhx 250 ft. Determines (dB)	Excess A Obstacle (dB)
a	22000	20	75	5	149.4	148.1	-1.3	150.7	1.3	150.4	1.0				
				10	155.4	164.1	8.7	157.7	2.3	157.7	2.3				
				15	158.9	168.4	9.5	162.8	3.9	162.8	3.9				
b	22000	20	125	5	153.8	161.8	7.8	161.5	7.7	161.7	7.9				
				10	159.8	166.4	6.6	169.1	9.5	169.3	9.5				
				15	163.3	169.1	5.8	175.0	11.7	175.0	11.7				
c	33000	20	125	2	145.8	146.7	0.9	149.4	3.6	149.4	3.6				
				5	153.8	152.7	-1.1	158.2	4.4	158.2	4.4				
				10	159.8	169.8	10.0	165.7	5.9	165.7	5.9	165.7	5.9	165.7	5.9
				15	163.3	174.4	11.1	170.6	7.3	170.6	7.3				
	33000	3	125	2	145.9	145.1	-0.8	149.6	3.7						
d	33000	20	200	2	149.9	156.5	6.6	159.3	9.4	180.7	30.8				
				5	157.8	167.0	9.2	170.0	12.2	187.1	29.3				
				10	163.8	173.0	9.2	178.5	14.7	195.8	32.0	178.8	15.0	190.4	26.6
				15	167.4	182.8	15.4	184.9	17.5	203.1	35.7				
	33000	3	200	2	149.9	172.0	22.1	166.8	16.9						
e	66000	20	125	10	159.8	167.7	7.9	160.9	1.1	160.9	1.1				
f	66000	20	200	10	163.9	175.1	11.2	171.3	7.4	171.3	7.4				

BASIC TRANSMISSION LOSS, $L_b(90,d)$ AND EXCESS PROPAGATION LOSS, $A(90,d)$

Surface Lobing Determines Median, Excess Loss =90 Per Cent Confidence Level - Free Space,
Desert Climate, Poor Ground, Isotropic Antennas, Circular Polarization

Table 3-7. Expected Values of Transmission Loss for Various Obstructions, Lobing Contributes to Variability

Case	Aircraft Antenna Height feet	Ground Antenna Height feet	Distance nmi	Frequency GHz	BASIC TRANSMISSION LOSS, $L_b(d)$ AND EXCESS PROPAGATION LOSS, $A(d)$									
					Free Space L_{bf} (dB)	Basic $\langle L_b \rangle$ Δhs 0 ft. Determines (dB)	Excess $\langle A \rangle$ Obstacle (dB)	Basic $\langle L_b \rangle$ Δhs 50 ft. Determines (dB)	Excess $\langle A \rangle$ Obstacle (dB)	Basic $\langle L_b \rangle$ 50 ft. at (dB)	Excess $\langle A \rangle$ Δhs 50 ft. Obstacle 0.6 nmi (dB)	Basic $\langle L_b \rangle$ Δhs Determines (dB)	Excess $\langle A \rangle$ 150 ft. Obstacle (dB)	Basic $\langle L_b \rangle$ Δhs Determines (dB)	Excess $\langle A \rangle$ 250 ft. Obstacle (dB)
a	22000	20	75	2	149.4	151.2	1.8	150.3	0.9	150.3	0.9				
				5	155.4	157.8	2.4	156.9	1.5	156.9	1.5				
				10	158.9	162.1	3.2	161.2	2.3	161.2	2.3				
				15											
b	22000	20	125	2	153.8	158.4	4.6	157.8	4.0	157.8	4.0				
				5	159.3	165.8	5.8	165.2	5.4	165.2	5.4				
				10	163.3	170.8	7.5	170.4	7.1	170.4	7.1				
				15											
c	33000	20	125	2	145.8	147.6	1.8	146.8	1.0	146.8	1.0				
				5	153.8	155.2	1.4	155.1	1.3	155.1	1.3				
				10	159.5	162.7	2.9	161.2	1.4	161.9	2.1	162.0	2.2	162.0	2.2
				15	163.9	167.2	3.3	166.5	2.6	166.5	2.6				
	33000	3	125	2	145.9	147.2	1.3	146.7	0.8						
d	33000	20	200	2	149.9	157.7	7.8	157.7	7.8	171.6	21.3				
				5	157.9	177.6	19.7	166.8	8.9	177.6	19.7				
				10	163.8	174.7	10.9	174.7	10.9	165.7	21.9	174.7	10.9	179.9	16.1
				15	167.4	180.8	13.4	180.8	13.4	192.6	25.2				
	33000	3	200	2	149.9	162.8	12.9	157.8	7.1						
e	66000	20	125	10	159.8	161.2	1.4	160.7	0.9	160.7	0.9				
f	66000	20	200	10	163.9	167.6	3.7	166.8	2.9	166.8	2.9				

Surface Lobing Contributes to Variability, Excess Loss = Expected Value - Free Space
Desert Climate, Poor Ground, Isotropic Antennas, Circular Polarization

Table 3-8. 90 Percent Confidence Levels of Transmission Loss for Various Obstructions, Lobing Contributes to Variability

Case	Aircraft Antenna Height feet	Ground Antenna Height feet	Distance nmi	Frequency GHz	Free Space L_{bf} (dB)	Basic L_b Δhs 0 ft. Determines Obstacle (dB)	Excess A Δhs 0 ft. Obstacle (dB)	Basic L_b Δhs 50 ft. Determines Obstacle (dB)	Excess A Δhs 50 ft. Obstacle (dB)	Basic L_b Δhs 50 ft. at 0.6 nmi (dB)	Excess A 50 ft. Obstacle at 0.6 nmi (dB)	Basic L_b Δhs 150 ft. Determines Obstacle (dB)	Excess A 150 ft. Obstacle (dB)	Basic L_b Δhs 250 ft. Determines Obstacle (dB)	Excess A 250 ft. Obstacle (dB)
a	22000	20	75	3	149.4	157.5	8.1	150.7	1.3	150.7	1.3				
				10	155.4	164.1	8.7	157.7	2.3	157.7	2.3				
				15	158.9	168.4	9.5	162.8	3.9	162.8	3.9				
b	22000	20	125	5	153.8	166.5	12.7	163.8	10.0	163.8	10.0				
				10	159.6	173.8	14.0	171.6	12.0	171.8	12.0				
				15	163.3	179.1	15.8	177.4	14.1	177.4	14.1				
c	33000	20	125	2	145.8	154.7	8.9	149.5	3.7	149.5	3.7				
				5	153.8	158.2	4.4	158.2	4.4	158.2	4.4				
				10	159.5	169.6	10.0	165.6	5.8	165.7	5.9	165.7	5.9	165.7	5.9
				15	163.4	174.4	11.0	170.6	8.4	170.8	7.2				
	33000	3	125	2	140.9	152.3	2.4	149.6	-0.3						
d	33000	20	200	2	149.9	158.5	8.6	167.4	17.5	180.7	30.8				
				5	157.8	187.6	29.8	178.9	19.1	187.1	29.3				
				10	163.9	185.6	21.7	169.8	5.9	195.8	31.9	185.6	21.7	190.3	26.4
				15	167.4	191.8	24.4	191.5	24.4	203.1	35.7				
	33000	3	200	2	149.9	172.0	22.1	167.7	17.8						
e	66000	20	125	10	159.8	167.7	7.9	160.9	1.1	160.9	1.1				
f	66000	20	200	10	163.9	175.1	11.2	171.3	7.4	171.3	7.4				

BASIC TRANSMISSION LOSS, $L_b(90,d)$ AND EXCESS PROPAGATION LOSS, A(90,d)

Surface Lobing Contributes to Variability, 90 Per Cent Confidence Level = Expected Value - Free Space, Desert Climate, Poor Ground, Isotropic Antennas, Circular Polarization

The basic transmission loss for h_2 = 22,000 ft and h_1 = 20 ft and various obstructed paths is plotted as a function of the distance d at a frequency of 5 GHz in figures 3-21 through 3-24; at 10 GHz in figures 3-25 through 3-28; and at 15 GHz in figures 3-29 through 3-32. The most distinctive feature of these figures is the reduction of the lobing pattern with increasing obstruction of the p agation path. For example, in figure 3-21 for Δh = 0 ft, the lobing pattern is pronounced; in figure 3-22 for Δh = 50 ft, only the lobe adjacent to the horizon is still evident; and in figure 3-24 for Δh = 50 ft with a 50-ft obstruction, no lobes are evident.

Similar trends are obtained for the following:

1. 2 GHz, h_2 = 33,000 ft, h_1 = 20 ft (see figures 3-33 through 3-36)
2. 2 GHz, h_2 = 33,000 ft, h_1 = 3 ft (see figures 3-37 and 3-38)
3. 5 GHz, h_2 = 33,000 ft, h_1 = 20 ft (see figures 3-39 through 3-42)
4. 10 GHz, h_2 = 33,000 ft, h_1 = 20 ft (see figures 3-43 through 3-48)
5. 15 GHz, h_2 = 33,000 ft, h_1 = 20 ft (see figures 3-49 through 3-52)
6. 10 GHZ, h_2 = 66,000 ft, h_1 = 20 ft (see figures 3-53 through 3-56)

A nearby site-specified obstacle (50-ft tall at a distance of 0.6 nmi from the ground antenna) with slightly rough terrain (interdecile height Δh = 50 ft) increases the excess propagation loss more than does slightly rough terrain alone. The site-specified obstacle reduces the distance to the radio horizon by approximately 30 nmi, whereas the slightly rough terrain has no such effect (compare figures 3-28 with 3-26, 3-32 with 3-30, 3-42 with 3-40, 3-46 with 3-44, and 3-52 with 3-50). A further increase in the terrain roughness (to Δh = 150 ft and 250 ft) also did not appreciably reduce the distance to the radio horizon (compare figures 3-44, 3-47, and 3-48).

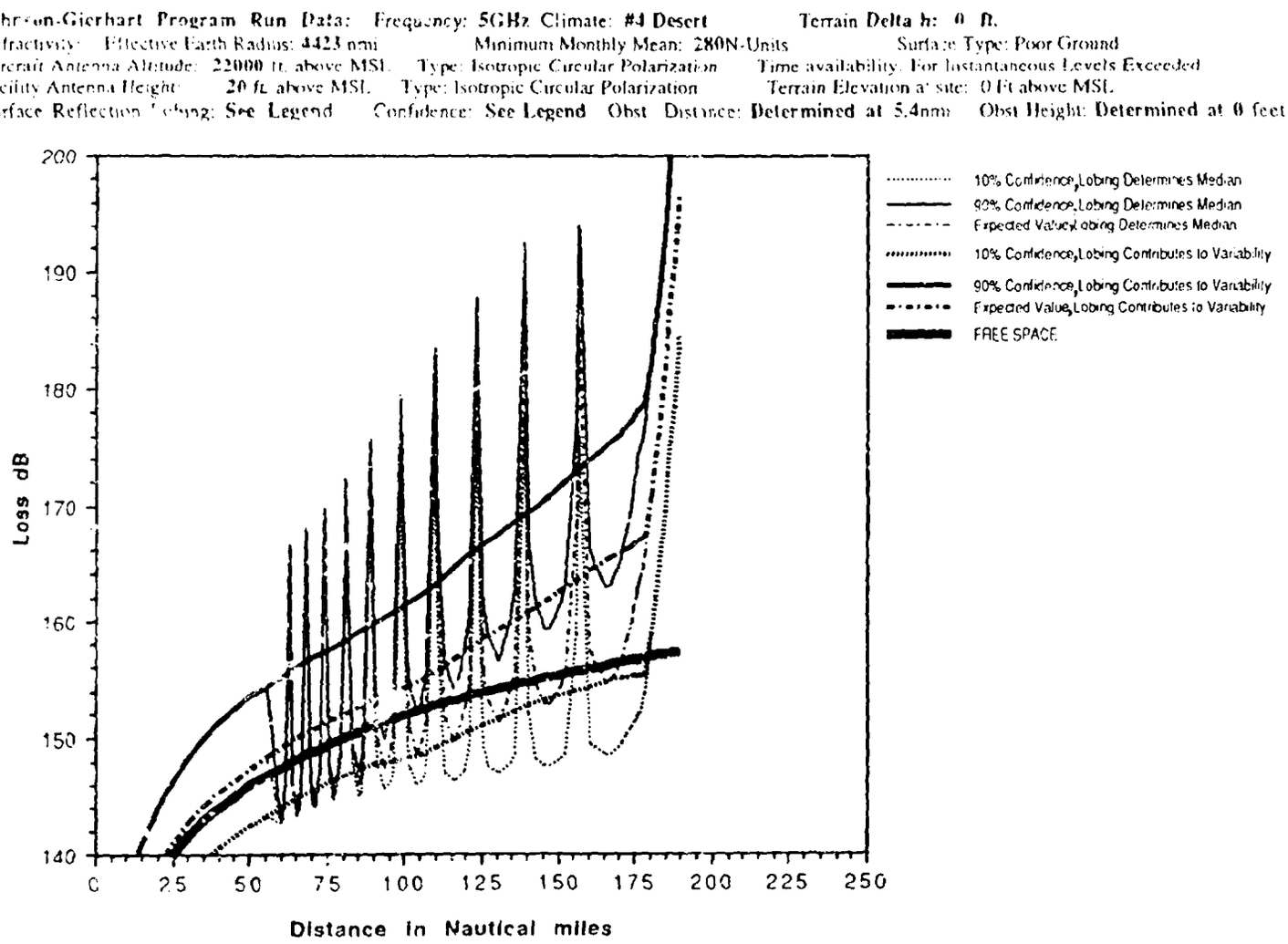

Figure 3-21. Basic Transmission Loss; Terrain Roughness Δh = 0, No Site-Specified Obstacle, 5 GHz, h2 = 22,000 ft, h1 = 20 ft

Johnson-Gierhart Program Run Data: Frequency: 5GHz Climate: #4 Desert Terrain Delta h: 50 ft.
Refractivity: Effective Earth Radius: 4423 nmi Maximum Monthly Mean: 280N-Units Surface Type: Poor Ground
Aircraft Antenna Altitude: 22000 ft. above MSL Type: Isotropic Circular Polarization Time availability: For Instantaneous Levels Exceeded
Facility Antenna Height: 20 ft. above MSL Type: Isotropic Circular Polarization Terrain Elevation at site: 0 Ft above MSL
Surface Reflection Lobing: See Legend Confidence: See Legend Obst Distance: Determined at 4.83 nmi Obst Height: Determined at 4 feet

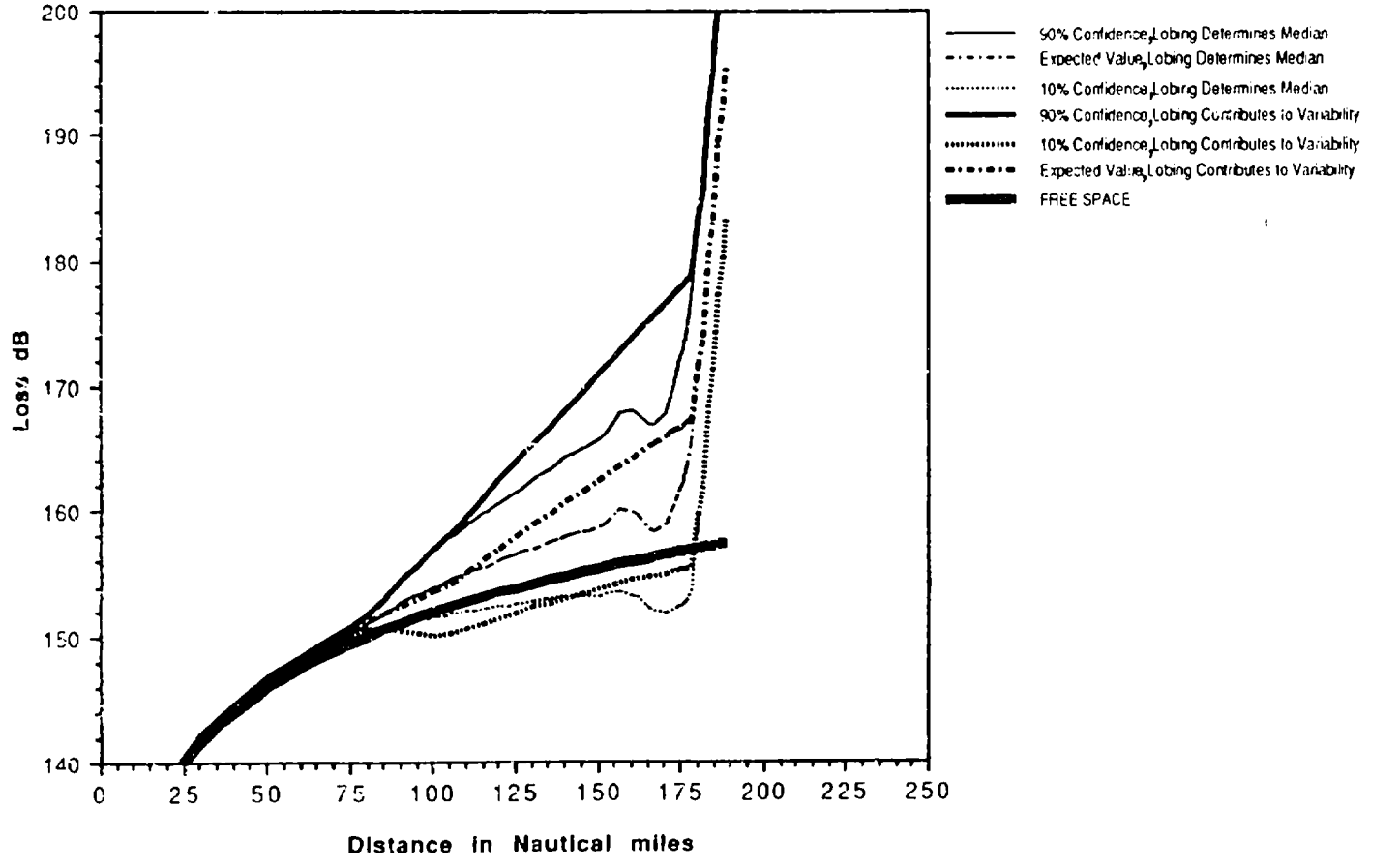

Figure 3-22. Basic Transmission Loss, Terrain Roughness Δh = 50 ft, No Site-Specified Obstacle, 5 GHz, h_2 = 22,000 ft, h_1 = 20 ft

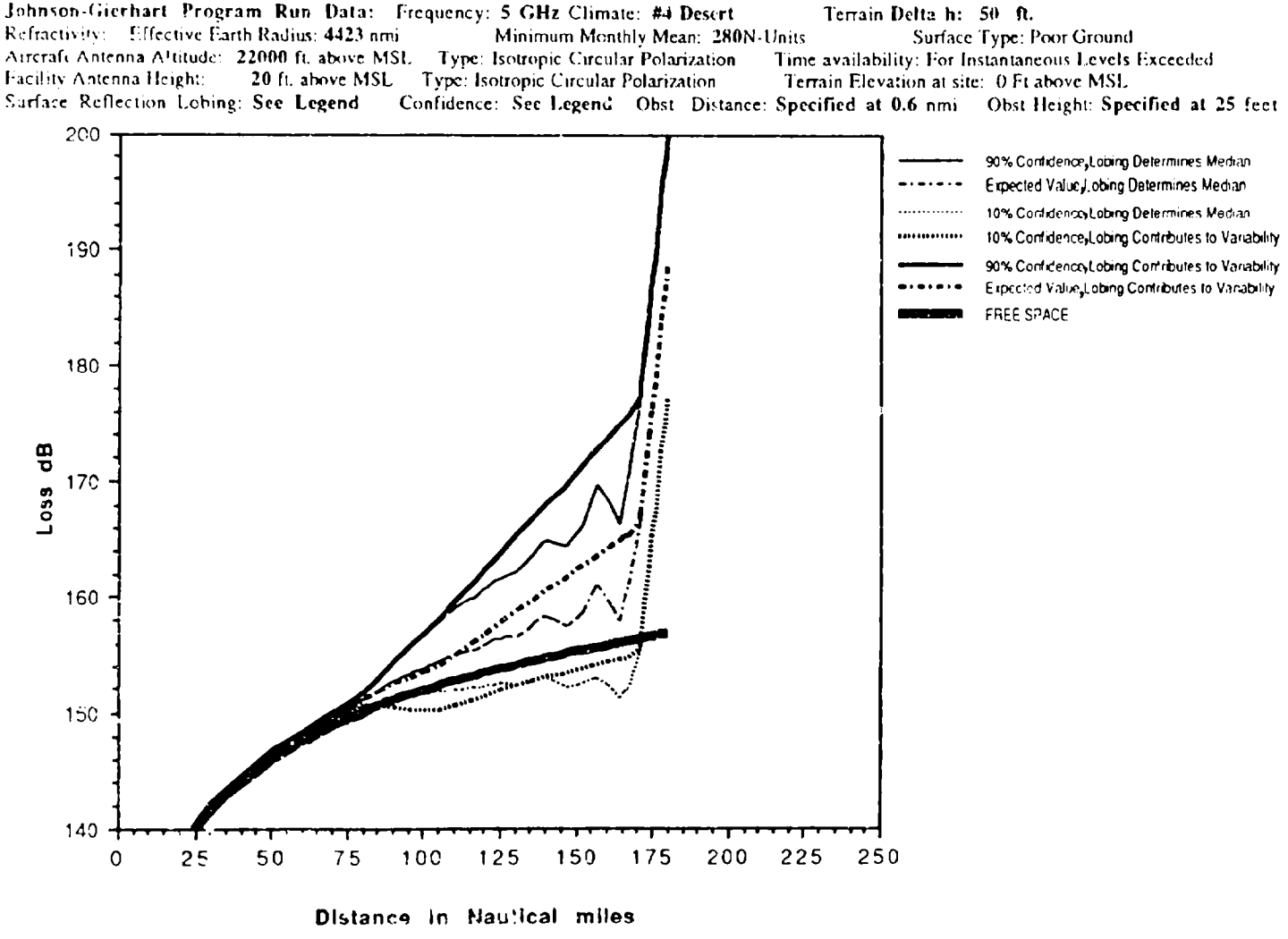

Figure 3-23. Basic Transmission Loss; Terrain Roughness Δh = 50 ft, 25-ft Obstacle, 5 GHz, h_2 = 22,000 ft, h_1 = 20 ft

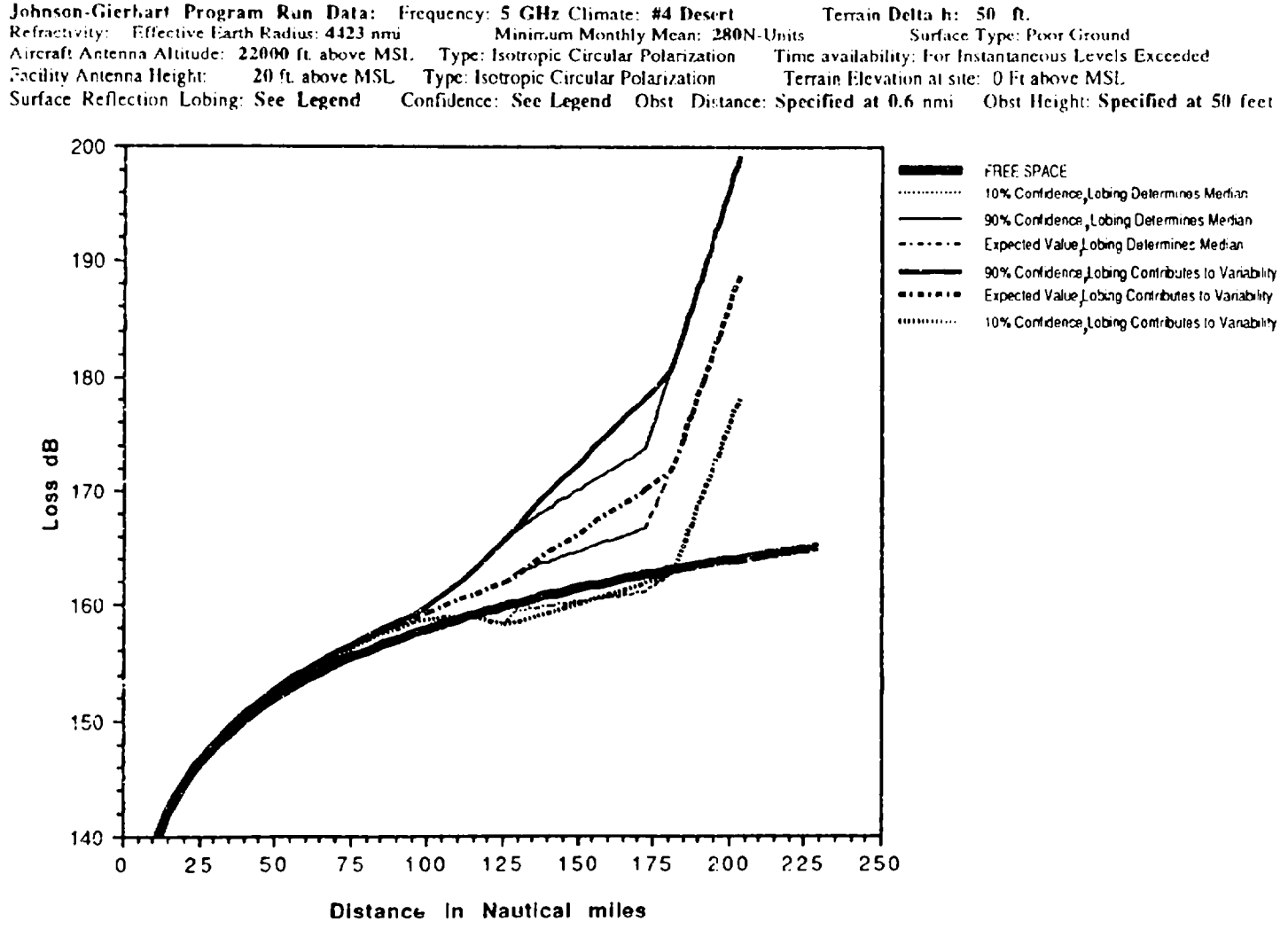

Figure 3-24. Basic Transmission Loss; Terrain Roughness Δh = 50 ft, 50-ft Obstacle 5 GHz, h_2 = 22,000 ft, h_1 = 20 ft

Johnson-Gierhart Program Run Data: Frequency: 10 GHz Climate: #4 Desert Terrain Delta h: 0 ft.
Refractivity: Effective Earth Radius: 4423 nmi Minimum Monthly Mean: 280N-Units Surface Type: Poor Ground
Aircraft Antenna Altitude: 22000 ft. above MSL Type: Isotropic Circular Polarization Time availability: For Instantaneous Levels Exceeded
Facility Antenna Height: 20 ft. above MSL Type: Isotropic Circular Polarization Terrain Elevation at site: 0 Ft above MSL
Surface Reflection Looing: See Legend Confidence: See Legend Obst Distance: Determined at 5.4 nmi Obst Height: Determined at 0 feet

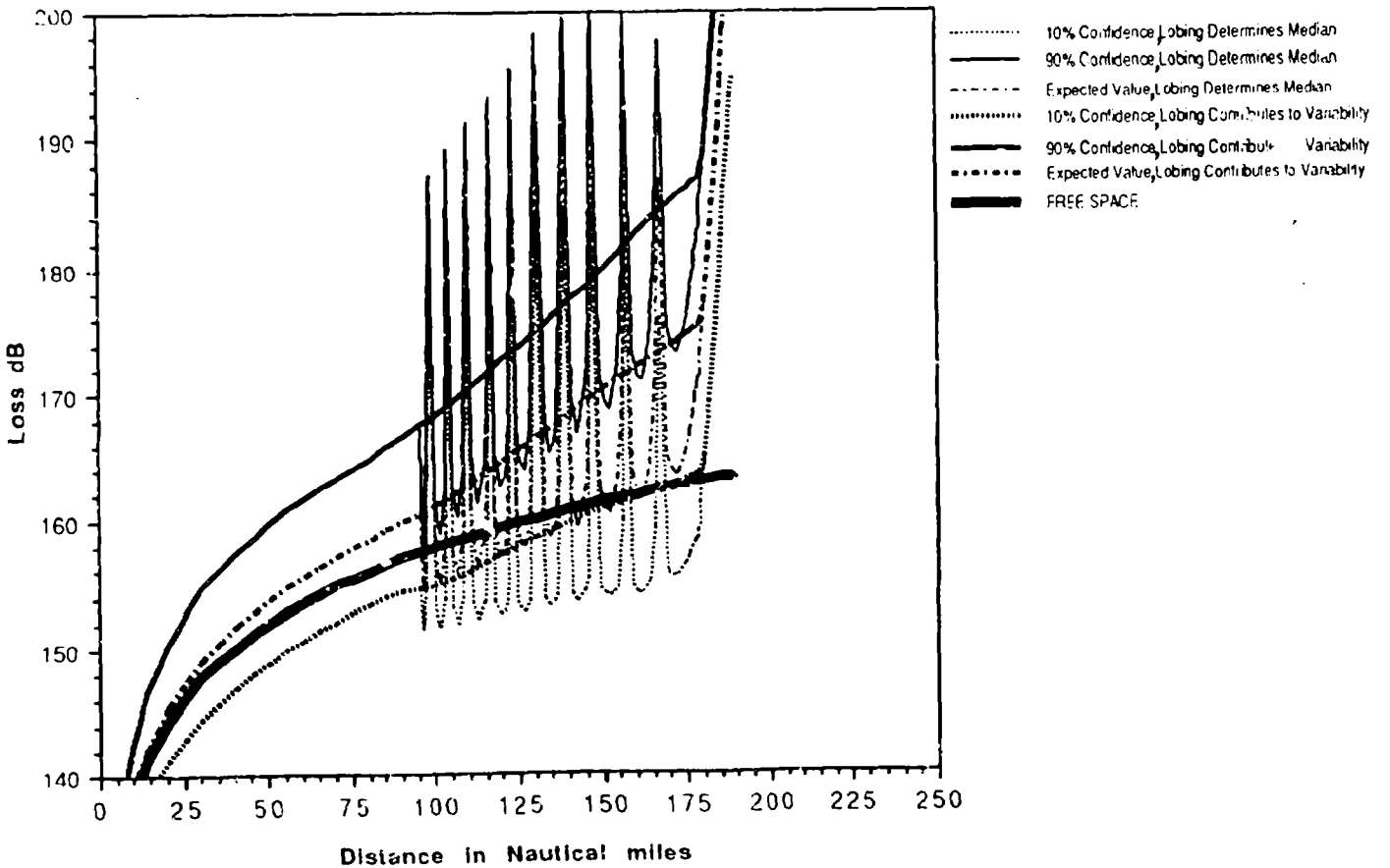

Figure 3-25. Basic Transmission Loss; Terrain Roughness Δh = 0, No Site-Specified Obstacle, 10 GHz, h_2 = 22,000 ft, h_1 = 20 ft

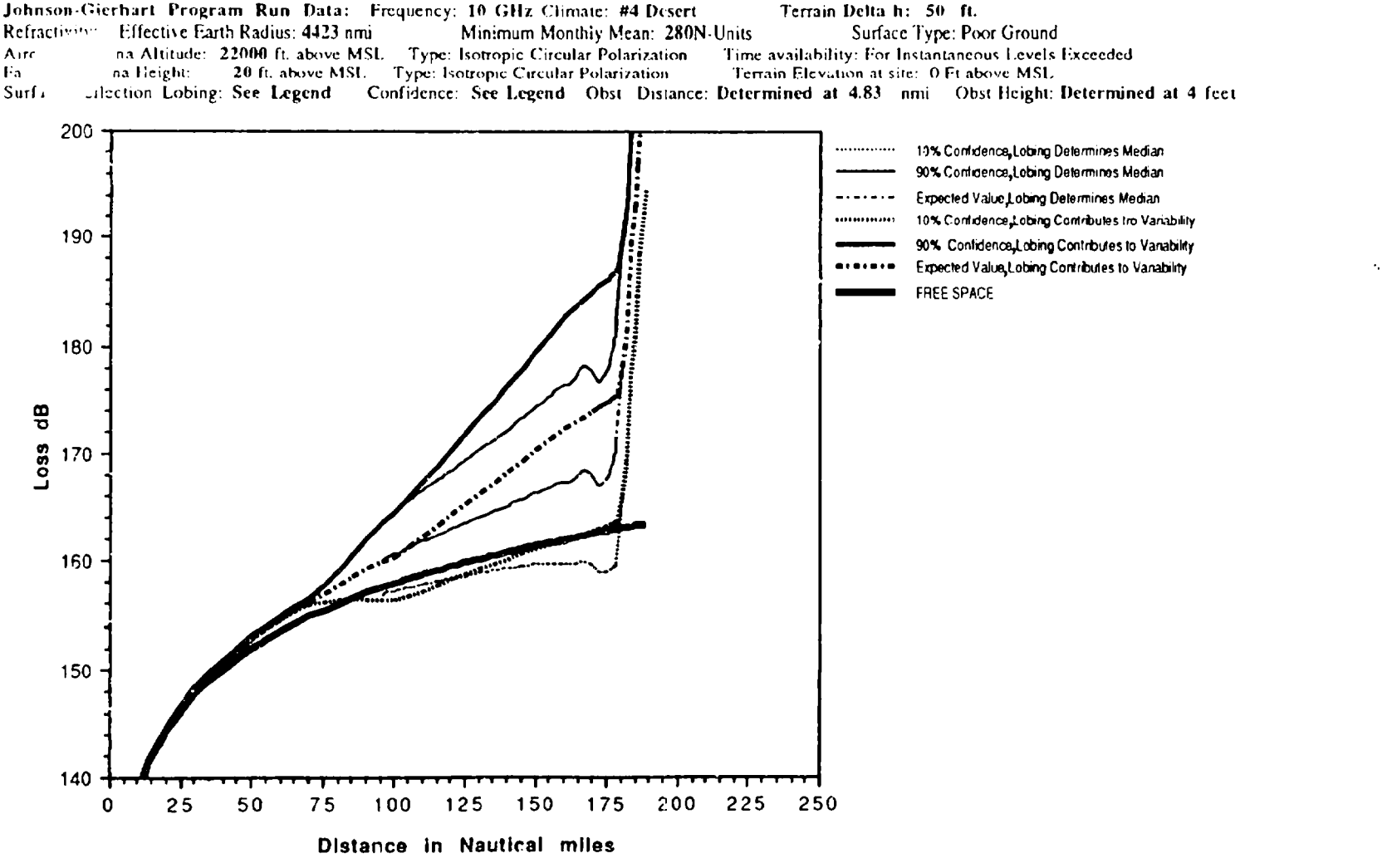

Figure 3-26. Basic Transmission Loss; Terrain Roughness Δh = 50 ft, No Site-Specified Obstacle, 10 GHz, h_2 = 22,000 ft, h_1 = 20 ft

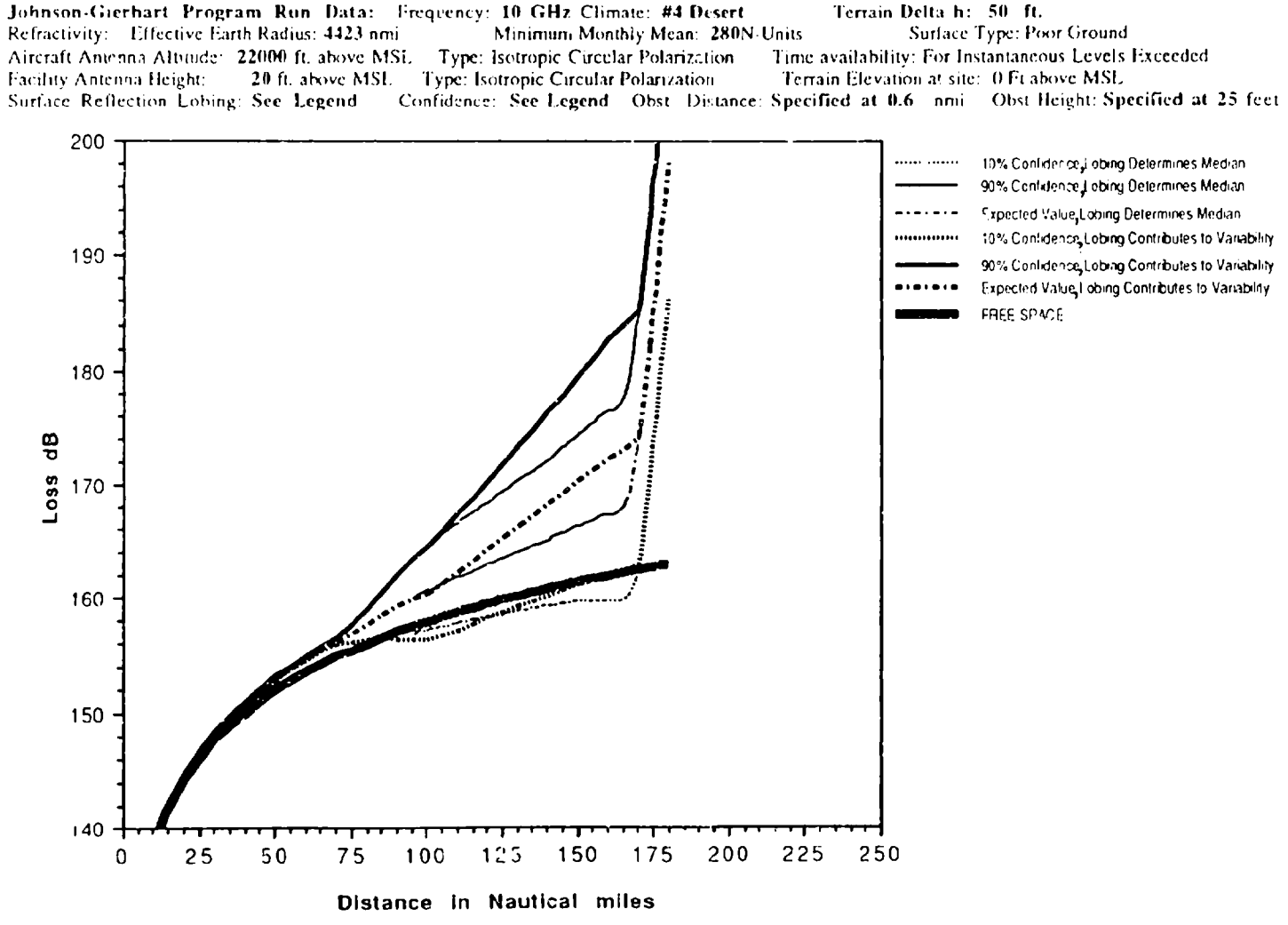

Figure 3-27. Basic Transmission Loss; Terrain Roughness Δh = 50 ft, 25-ft Obstacle, 10 GHz, h_2 = 22,000 ft, h_1 = 20 ft

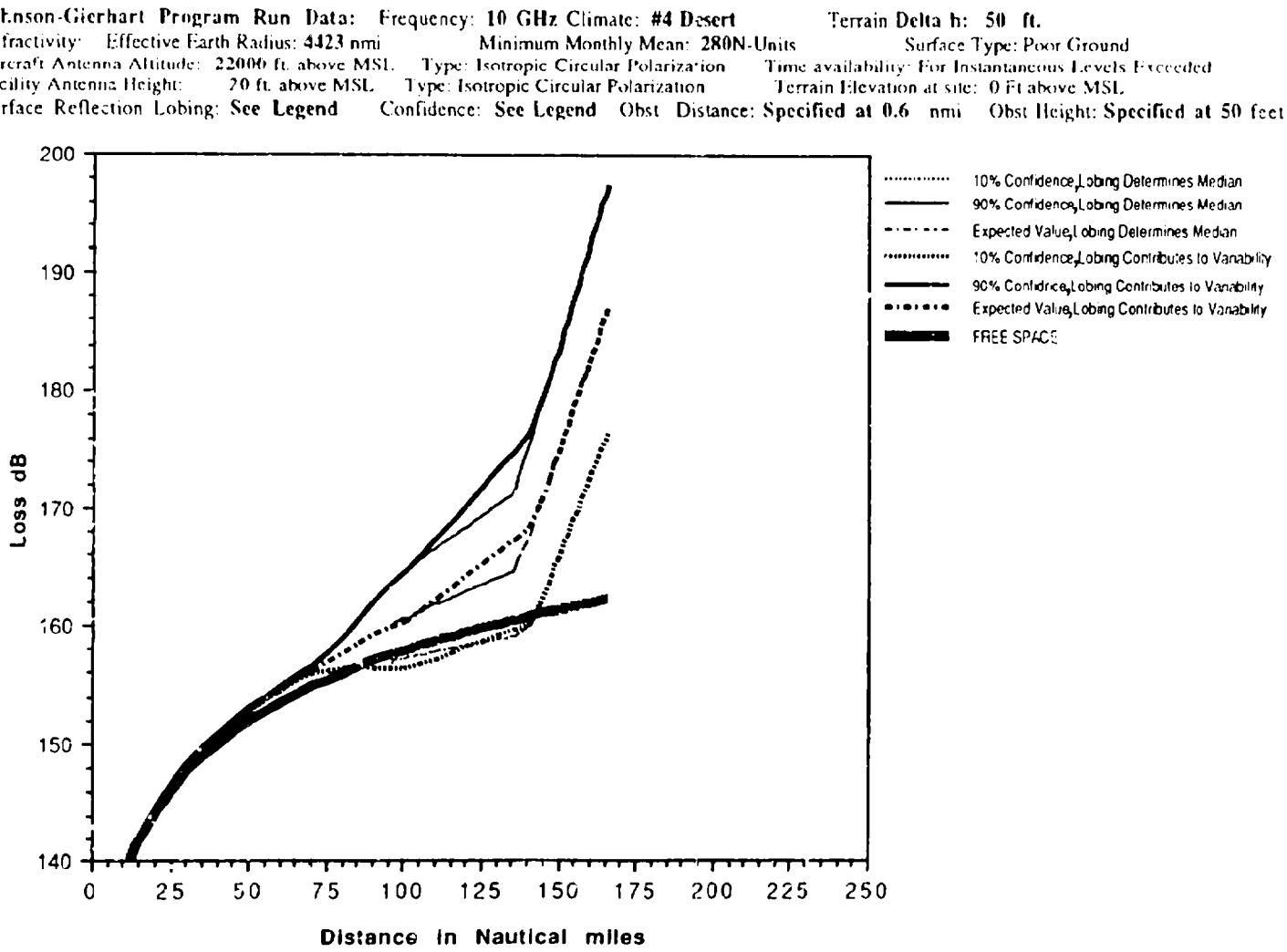

Figure 3-28. Basic Transmission Loss; Terrain Roughness Δh = 50 ft, 50-ft Obstacle, 10 GHz, h_2 = 22,000 ft, h_1 = 20 ft

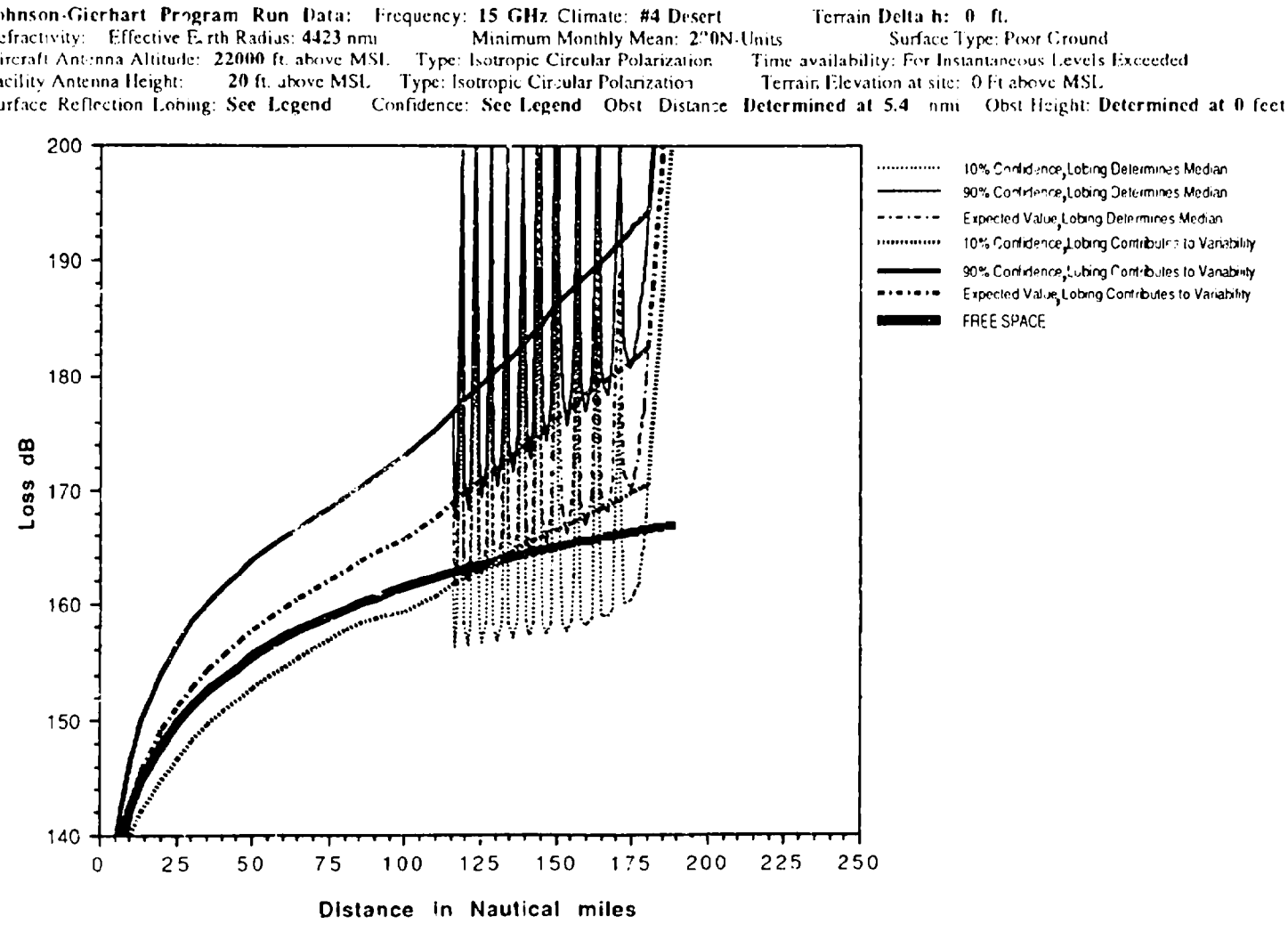

Figure 3-29. Basic Transmission Loss; Terrain Roughness Δh = 0, No Site-Specified Obstacle, 15 GHz, h_2 = 22,000 ft, h_1 = 20 ft

Johnson-Gierhart Program Run Data: Frequency: 15 GHz Climate: #4 Desert Terrain Delta h: 50 ft.
Refractivity: Effective Earth Radius: 4423 nmi Minimum Monthly Mean: 280N-Units Surface Type: Poor Ground
Aircraft Antenna Altitude: 22000 ft. above MSL Type: Isotropic Circular Polarization Time availability: For Instantaneous Levels Exceeded
Facility Antenna Height: 20 ft. above MSL Type: Isotropic Circular Polarization Terrain Elevation at site: 0 Ft above MSL
Surface Reflection Lobing: See Legend Confidence: See Legend Obst Distance: Determined at 4.83 nmi Obst Height: Determined at 4 feet

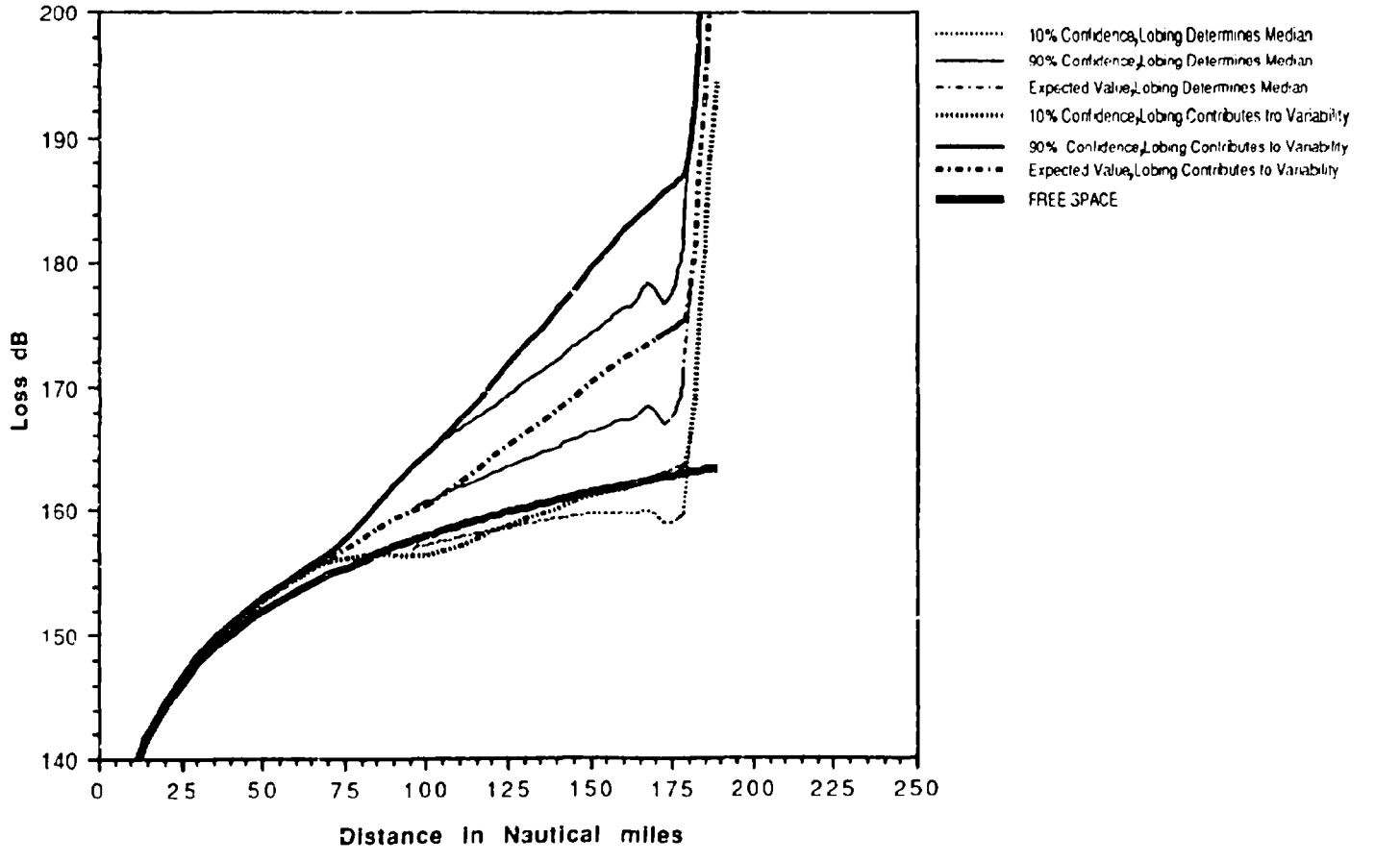

Figure 3-30. Basic Transmission Loss; Terrain Roughness Δh = 50 ft, No Site-Specified Obstacle, 15 GHz, h_2 = 22,000 ft, h_1 = 20 ft

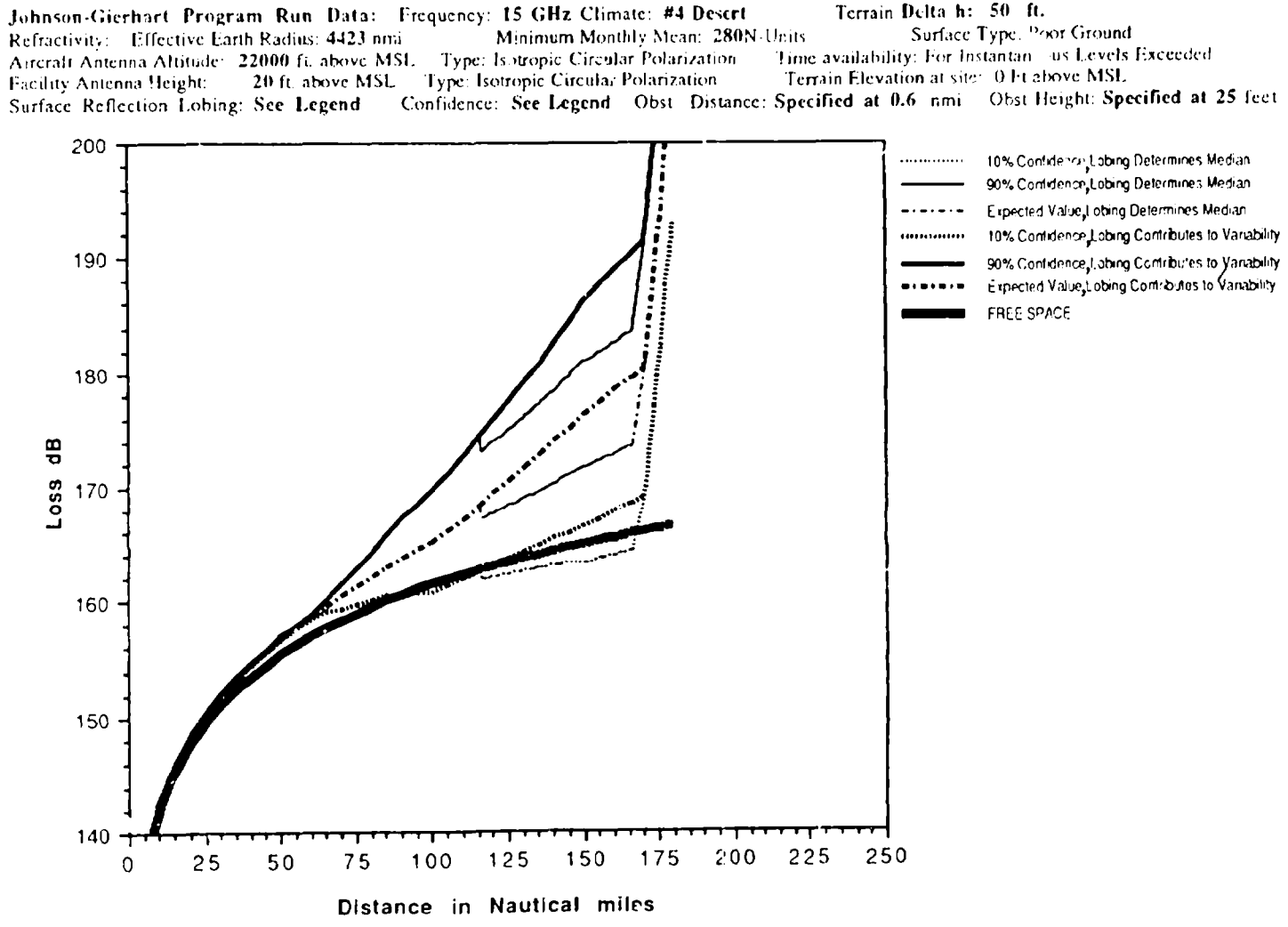

Figure 3-31. Basic Transmission Loss; Terrain Roughness Δh = 50 ft, 25-ft Obstacle, 15 GHz, h_2 = 22,000 ft, h_1 = 20 ft

Johnson-Gierhart Program Run Data: Frequency: 15 GHz Climate: #4 Desert Terrain Delta h: 50 ft.
Refractivity: Effective Earth Radius: 4423 nmi Minimum Monthly Mean: 280N-Units Surface Type: Poor Ground
Aircraft Antenna Altitude: 22000 ft. above MSL Type: Isotropic Circular Polarization Time availability: For Instantaneous Levels Exceeded
Facility Antenna Height: 20 ft. above MSL Type: Isotropic Circular Polarization Terrain Elevation at site: 0 Ft above MSL
Surface Reflection Lobing: See Legend Confidence: See Legend Obst Distance: Specified at 0.6 nmi Obst Height: Specified at 50 feet

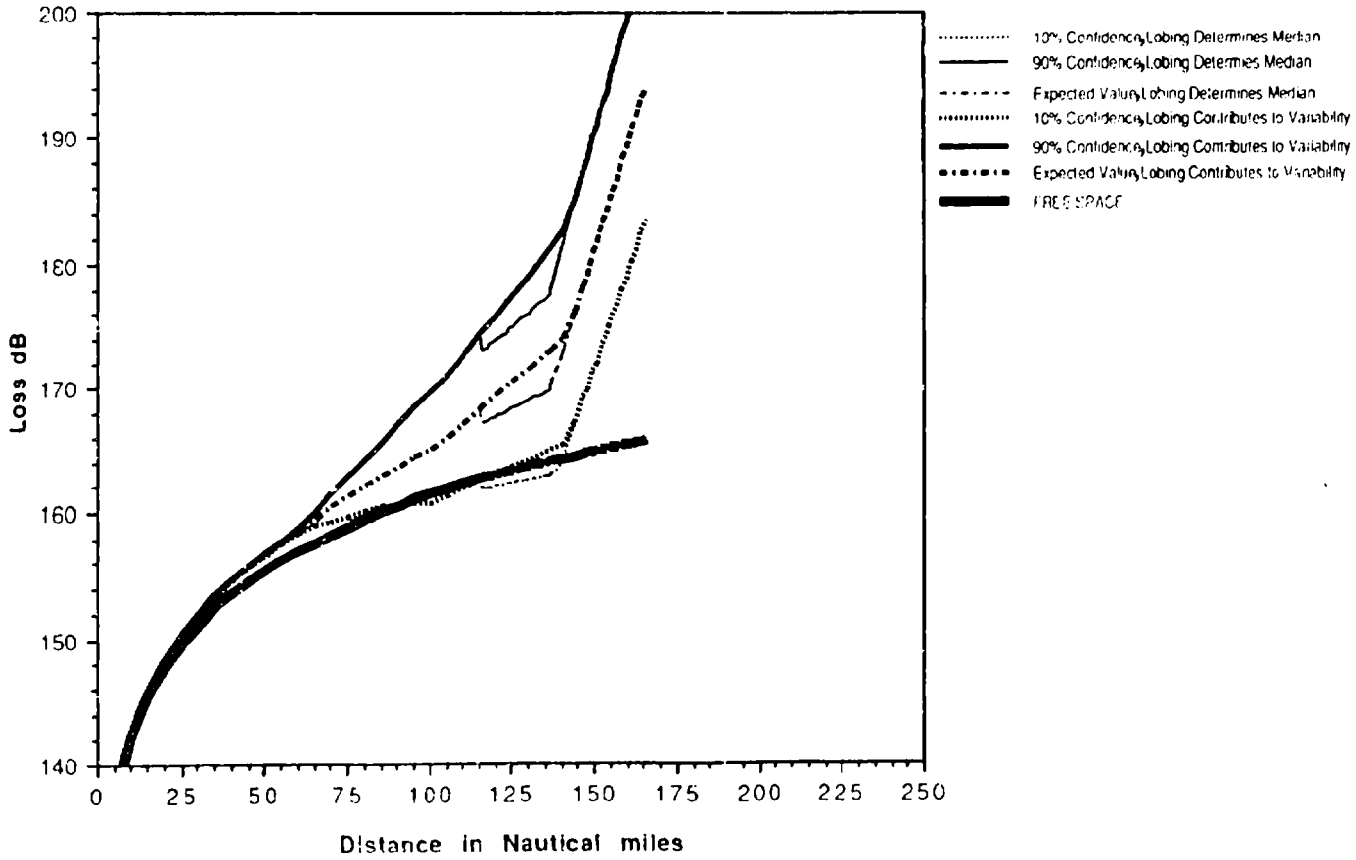

Figure 3-32. Basic Transmission Loss; Terrain Roughness Δh = 50 ft, 50-ft Obstacle, 15 GHz, h_2 = 22,000 ft, h_1 = 20 ft

Johnson-Gierhart Program Run Data: Frequency: 2 GHz Climate: #4 Desert Terrain Delta h: 0 ft.
Refractivity: Effective Earth Radius: 4423 nmi Minimum Monthly Mean: 280N-Units Surface Type: Poor Ground
Aircraft Antenna Altitude: 32000 ft. above MSL Type: Isotropic Circular Polarization Time availability: For Instantaneous Levels Exceeded
Facility Antenna Height: 20 ft. above MSL Type: Isotropic Circular Polarization Terrain Elevation at site: 0 Ft above MSL
Surface Reflection Lobing: See Legend Confidence: See Legend Obst Distance: Determined at 5.4 nmi Obst Height: Determined at 0 feet

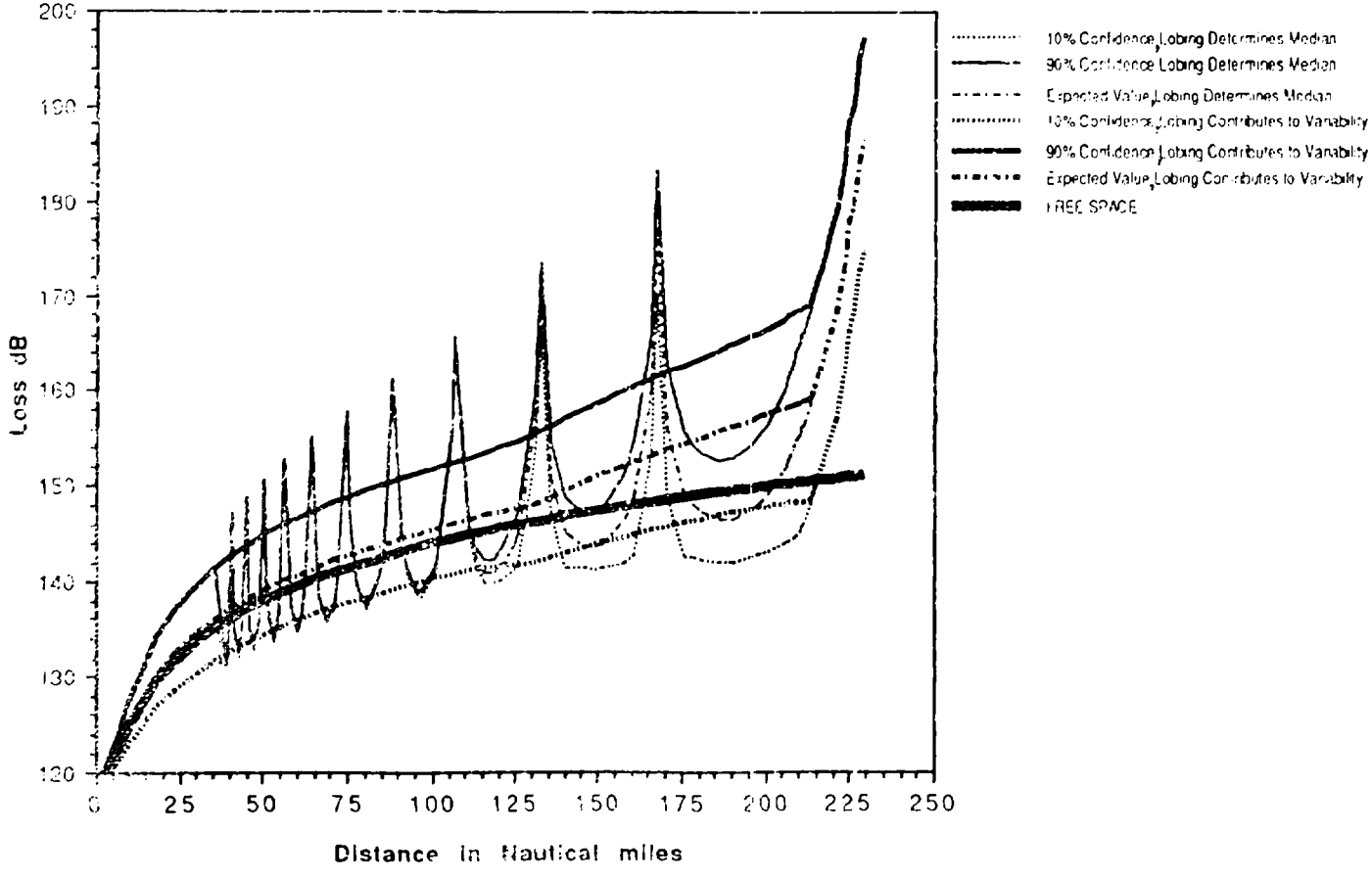

Figure 3-33. Basic Transmission Loss; Terrain Roughness Δh = 0, No Site-Specified Obstacle, 2 GHz, h_2 = 33,000 ft, h_1 = 20 ft

Johnson-Gierhart Program Run Data: Frequency: 2 GHz Climate: #4 Desert Terrain Delta h: 50 ft.
Refractivity: Effective Earth Radius: 4423 nmi Minimum Monthly Mean: 280N-Units Surface Type: Poor Ground
Aircraft Antenna Altitude: 33000 ft. above MSL Type: Isotropic Circular Polarization Time availability: For Instantaneous Levels Exceeded
Facility Antenna Height: 20 ft. above MSL Type: Isotropic Circular Polarization Terrain Elevation at site: 0 Ft above MSL
Surface Reflection Lobing: See Legend Confidence: See Legend Obst Distance: Determined at 4.83 nmi Obst Height: Determined at 4feet

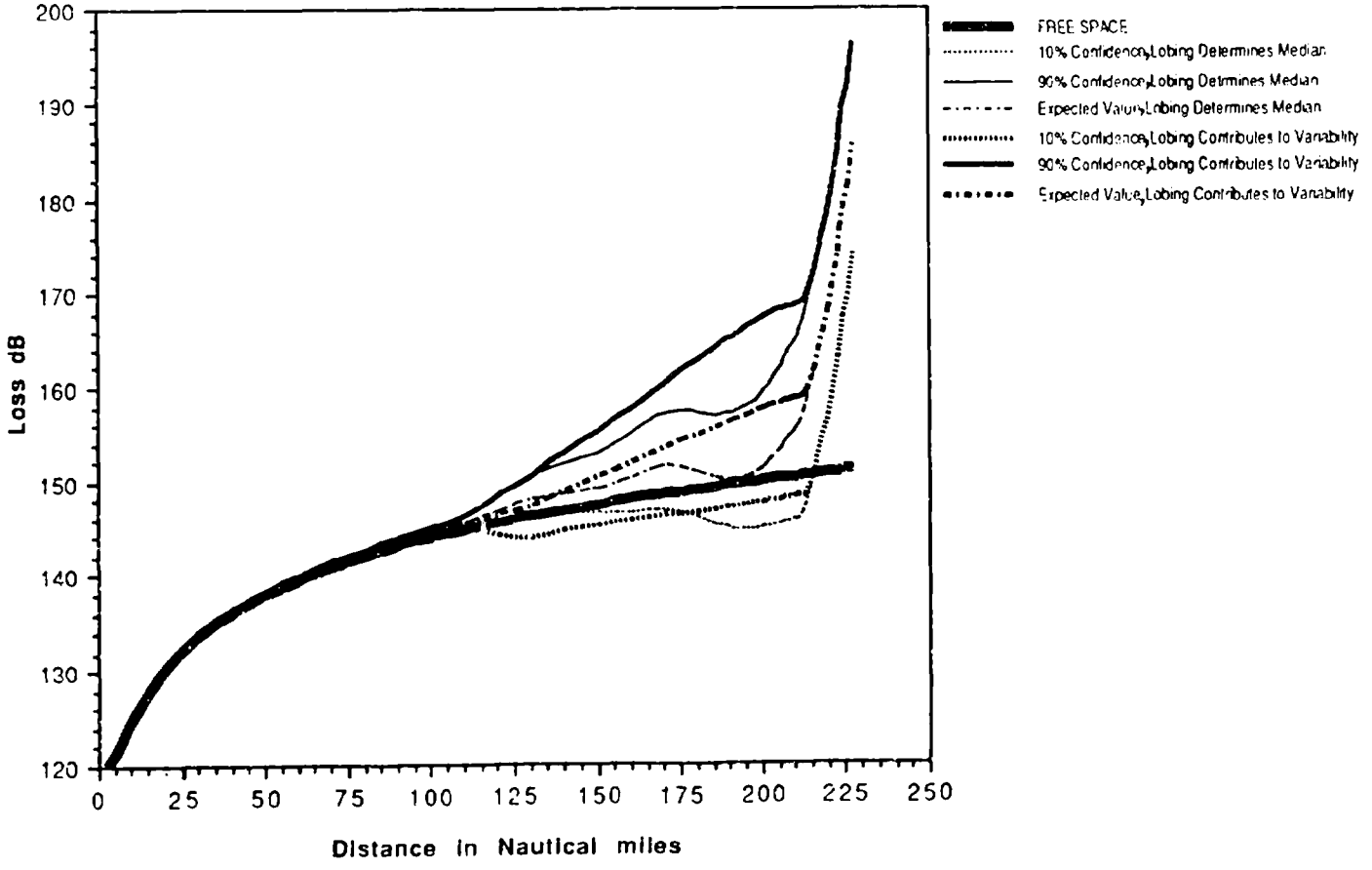

Figure 3-34. Basic Transmission Loss; Terrain Roughness Δh = 50 ft, No Site-Specified Obstacle, 2 GHz, h_2 = 33,000 ft, h_1 = 20 ft

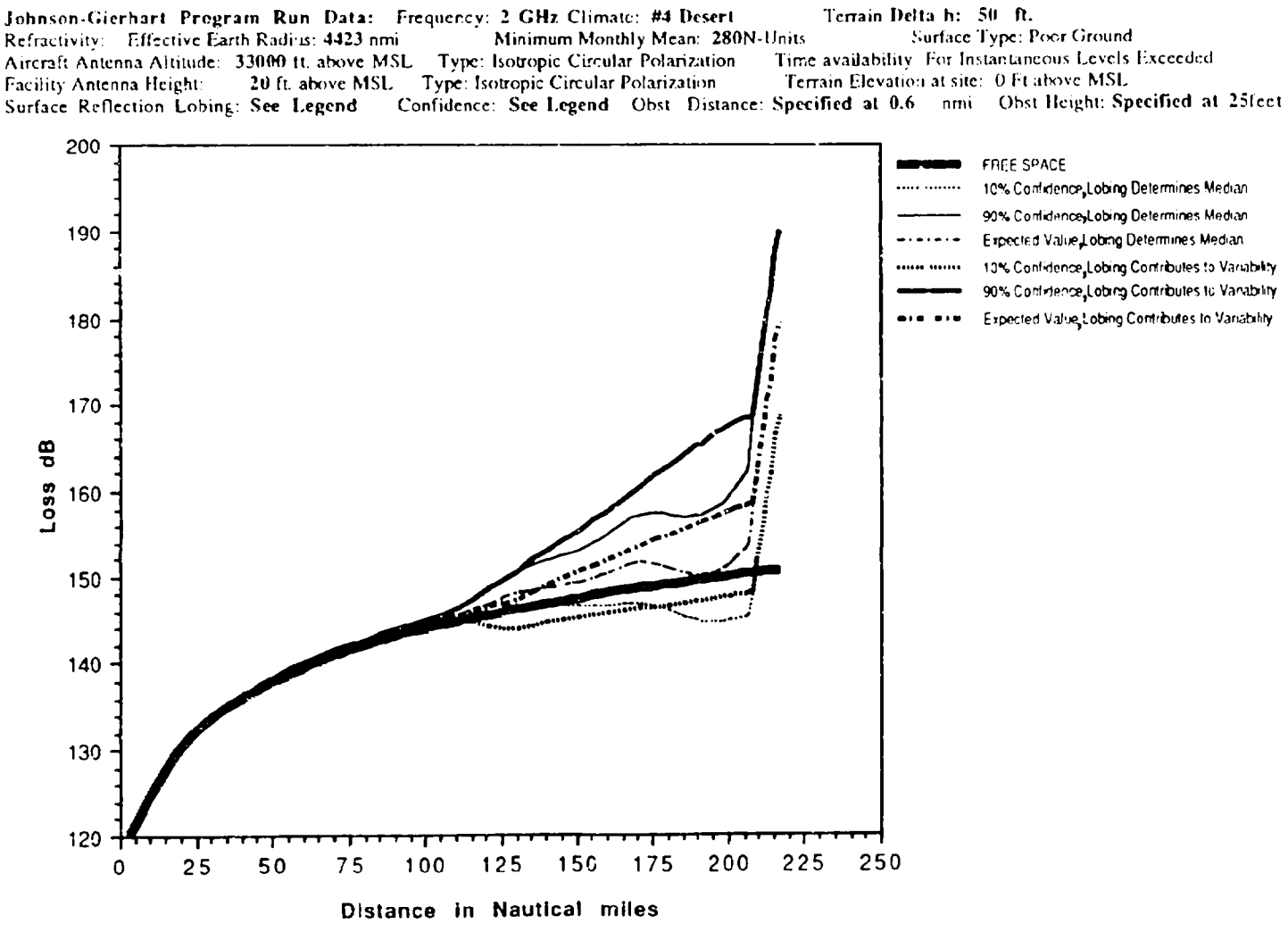

Figure 3-35. Basic Transmission Loss; Terrain Roughness Δh = 50 ft, 25-ft Obstacle, 2 GHz, h_2 = 33,000 ft, h_1 = 20 ft

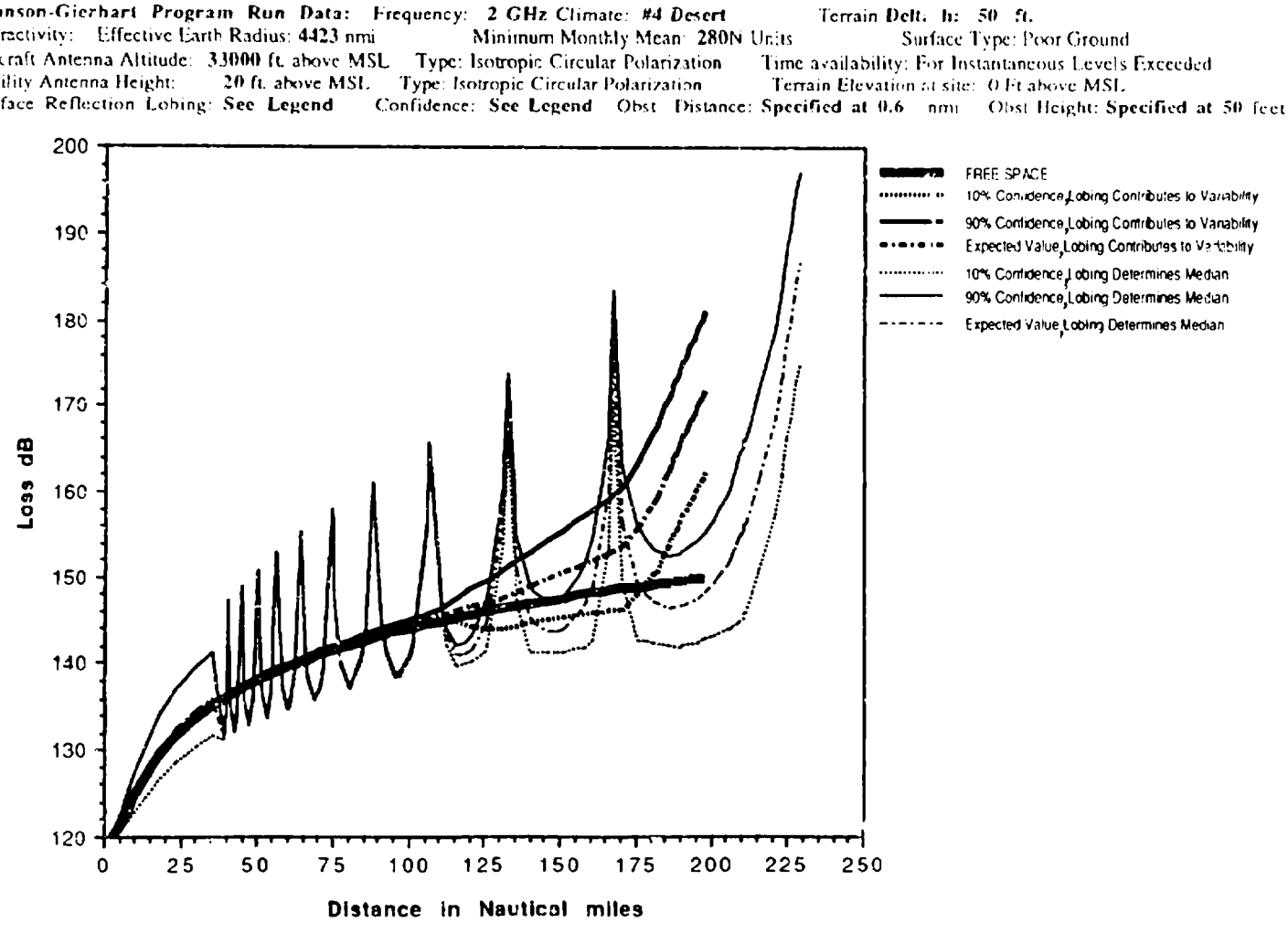

Figure 3-36. Basic Transmission Loss; Terrain Roughness Δh = 50 ft, 50-ft Obstacle, 2 GHz, h_2 = 33,000 ft, h_1 = 20 ft

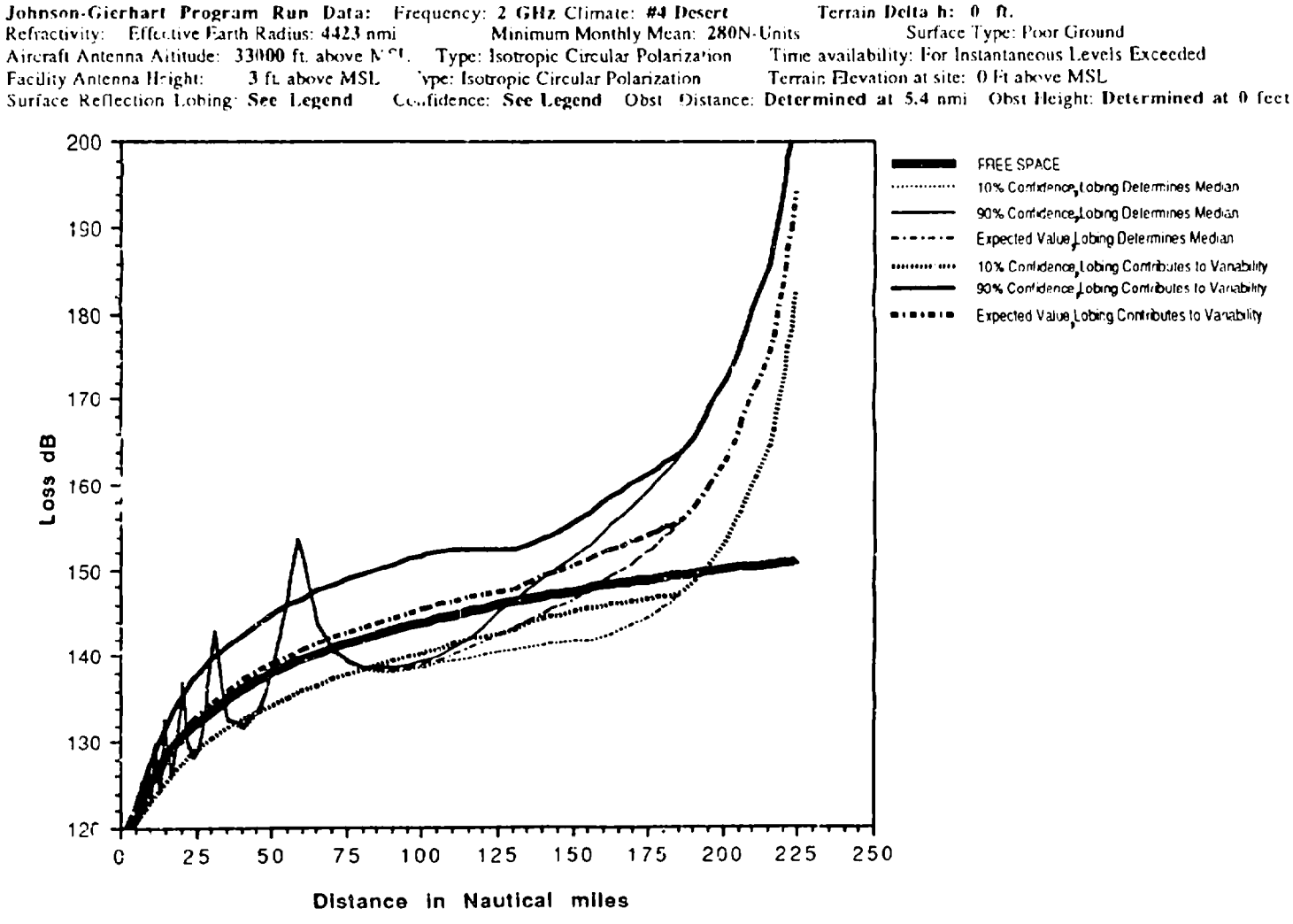

Figure 3-37. Basic Transmission Loss; Terrain Roughness $\Delta h = 0$, No Site-Specified Obstacle, 2 GHz, h_2 = 33,000 ft, h_1 = 3 ft

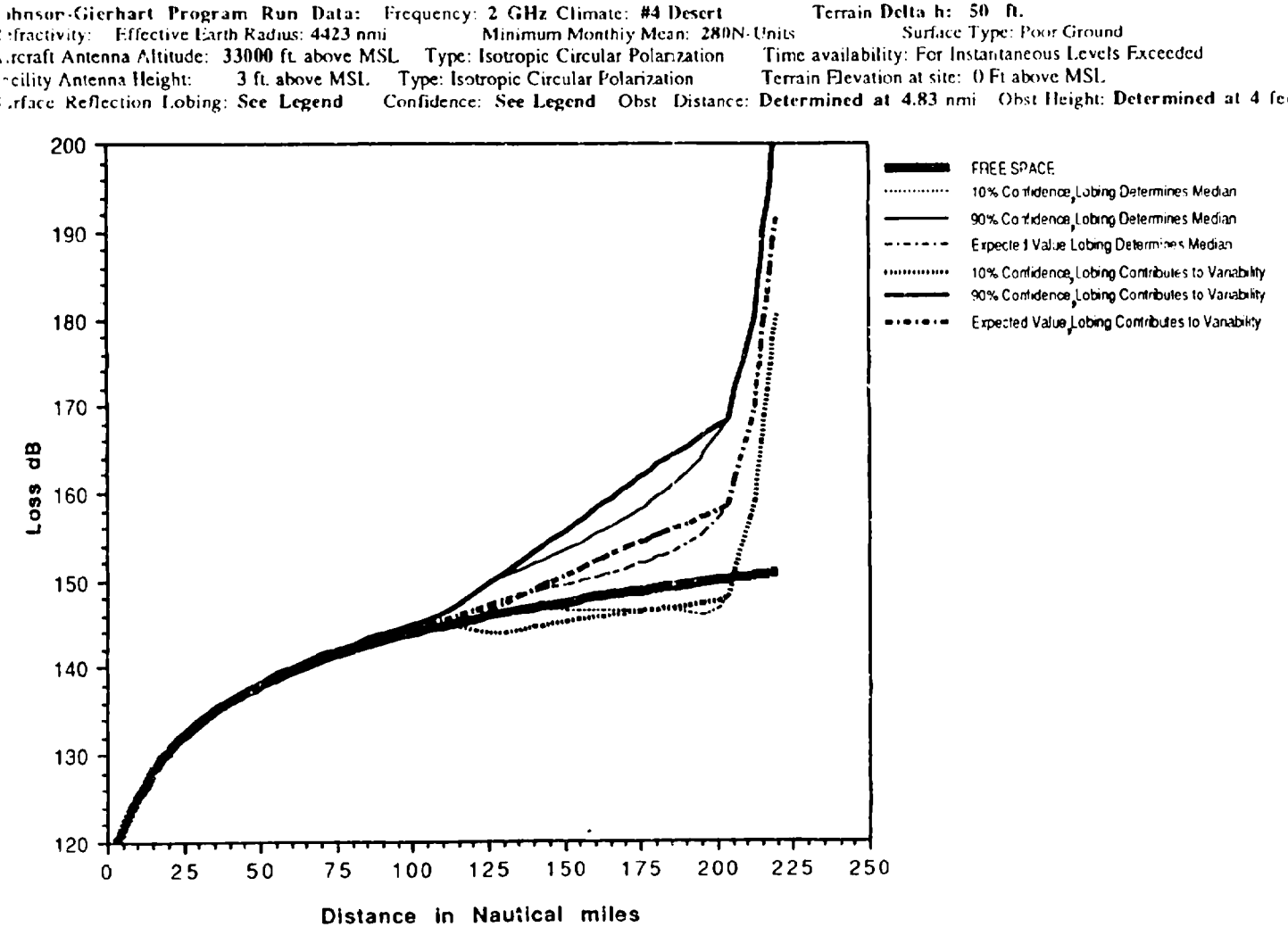

Figure 3-38. Basic Transmission Loss; Terrain Roughness Δh = 50 ft, No Site-Specified Obstacle, 2 GHz, h_2 = 33,000 ft, h_1 = 3 ft

Johnson-Gierhart Program Run Data: Frequency: 5 GHz Climate: #4 Desert Terrain Delta h: 0 ft.
Refractivity: Effective Earth Radius: 4423 nmi Minimum Monthly Mean: 280N-Units Surface Type: Poor Ground
Aircraft Antenna Altitude: 33000 ft. above MSL. Type: Isotropic Circular Polarization Time availability: For Instantaneous Levels Exceeded
Facility Antenna Height: 20 ft. above MSL Type: Isotropic Circular Polarization Terrain Elevation at site: 0 Ft above MSL
Surface Reflection Lobing: See Legend Confidence: See Legend Obst Distance: Determined at 5.4 nmi Obst Height: Determined at 0 feet

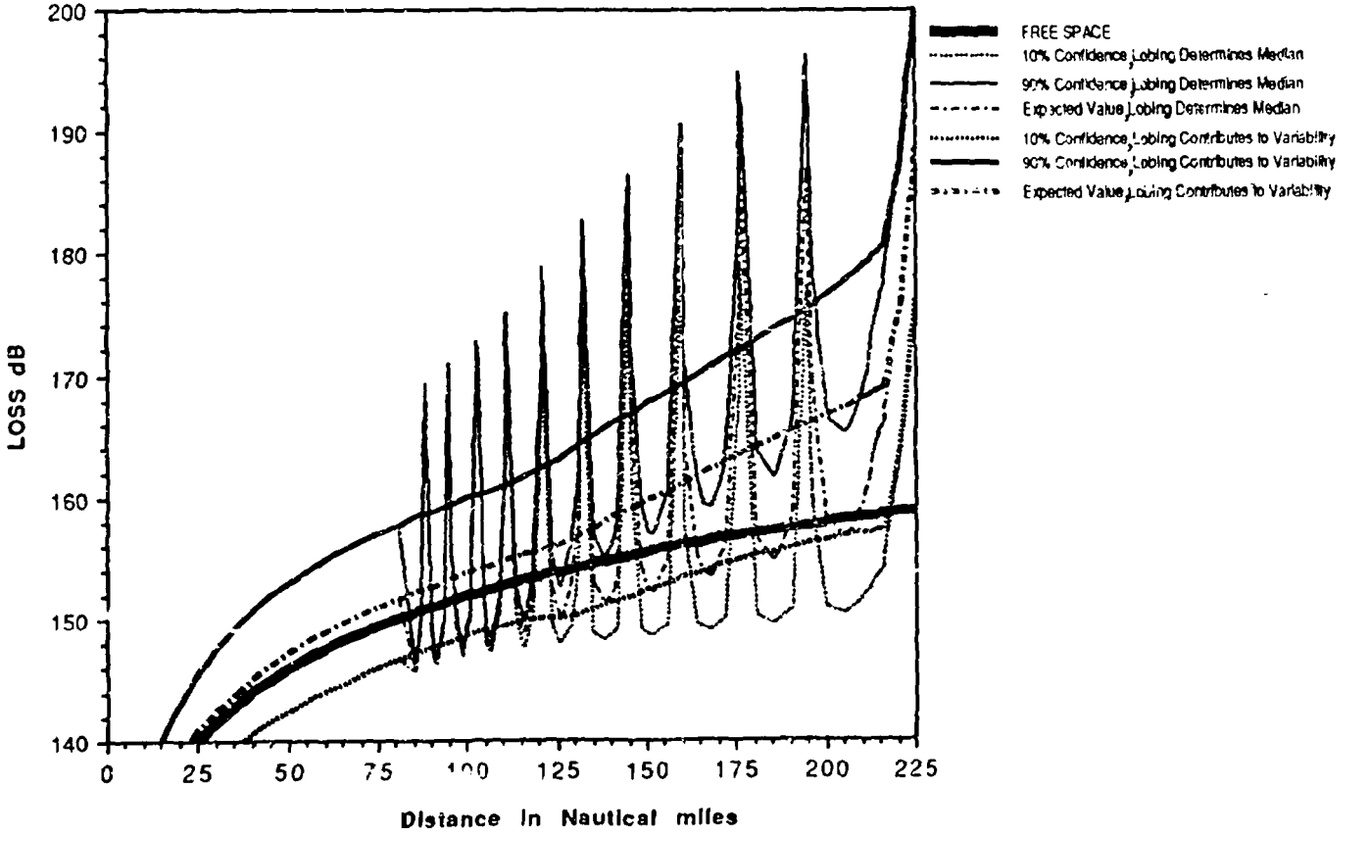

Figure 3-39. Basic Transmission Loss; Terrain Roughness Δh = 0, No Site-Specified Obstacle, 5 GHz, h_2 = 33,000 ft, h_1 = 20 ft

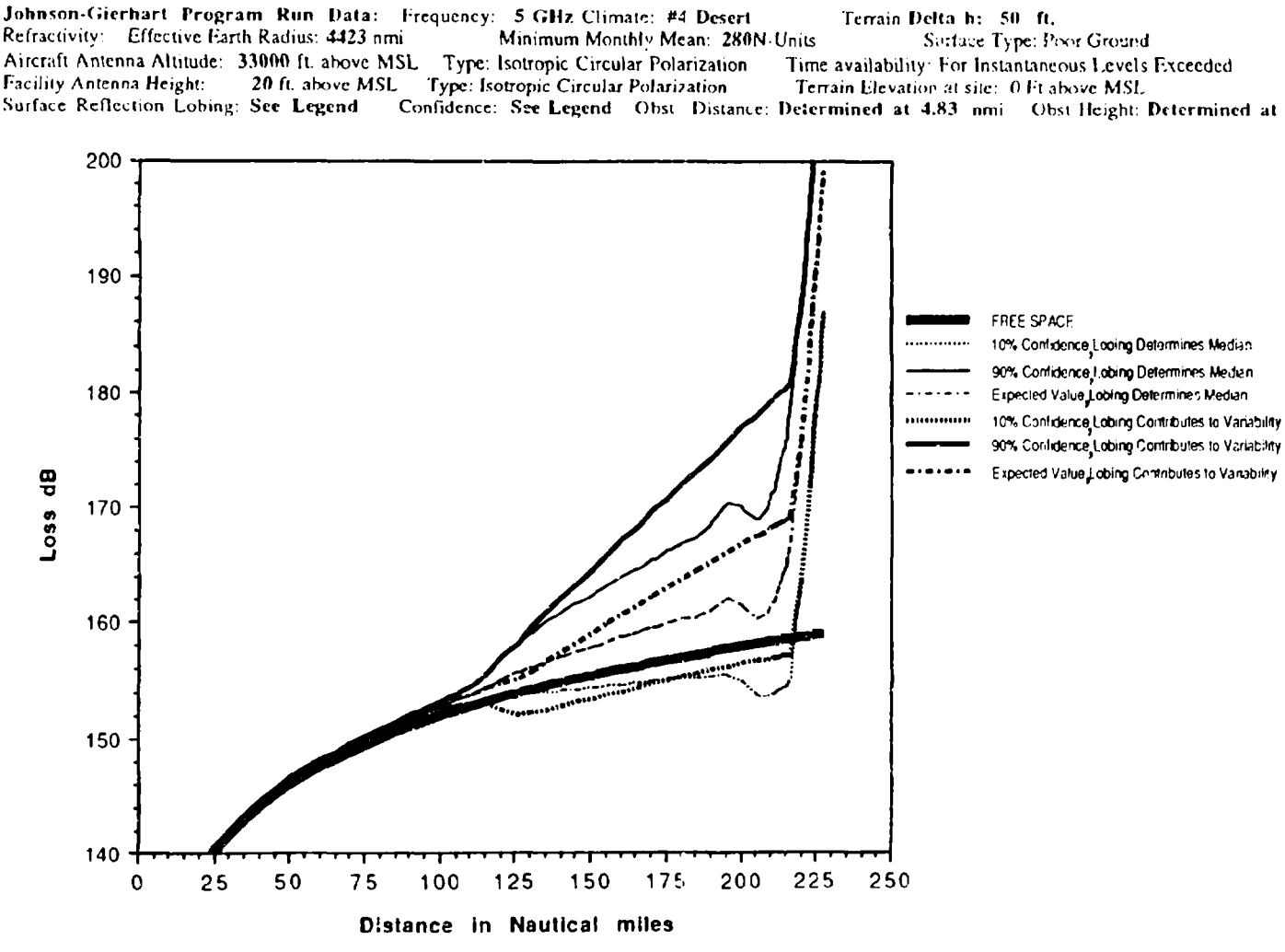

Figure 3-40. Basic Transmission Loss; Terrain Roughness Δh = 50 ft, No Site-Specified Obstacle, 5 GHz, h_2 = 33,000 ft, h_1 = 20 ft

Johnson-Gierhart Program Run Data: Frequency: 5 GHz Climate: #4 Desert Terrain Delta h: 50 ft.
Refractivity: Effective Earth Radius: 4423 nmi Minimum Monthly Mean: 280N-Units Surface Type: Poor Ground
Aircraft Antenna Altitude: 33000 ft. above MSL. Type: Isotropic Circular Polarization Time availability: For Instantaneous Levels Exceeded
Facility Antenna Height: 20 ft. above MSL Type: Isotropic Circular Polarization Terrain Elevation at site: 0 Ft above MSL
Surface Reflection Lobing: See Legend Confidence: See Legend Obst Distance: Specified at 0.6 nmi Obst Height: Specified at 25 feet

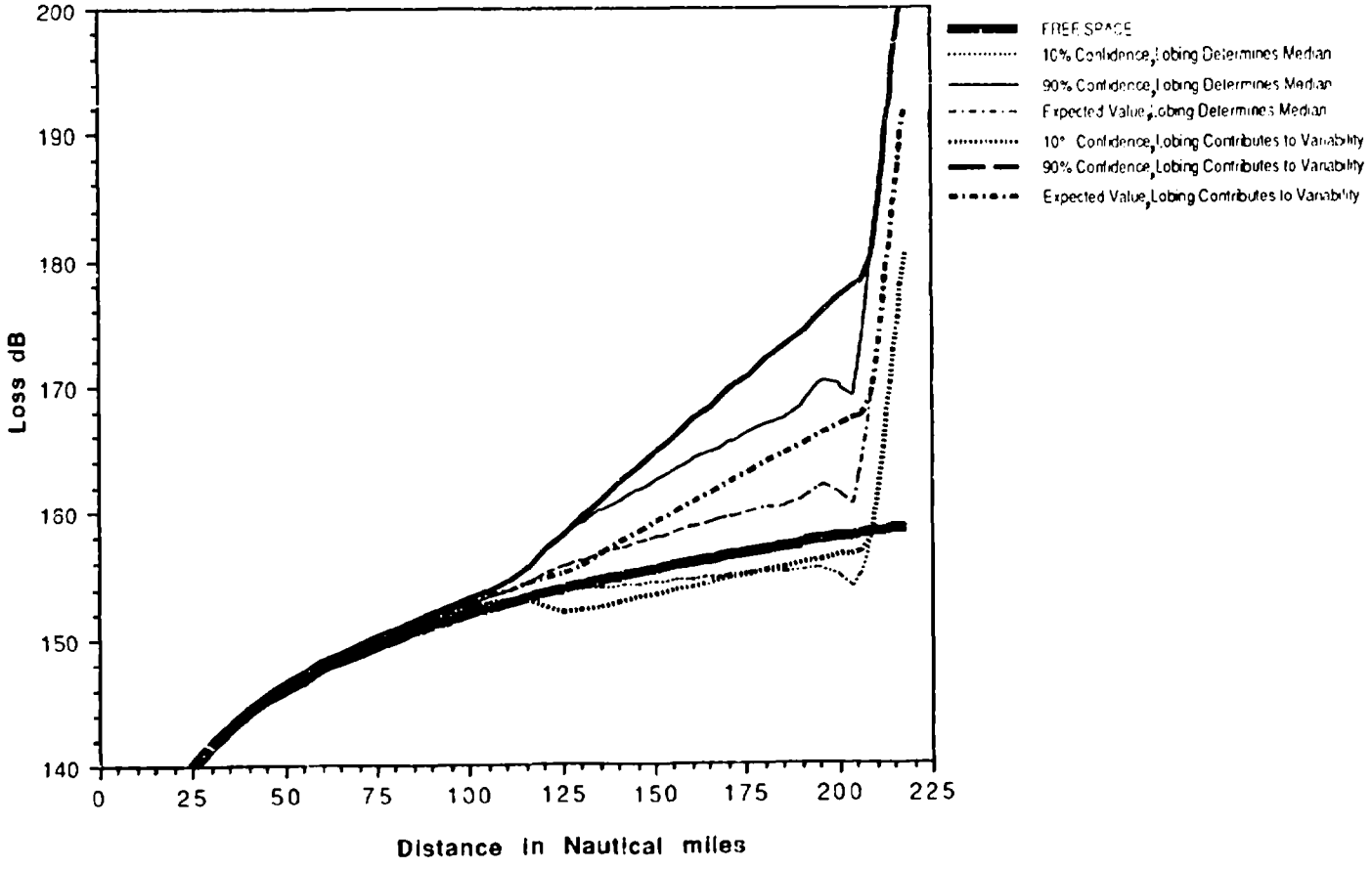

Figure 3-41. Basic Transmission Loss; Terrain Roughness Δh = 50 ft, 25-ft Obstacle, 5 GHz, h_2 = 33,000 ft, h_1 = 20 ft

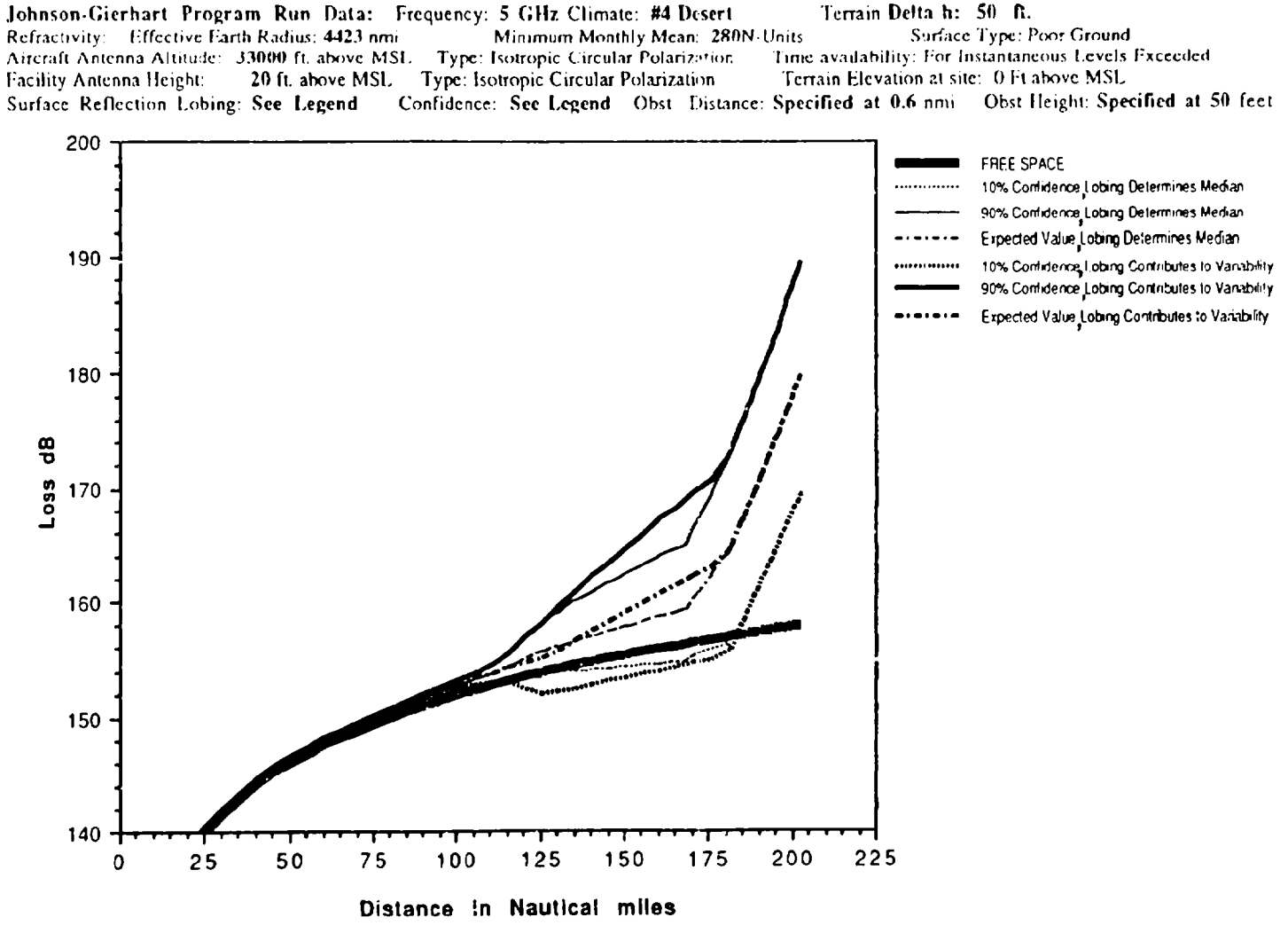

Figure 3-42. Basic Transmission Loss; Terrain Roughness Δh = 50 ft, 50-ft Obstacle, 5 GHz, h_2 = 33,000 ft, h_1 = 20 ft

Johnson-Gierhart Program Run Data: Frequency: 10 GHz Climate: #4 Desert Terrain Delta h: 0 ft.
Refractivity: Effective Earth Radius: 4423 nmi Minimum Monthly Mean: 280N-Units Surface Type: Poor Ground
Aircraft Antenna Altitude: 33000 ft. above MSL Type: Isotropic Circular Polarization Time availability: For Instantaneous Levels Exceeded
Facility Antenna Height: 20 ft. above MSL Type: Isotropic Circular Polarization Terrain Elevation at site: 0 Ft above MSL
Surface Reflection Lobing: See Legend Confidence: See Legend Obst Distance: Determined at 5.4nmi Obst Height: Determined at 0 feet

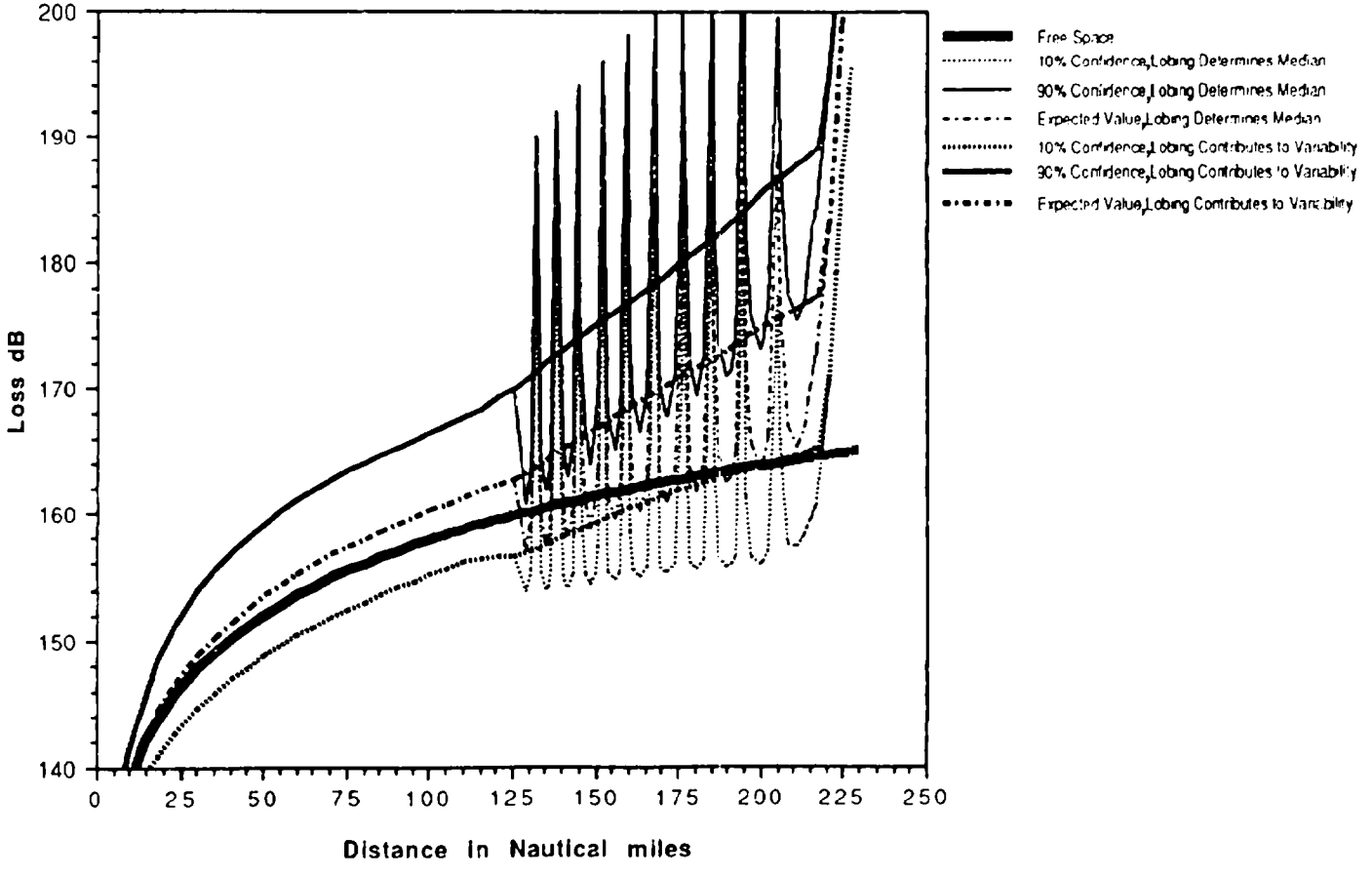

Figure 3-43. Basic Transmission Loss; Terrain Roughness Δh = 0, No Site-Specified Obstacle, 10 GHz, h_2 = 33,000 ft, h_1 = 20 ft

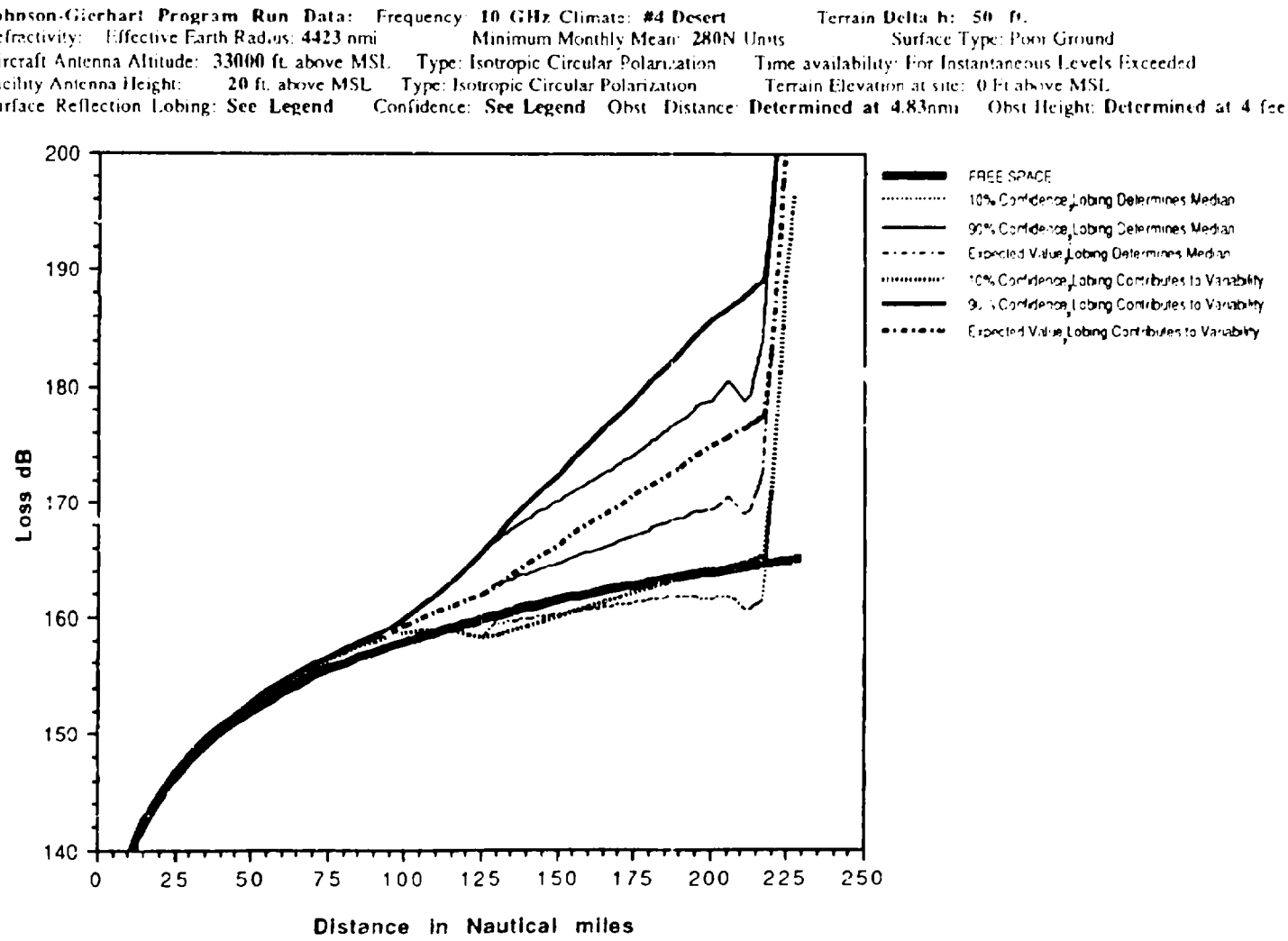

Figure 3-44. Basic Transmission Loss; Terrain Roughness Δh = 50 ft, No Site-Specified Obstacle, 10 GHz, h_2 = 33,000 ft, h_1 = 20 ft

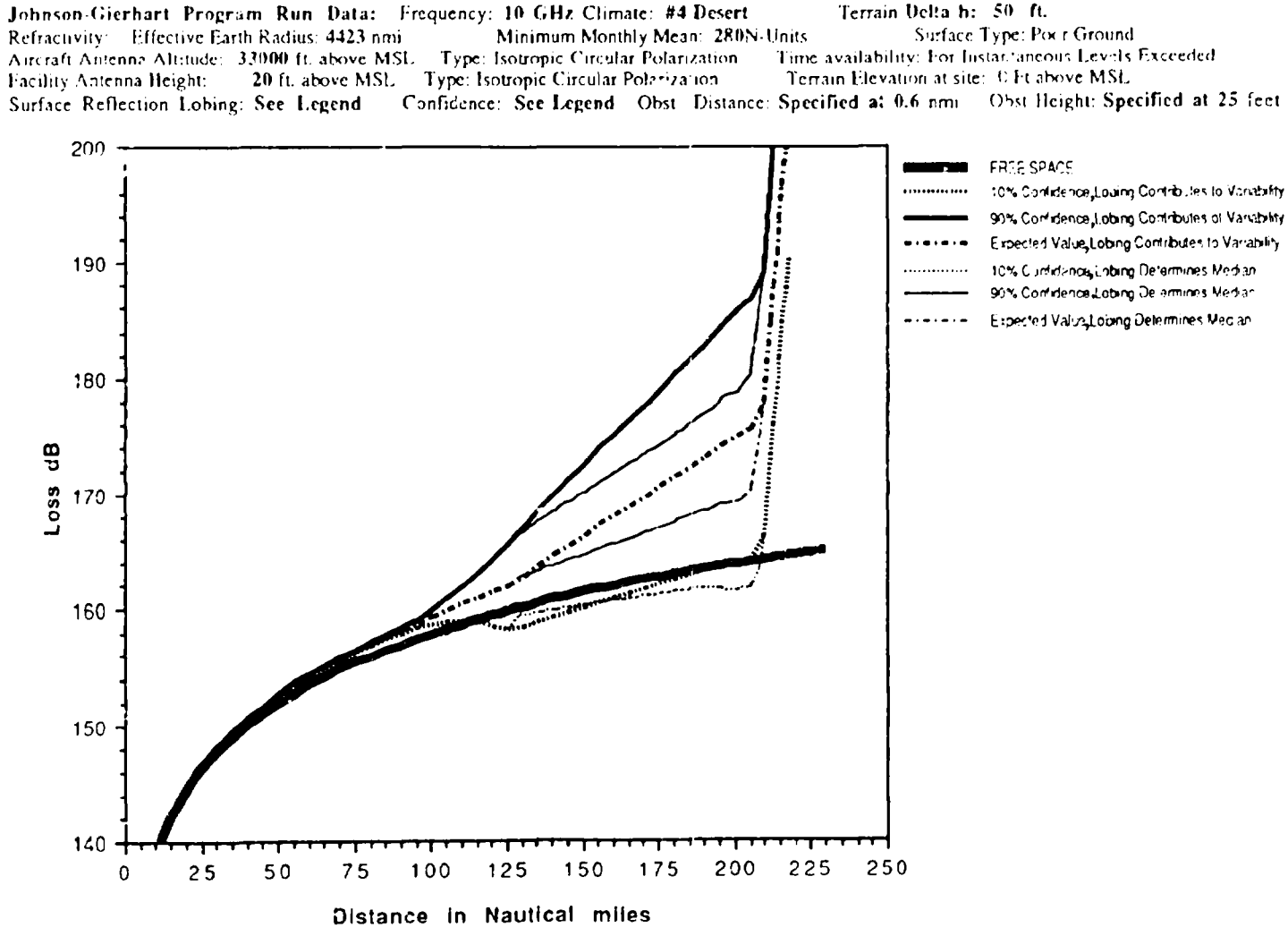

Figure 3-45. Basic Transmission Loss; Terrain Roughness Δh = 50 ft, 25-ft Obstacle, 10 GHz, h_2 = 33,000 ft, h_1 = 20 ft

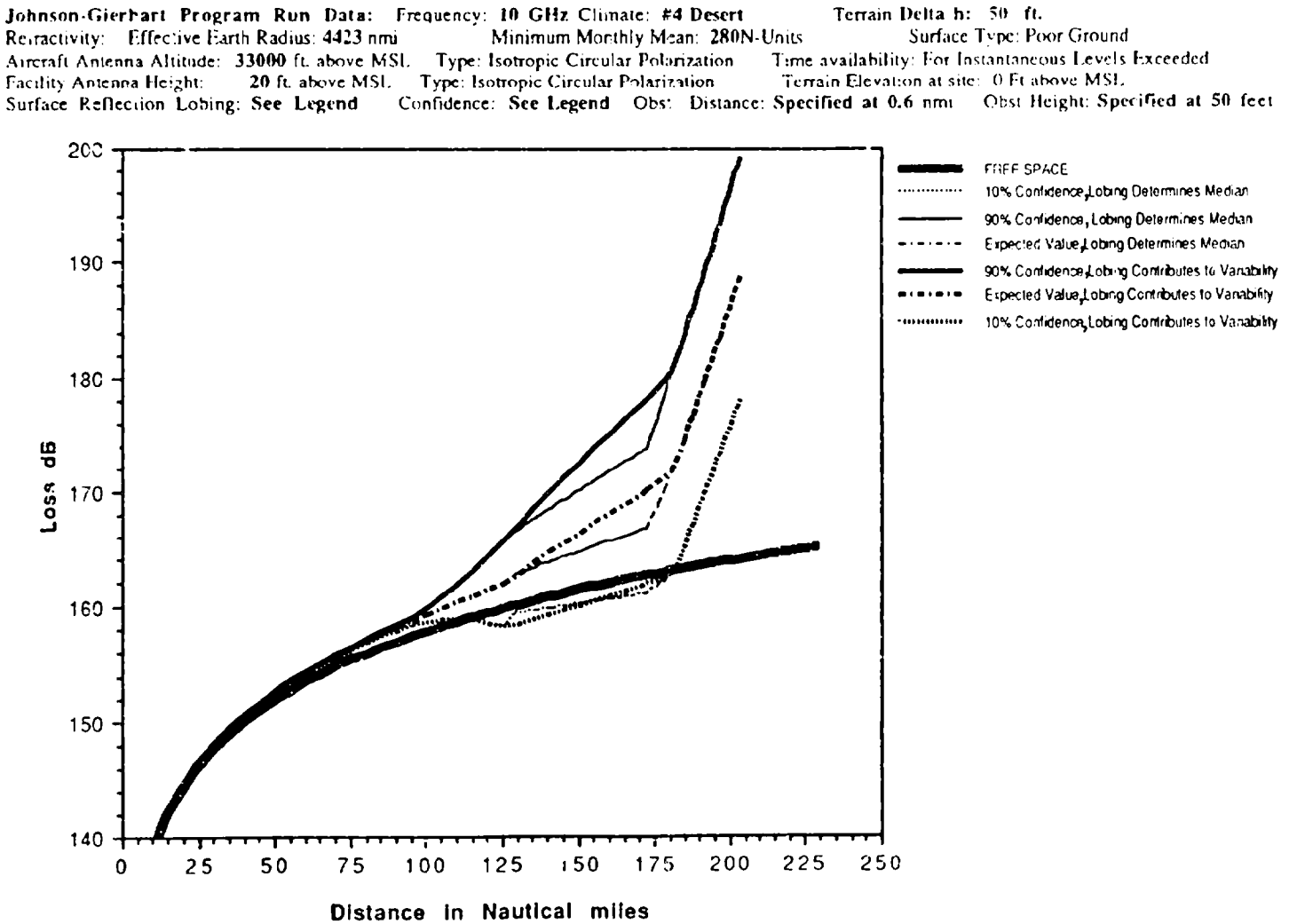

Figure 3-46. Basic Transmission Loss; Terrain Roughness Δh = 50 ft, 50-ft Obstacle, 10 GHz, h_2 = 33,000 ft, h_1 = 20 ft

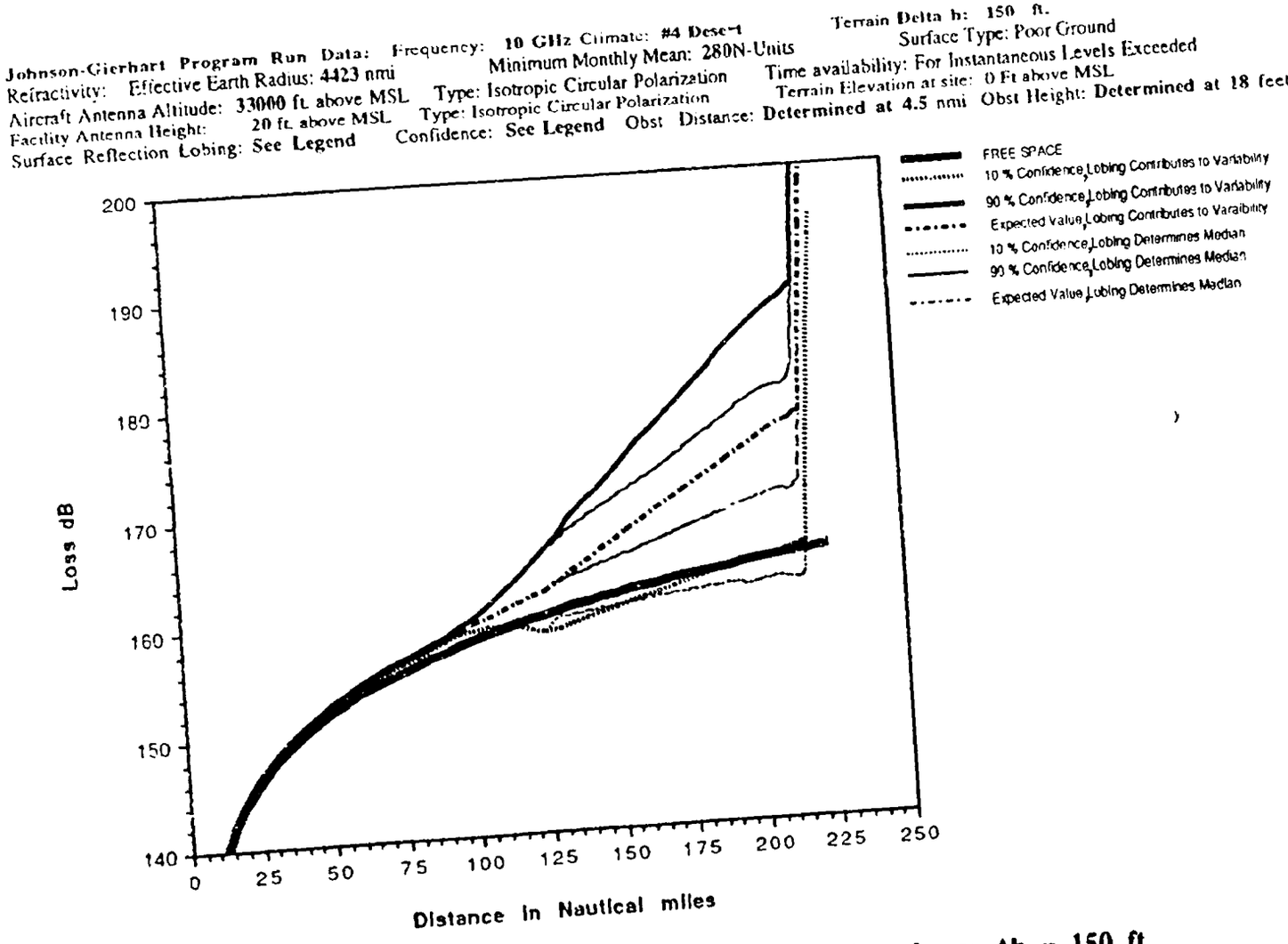

Figure 3-47. Basic Transmission Loss; Terrain Roughness Δh = 150 ft, No Site-Specified Obstacle, 10 GHz, h2 = 33,000 ft, h1 = 20 ft

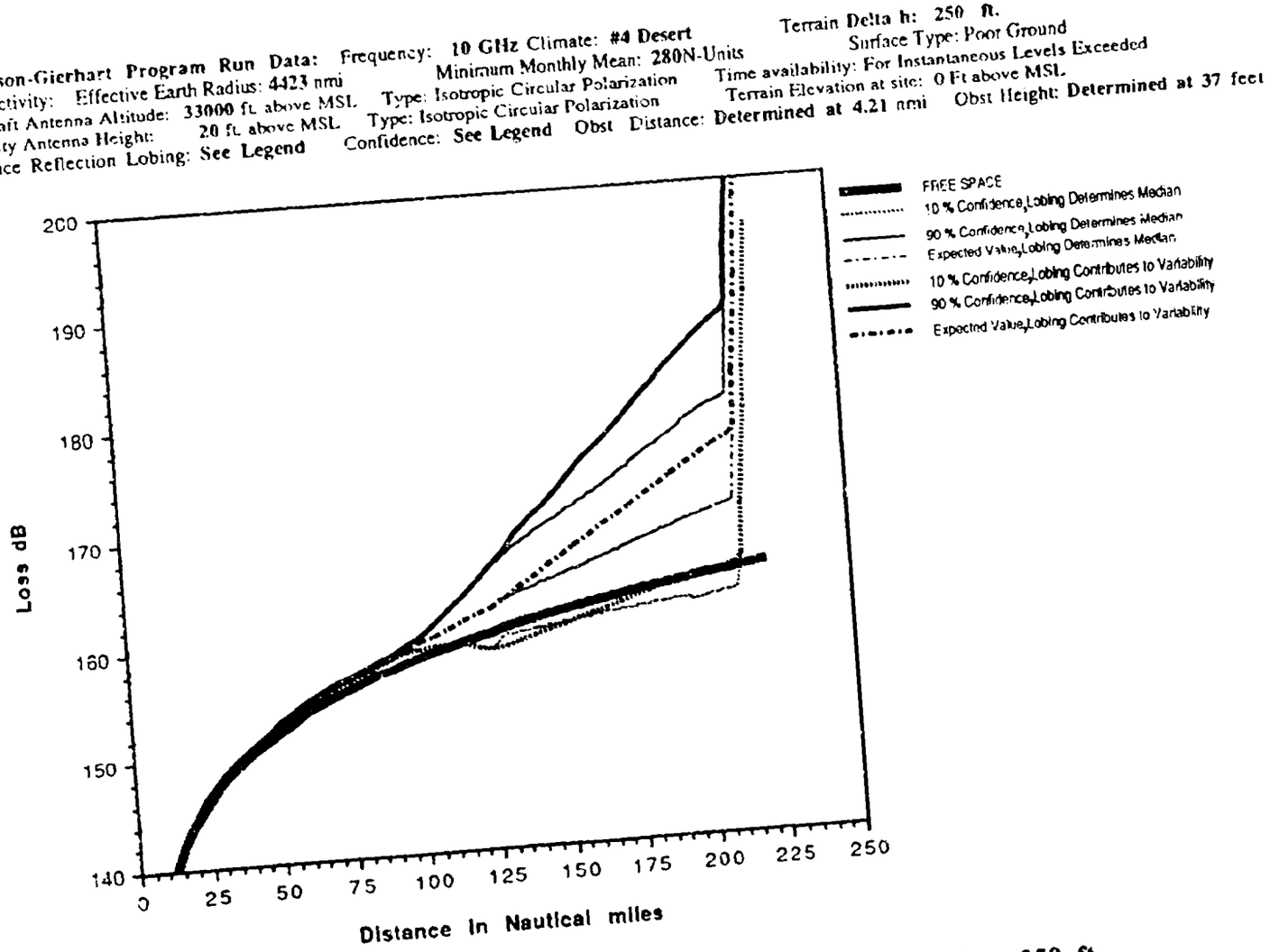

Figure 3-48. Basic Transmission Loss; Terrain Roughness Δh = 250 ft, No Site-Specified Obstacle, 10 GHz, h2 = 33,000 ft, h1 = 20 ft

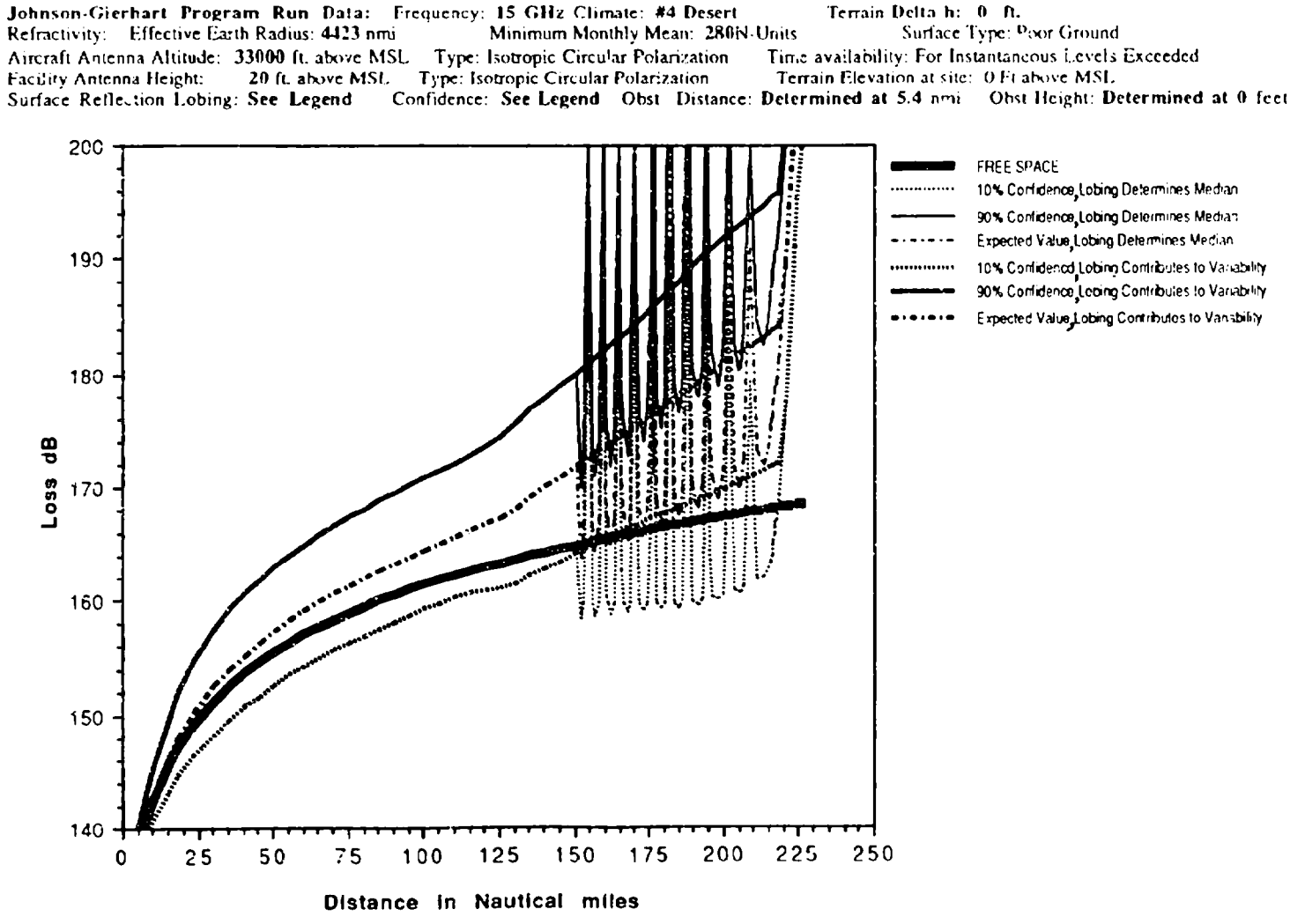

Figure 3-49. Basic Transmission Loss; Terrain Roughness Δh = 0, No Site-Specified Obstacle, 15 GHz, h_2 = 33,000 ft, h_1 = 20 ft

Johnson-Gierhart Program Run Data: Frequency: 15 GHz Climate: #4 Desert Terrain Delta h: 50 ft.
Refractivity: Effective Earth Radius: 4423 nmi Minimum Monthly Mean: 280N-Units Surface Type: Poor Ground
Aircraft Antenna Altitude: 33000 ft. above MSL Type: Isotropic Circular Polarization Time availability: For Instantaneous Levels Exceeded
Facility Antenna Height: 20 ft. above MSL Type: Isotropic Circular Polarization Terrain Elevation at site: 0 Ft above MSL
Surface Reflection Lobing: See Legend Confidence: See Legend Obst Distance: Determined at 4.83 nmi Obst Height: Determined at 4 feet

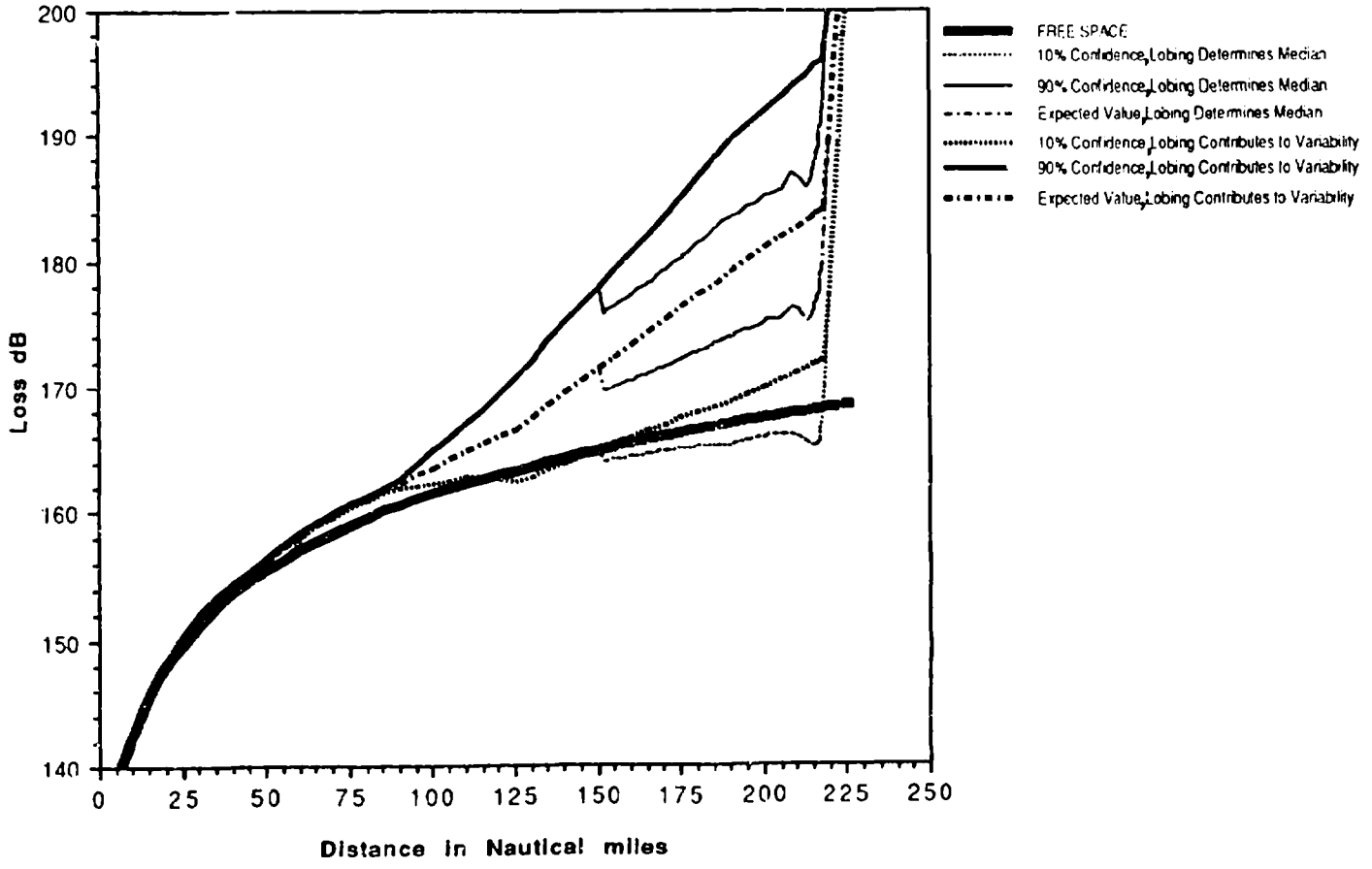

Figure 3-50. Basic Transmission Loss; Terrain Roughness Δh = 50 ft, No Site-Specified Obstacle, 15 GHz, h_2 = 33,000 ft, h_1 = 20 ft

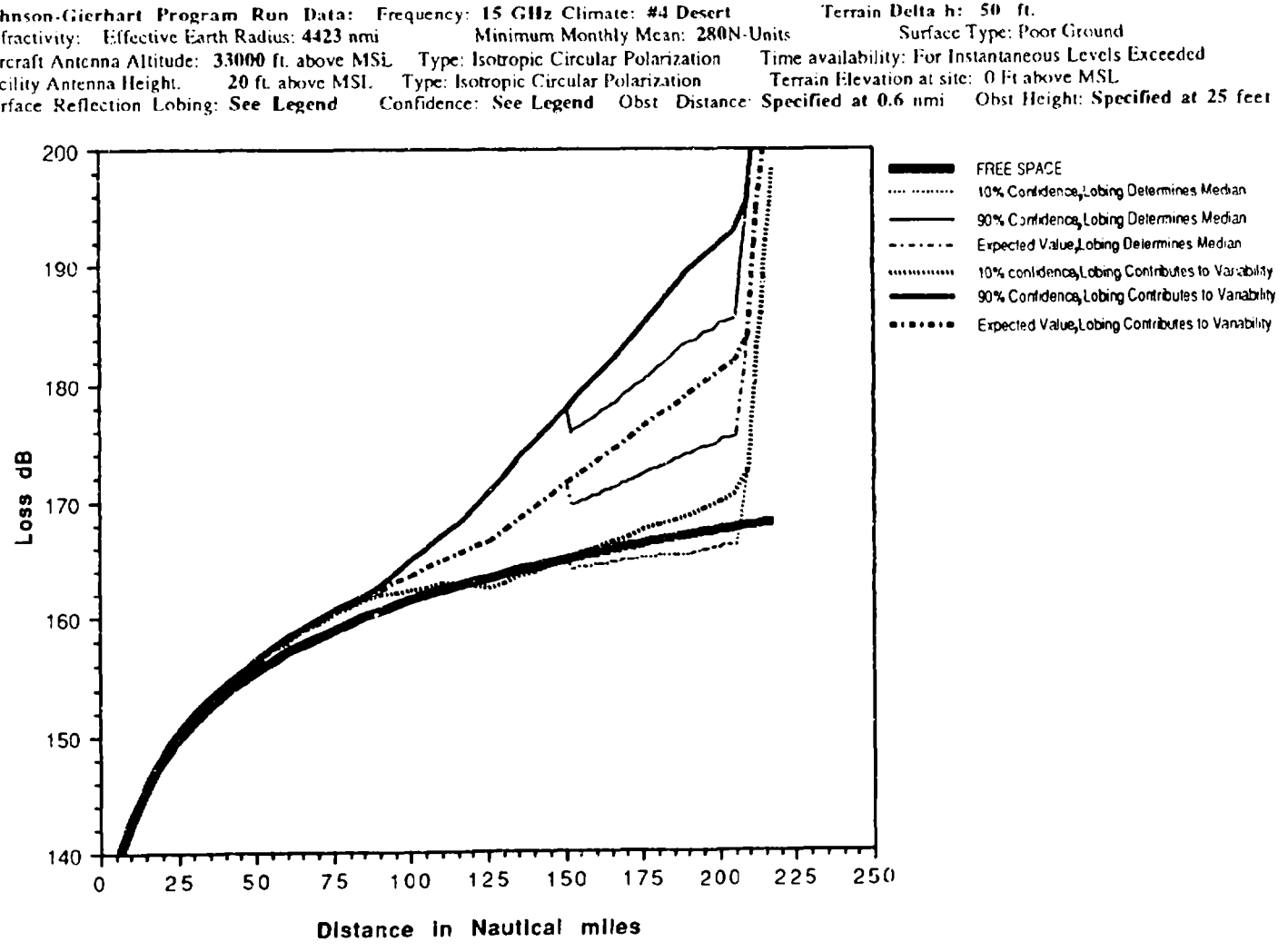

Figure 3-51. Basic Transmission Loss; Terrain Roughness Δh = 50 ft, 25-ft Obstacle, 15 GHz, h_2 = 33,000 ft, h_1 = 20 ft

Johnson-Gierhart Program Run Data: Frequency: 15 GHz Climate: #4 Desert Terrain Delta h: 50 ft.
Refractivity: Effective Earth Radius: 4423 nmi Minimum Monthly Mean: 280N-Units Surface Type: Poor Ground
Aircraft Antenna Altitude: 33000 ft. above MSL Type: Isotropic Circular Polarization Time availability: For Instantaneous Levels Exceeded
Facility Antenna Height: 20 ft. above MSL Type: Isotropic Circular Polarization Terrain Elevation at site: 0 Ft above MSL
Surface Reflection Lobing: See Legend Confidence: See Legend Obst Distance: Specified at 0.6 nmi Obst Height: Specified at 50 feet

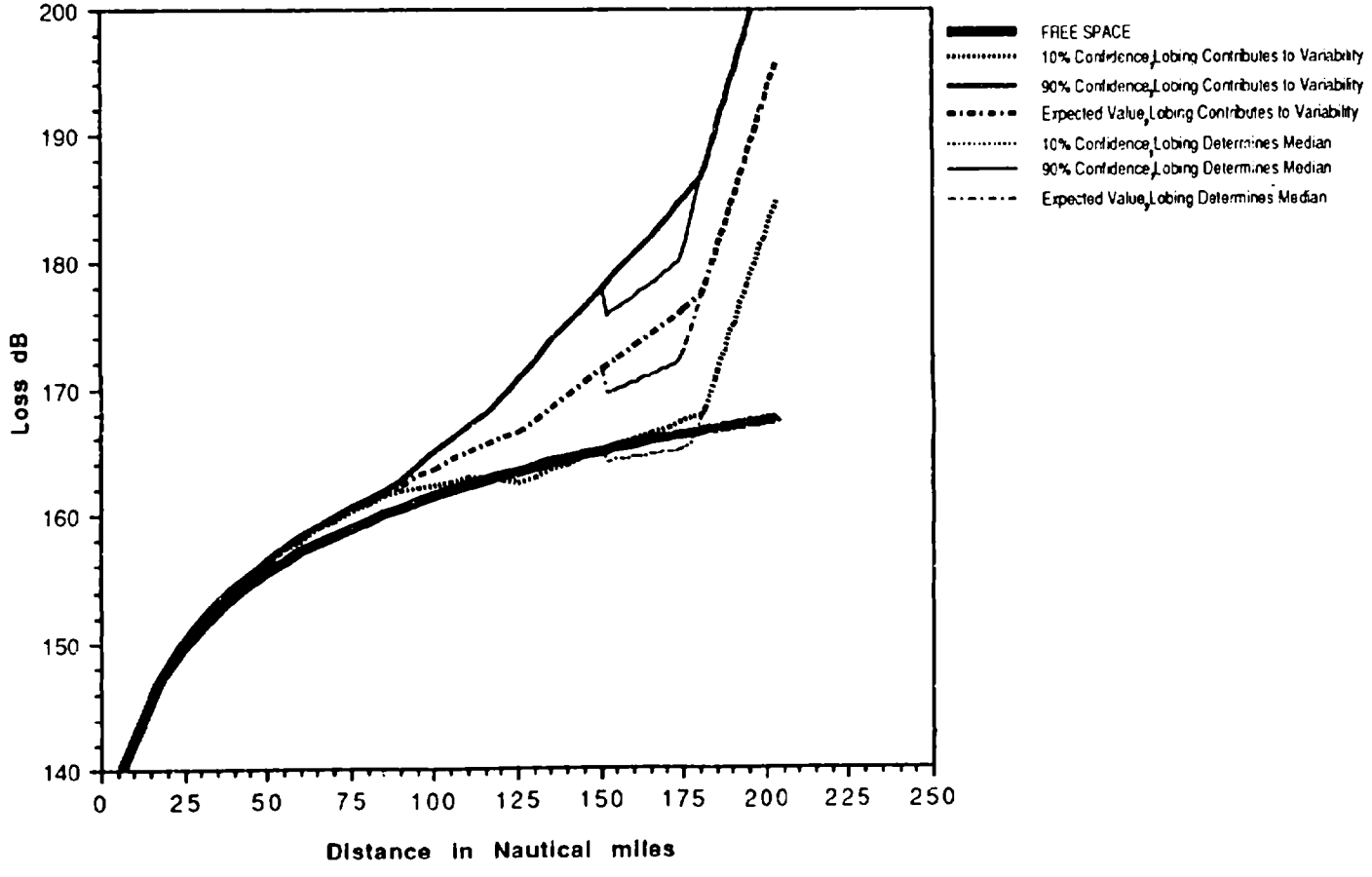

Figure 3-52. Basic Transmission Loss; Terrain Roughness Δh = 50 ft, 50-ft Obstacle, 15 GHz, h_2 = 33,000 ft, h_1 = 20 ft

Johnson-Gierhart Program Run Data: Frequency: 10 GHz Climate: #4 Desert Terrain Delta h: 0 ft.
Refractivity: Effective Earth Radius: 4423 nmi Minimum Monthly Mean: 280N-Units Surface Type: Poor Ground
Aircraft Antenna Altitude: 66000 ft. above MSL Type: Isotropic Circular Polarization Time availability: For Instantaneous Levels Exceeded
Facility Antenna Height: 20 ft. above MSL Type: Isotropic Circular Polarization Terrain Elevation at site: 0 ft above MSL
Surface Reflection Lobing: See Legend Confidence: See Legend Obst Distance: Determined at 5.4nmi Obst Height: Determined at 0feet

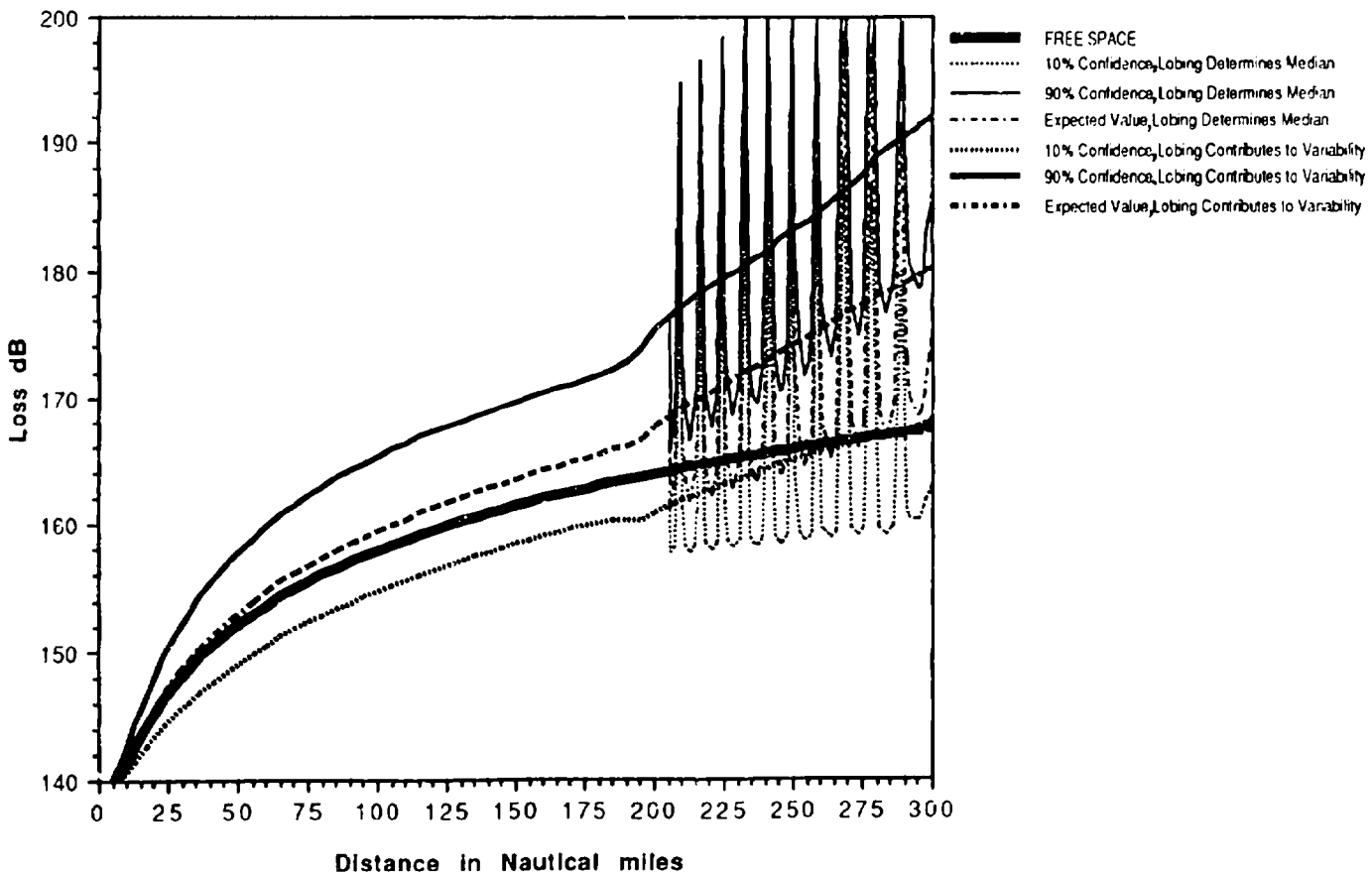

Figure 3-53. Basic Transmission Loss; Terrain Roughness Δh = 0, No Site-Specified Obstacle, 10 GHz, h_2 = 66,000 ft, h_1 = 20 ft

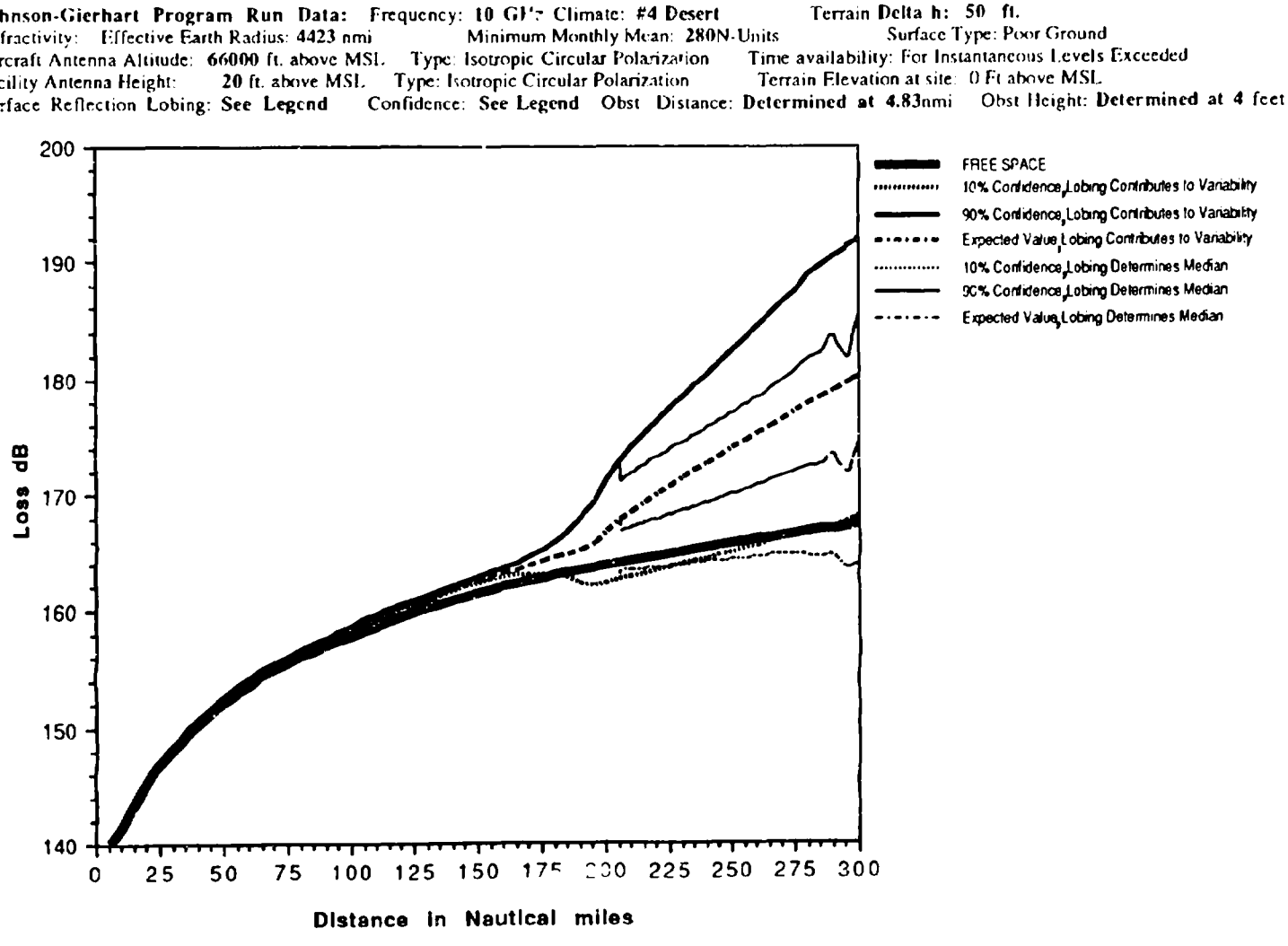

Figure 3-54. Basic Transmission Loss; Terrain Roughness Δh = 50 ft, No Site-Specified Obstacle, 10 GHz, h_2 = 66,000 ft, h_1 = 20 ft

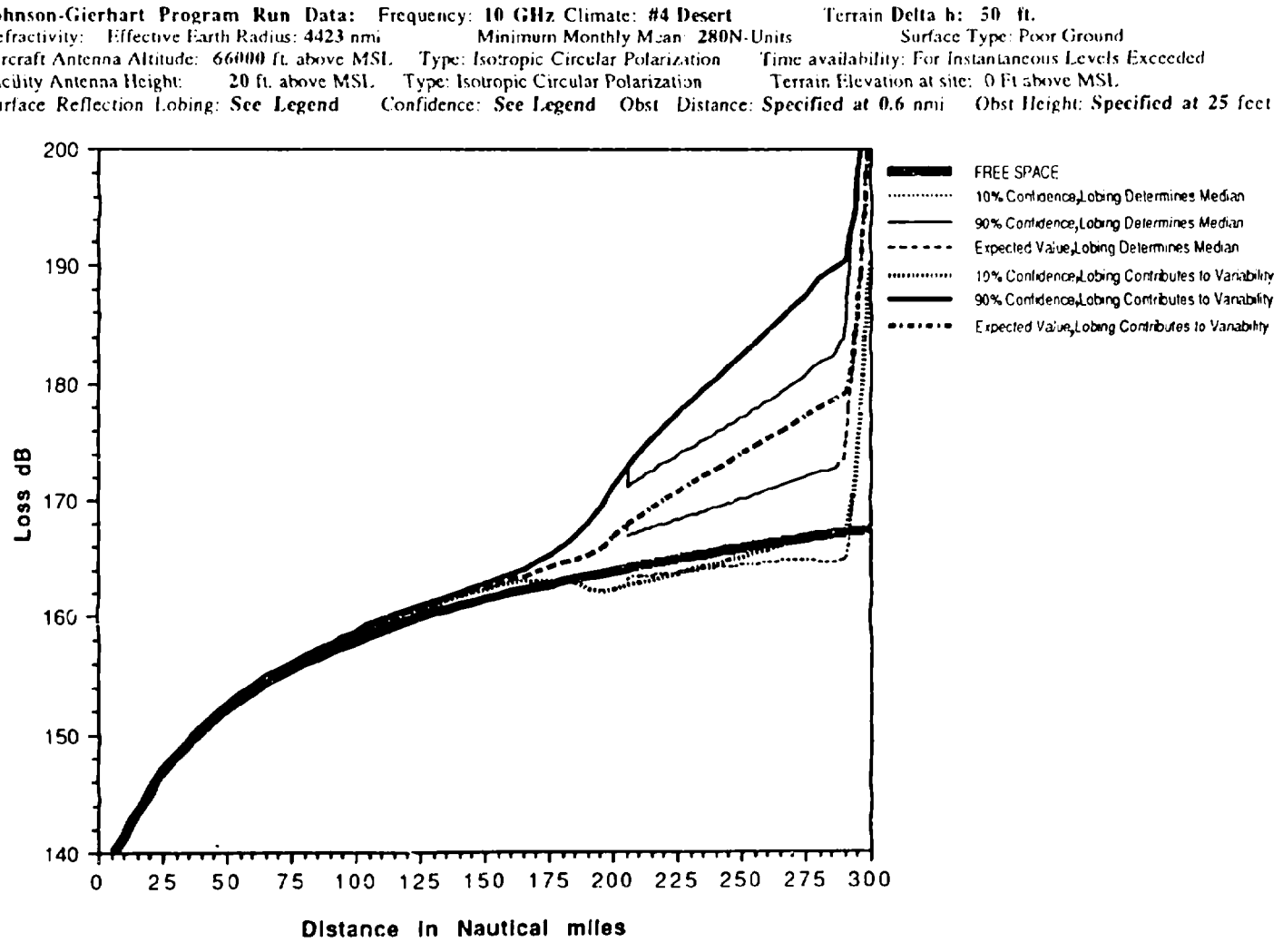

Figure 3-55. Basic Transmission Loss; Terrain Roughness Δh = 50 ft, 25-ft Obstacle, 10 GHz, h_2 = 66,000 ft, h_1 = 20 ft

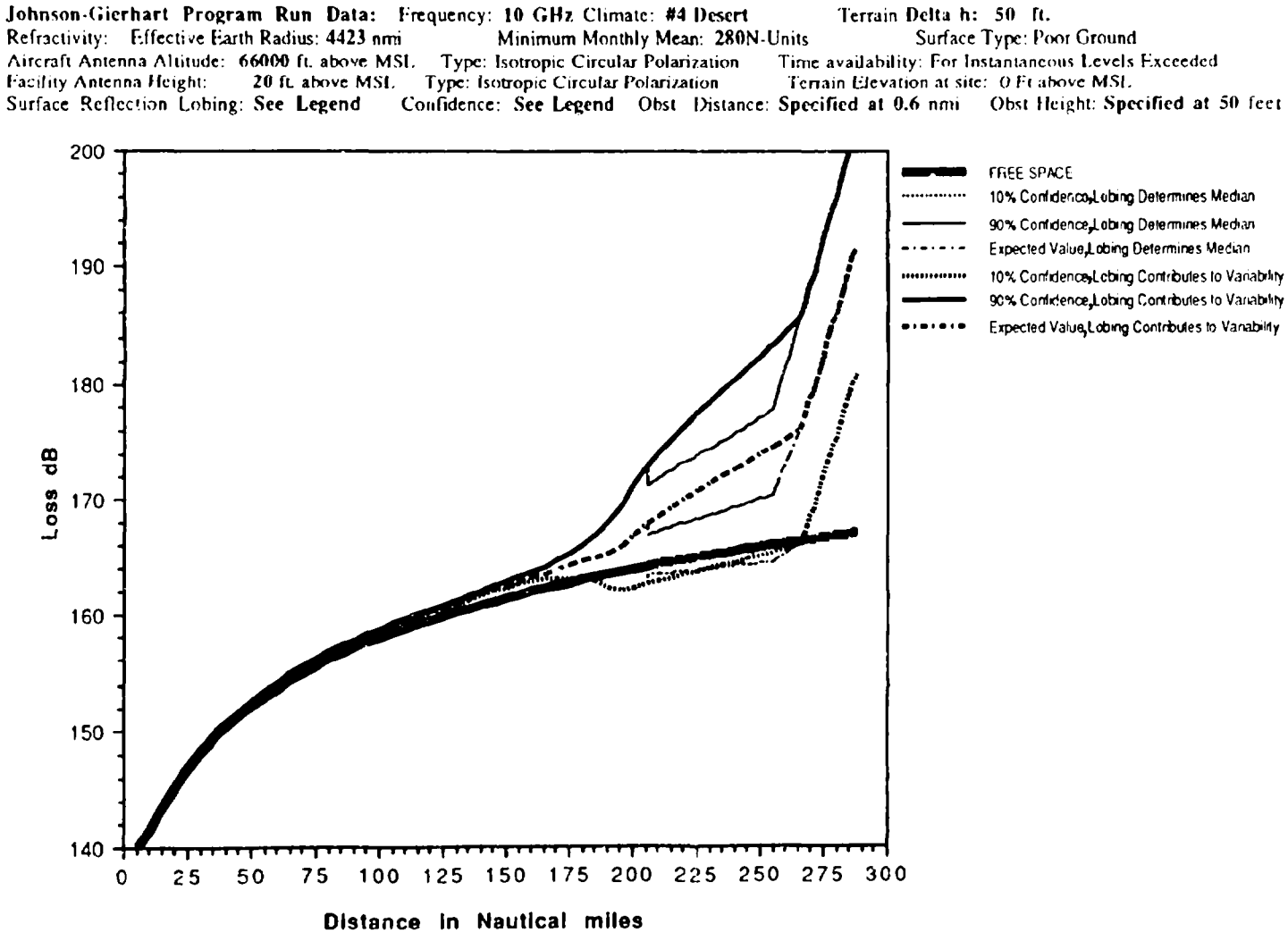

Figure 3-56. Basic Transmission Loss; Terrain Roughness Δh = 50 ft, 50-ft Obstacle, 10 GHz, h_2 = 66,000 ft, h_1 = 20 ft

SECTION 4

APPLICABILITY TO PROBABILITY OF DETECTION

Since the basic transmission loss expressed as a numeric $l_b(d)$ is log-normally distributed or two-piecewise log-normally distributed for the scenarios of interest (see figure 2-3), care should be exercised in how one uses the quantiles of basic transmission loss in determining the probability of detection. The probability of detection for a system whose numeric system margin **m** is log-normally distributed can be significantly less than that for a system whose numeric system margin **m** is composed of deterministic signal power and exponentially-distributed noise power. The selected model for the probability of detection of single-detection events is similar to that reported by Hagn [31].

The components of the model are discussed in the following sequence: system margin parameters, channel adequacy, required system margin, signal-to-noise ratio for a system margin of zero decibels, and mean signal-to-noise ratio required to required to achieve channel adequacy.

4.1 SYSTEM MARGIN PARAMETERS

The system margin $M(d,r_i)$ in decibels is defined as

$$M(d,r_i) = S(d) - N - R(r_i) \tag{4.1}$$

where

S(d) = available signal power referred to the output terminals of the equivalent loss-free receiving antenna at a great circle distance d from the transmitting antenna (dBm)

N = system available noise power referred to the output terminals of the equivalent loss-free receiving antenna (dBm)

$R(r_i)$ = $\left[\left(\langle S(d)\rangle - \langle N\rangle\right) \mid \langle M\rangle = 0\right]$ = predetection mean signal-to-noise ratio required for a long-term mean system margin $\left\langle M(d,r_i)\right\rangle = 0$ *decibels* (numeric system margin $\langle m\rangle = 1$) with information of quality r_i (dB). Mean signal-to-noise ratio in decibels is defined as $\langle S(d)\rangle - \langle N\rangle$. Long-term system margin is defined in subsection 4.2.

The information quality r_i might be the bit error probability in a digital communications system or the false alarm probability in a radar system.

If the system available noise power is primarily from an interferer at a great-circle distance d_2 from the receiving antenna and N is explicitly given as $N(d_2)$, then the system margin M is given by

$$M(d_1, d_2, r_i) = S(d_1) - N(d_2) - R(r_i) \tag{4.2}$$

where d_1 is the great-circle distance of the signal source. The quantiles of basic transmission loss obtained from the Johnson-Gierhart program may be used to determine both $S(d_1)$ and $N(d_2)$ if the propagation paths from the signal source and interferer are applicable to the Johnson-Gierhart program. In order to simplify the notation, the following discussion will use the notation of equation 4.1, although the discussion is equally applicable to equation 4.2.

The available signal noise S(d) and the system available noise power N may be expressed as

$$S(d) = \sum_{j=1}^{J} X_j + L_b(d) \tag{4.3}$$

$$N = \sum_{k=1}^{K} Y_k \tag{4.4}$$

where X and Y are statistically-independent stochastic (or deterministic) parameters (expressed in decibels) that contribute to the signal S(d) and noise N, respectively. In the above expressions, X and Y are assumed to be independent of the great-circle distance d. The parameters X_j and Y_k are given in reference 29 for a radio system. The corresponding numeric parameters x_j and y_k are given in reference 30 for a radar system.

Since the expected value of a sum of statistically-independent random variables is equal to the sum of each random variable's expected value, the expected value in decibels of the system margin $M(d,r_i)$ is given by

$$\langle M(d,r_i)\rangle = \sum_{j=1}^{J}\langle X_j\rangle - \sum_{k=1}^{K}\langle Y_k\rangle + \langle L_b(d)\rangle - R(r_i) \tag{4.5}$$

where $R(r_i)$ is treated as a deterministic quantity.

Since the variance of a sum of statistically-independent random variables is equal to the sum of the respective variances, the standard deviation (square root of variance) in decibels of the system margin $M(d,r_i)$ is given by

$$\sigma_M = \left[\sum_{j=1}^{J}\sigma_{X_j}^2 + \sum_{k=1}^{K}\sigma_{Y_k}^2 + \sigma_{L_b(d)}^2\right]^{\frac{1}{2}} \tag{4.6}$$

The model, which one selects to estimate each margin stochastic parameter in equations 4.1 through 4.4, has an uncertainty associated with it. The model uncertainty occurs because the empirical data base has a situation variability (resulting from uncertainties in the experimental set-up at each time and location) that is in addition to time and location variabilities.

The model uncertainties are assumed to be independent random variables whose sum is a zero-mean random variable. In equation 4.6, the model uncertainty associated with each margin parameter is included in the variances of each margin parameter. The variance of each margin parameter is the sum of the variances of the location variability, time variability, and model uncertainty of the margin parameter.

4.2 CHANNEL ADEQUACY

If the system margin $M(d,r_i)$ were a deterministic quantity, channel adequacy would be characterized by the successful detection of a single-detection event and would occur when $M(d,r_i) \geq 0$. However, the system margin $M(d,r_i)$ is a stochastic parameter with short-term (local) and long-term probability density functions. Short-term refers to time periods less than or equal to a single-event detection time. Long-term refers to time periods greater than a single-event detection time. For example, the numeric system margin $m(d,r_i)$ might be composed of noise power that is exponentially-distributed locally but log-normally distributed in the long-term.

Since the system margin $M(d,r_i)$ is a stochastic parameter, channel adequacy is characterized in terms of the probability of the event $[M(d,r_i) \geq 0]$, denoted $\text{prob}[M(d,r_i) \geq 0]$. The quantity $\text{prob}[M(d,r_i) \geq 0]$ is also referred to as the "channel availability," "channel accessibility," or "probability of detection of a single-detection event." The channel availability is equal to the fraction of successful single detection attempts to the total number of single detection attempts. A successful detection event is defined as a detection event that provides information of quality r_i or better. The channel of the entire system is defined to be adequate if

$$\text{prob}\left[M(d,r_i) \geq 0\right] \geq p_r \tag{4.7}$$

where

p_r = required channel availability (or required probability of detection of a single-detection event)

= minimum required fraction of successful single-detection attempts to the total number of single-detection attempts

The minimum value of $\text{prob}\left[M(d,r_i) \geq 0\right]$ that achieves channel adequacy occurs when the equality sign of equation 4.7 is satisfied, namely, $\text{prob}\left[M(d,r_i) \geq 0\right] = p_r$.

The signal-to-noise ratio expected value $\langle S(d)\rangle - \langle N\rangle|p_r$ that satisfies the minimum condition for channel adequacy is found from equation 4.7 to be

$$\begin{aligned}\left(\langle S(d)\rangle - (N)\right)|p_r &= \left\langle M(d,r_i)\right\rangle|p_r + R(r_i)\rangle \\ &= \sigma_M \cdot \left[\left(\langle M\rangle / \sigma_M\right)|p_r\right] + R(r_i)\end{aligned} \tag{4.8}$$

where $\left\langle M(d,r_i)\right\rangle|p_r$ is the expected value of the system margin required to achieve the channel adequacy p_r and $R(r_i)$ is defined to be a deterministic quantity equal to the signal-to-noise ratio required to achieve information of quality r_i with $\langle M\rangle = 0$ decibels. The determination of these parameters, for numeric system margins that are log-normally distributed, are discussed in subsections 4.3 through 4.5. It should be noted that if a numeric system margin m is log-normally distributed, then the signal-to-noise voltage envelope $m^{1/2}$ is also log-normally distributed.

4.3 REQUIRED SYSTEM MARGIN

For a normally-distributed system margin $M(d,r_i)$ in decibels, expected value $\langle M \rangle$ in decibels, and standard deviation σ_M in decibels, the probability of a non-negative system margin is given by equations (A.5) and (A.6) of appendix A as

$$\text{prob}\left[M(d,r_i) \geq 0\right] = F_Z(\langle M \rangle/\sigma_M), \text{ M normally-distributed} \tag{4.9}$$

where

$F_Z(\langle M \rangle/\sigma_M)$ = cumulative distribution function, evaluated at the quantile $\langle M \rangle/\sigma_M$, of the normally-distributed random variable $Z = (M - \langle M \rangle)/\sigma_M$ with zero mean and unit variance.

It should be noted that equation 4.9 is a correction to the expression for $\text{prob}\left[M(d,r_i) \geq 0\right]$ given by Hagn [31]. The probability of a non-negative system margin (channel availability, probability of detection of a single detection event) given by equation 4.9 is plotted in figure 4-1 on normal probability paper as a function of the quantile $\langle M \rangle/\sigma_M$. For example, $\text{prob}\left[M(d,r_i) \geq 0\right]$ equals 10, 50, and 90 percent for $\langle M \rangle/\sigma_M$ equal to -1.25, 0, and 1.25, respectively.

Consider now a two-piecewise normally-distributed system margin $M(d,r_i)$ in decibels with a breakpoint at the value M_0 and whose probability density function $f_M(M)$ is composed of the probability density functions $(1/A)f_{M_1}(M)$ for $-\infty \leq M \leq M_0$ and $(1/A)f_{M_2}(M)$ for $M_0 \leq M \leq \infty$ where $f_{M_1}(0) \geq f_{M_2}(0)$ and A is a normalizing constant so that the cumulative distribution functions of M evaluated at $M = 0$ is equal to unity $\left[F_M(\infty) = 1\right]$. The probability

IL3223

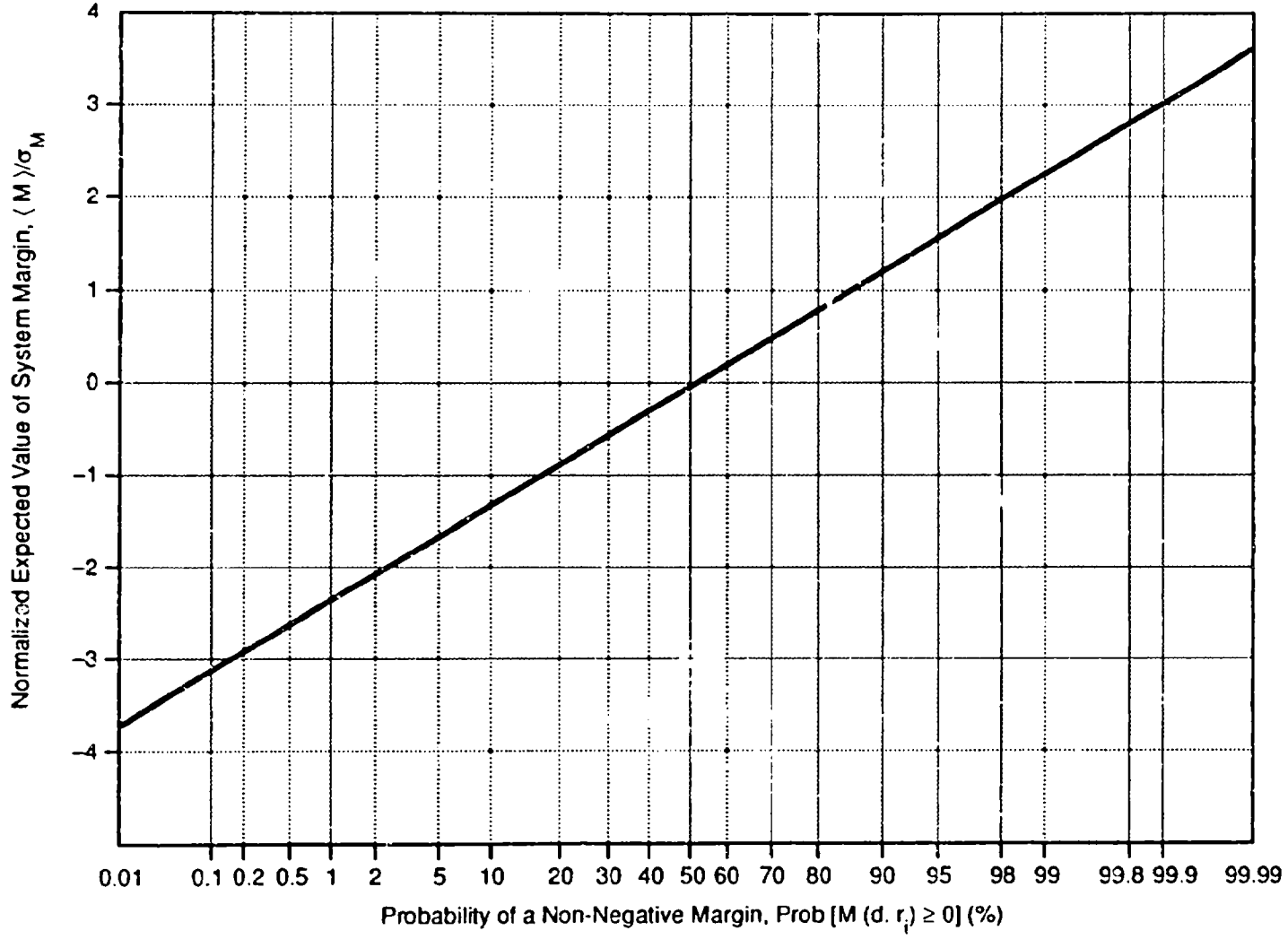

Figure 4-1. Probability M ≥ 0 Margin for a Normally-Distributed System Margin M in Decibels

density functions $f_{M_1}(M)$ and $f_{M_2}(M)$, defined over the infinite domain, have expected values $\langle M_1 \rangle$ and $\langle M_2 \rangle$, respectively, and standard deviations σ_{M_1} and σ_{M_2}, respectively. The probability of a non-negative system margin is given by equations B.7 and B.8 of appendix B for a two-piecewise normally-distributed random variable as

$$\text{prob}[M \geq 0] = \begin{cases} 1 - (1/A) F_{z_1}\left[-\langle M_1 \rangle / \sigma_{M_1} \right], & M_O \geq 0 \\ 1 - \frac{1}{A}\left\{ F_{z_1}\left[-\langle M_1 \rangle / \sigma_{M_1} \right] + F_{z_2}\left[\left(M_O - \langle M_2 \rangle \right) / \sigma_{M_2} \right] \right\} - F_{z_1}\left[\left(M_O - \langle M_1 \rangle \right) / \sigma_{M_1} \right], & \\ M_O < 0 \end{cases} \tag{4.10}$$

where

M = two-piecewise normally-distributed system margin with a breakpoint at the value M_O (dB)

$A = F_{Z_1}\left[\left(M_o - \langle M_1 \rangle \right) / \sigma_{M_1} \right] + F_{Z_2}\left[-\left(M_0 - \langle M_2 \rangle \right) / \sigma_{M_2} \right]$

$F_{Z_1}(z_1)$ = cumulative distribution function, evaluated at the quantile z_1, of the normally-distributed random variable $Z_1 = \left(M_1 - \langle M \rangle \right) / \sigma_{M_1}$ with zero-mean and unit variance.

$F_{Z_2}(z_2)$ = cumulative distribution function, evaluated at the quantile z_2, of the normally-distributed random variable $Z_2 = \left(M_2 - \langle M \rangle \right) / \sigma_{M_2}$ with zero-mean and unit variance.

The quantities $F_{Z_i}(z_i)$ for $i = 1, 2$ are readily evaluated from figure 4-1 if one substitutes $F_{Z_i}(z_i)$ for the abscissa and z_i for the ordinate.

For a normally-distributed system margin $M(d,r_i)$ in decibels, the expected value $\langle M(d,r_i)\rangle|p_r$ that satisfies the minimum condition for channel adequacy in equation 4.7 is given by

$$\langle M(d,r_i)\rangle|p_r = \sigma_M \bullet F_Z^{-1}\left[(\langle M\rangle / \sigma_M)|p_r\right], \text{ M normally-distributed} \qquad (4.11)$$

where

$$F_Z\left[\left(\langle M\rangle / \sigma_M\right)|p_r\right] = \text{prob}\left[M(d,r_i) \geq 0\right] = p_r$$

and σ_M = system margin standard deviation given by equation 4.6.

It should be noted that σ_M in equation 4.5 is independent of the required channel adequacy p_r. The quantity $(\langle M\rangle / \sigma_M)|p_r$ is the quantile $\langle M\rangle/\sigma_M$ in figure 4-1 that corresponds to $\text{prob}\left[M(d,r_i) \geq 0\right] = p_r$.

For a two-piecewise normally-distributed system margin $M(d,r_i)$, the quantile $(\langle M\rangle / \sigma_M)|p_r$ may be determined by relating $\langle M\rangle$ and σ_M to $\langle M_1\rangle$, $\langle M_2\rangle$, σ_{M_1} and σ_{M_2}. These relationships can be determined from the given system margin probability density function analogous to equation B.1 of appendix B but will not be demonstrated here.

4.4 SIGNAL-TO-NOISE RATIO FOR A SYSTEM MARGIN OF ZERO DECIBELS

The mean signal-to-noise ratio $R(r_i)$ required to achieve information of quality r_i with $\langle M\rangle = 0$ (see equation 4.8) is a function of the signal and noise power probability density functions, the signal waveform, the type of detector, and the detection process. A concise history of the development of the statistical theory of detection with emphasis on radar detection is given by Blake [33].

Long-term numerical values of $R(r_i)$ may be assigned to several cases in which the numeric system margin $m(d,r_i)$ is composed of numeric available noise power n that is exponentially-distributed (both locally and long-term) and numeric available signal power s(d) that is locally constant [34, 35]. For a non-fading constant signal power s_o, numeric available noise power n that is exponentially-distributed with mean <n>, and a numeric zero system margin r_o, the probability density function of the numeric system random variable m is given by

$$f_m(m) = \begin{cases} m^{-2} m_o \exp(-m_o / m), & m \geq 0 \\ 0 & , \quad m < 0 \end{cases} \tag{4.12}$$

where $m_o = s_o/(<n>r_o)$.

The density function $f_m(m)$ is inverted-gamma-1 distributed with a mean <m> and standard deviation σ_m that are infinite [36]. The signal plus noise amplitude modulus (envelope) is Rician-distributed. Noise power that is exponentially-distributed has a noise amplitude with real and imaginary quadrature components that are normally distributed, a modulus (envelope) that is Rayleigh-distributed and an angle (phase) that is uniformly distributed. The signal power is defined to be locally constant if its variance, over a time interval less than a single-event detection time, is small compared to its mean power level over that interval. In references 34 and 35, the long-term signal is either constant (non-fading) or Rayleigh distributed (non-selective slow fading that is slow compared to a single-event detection time but fast compared to seasonal or hourly variations).

For these cases, a single look-up table or curve is sufficient to specify $R(r_i)$. For example, with r_i = probability of bit error in a communication system, the signal-to-noise ratio $R(r_i)$ is constructed from reference 34 and is plotted in figure 4-2 for several different signal waveforms and detection processes and for both non-fading and fading signals. Figure 4-2 is constructed from reference 34 by arbitrarily assigning a system margin $\langle M \rangle = 0$ decibels (numeric margin <m> = 1) to the values given in reference 34 and by treating $R(r_i)$ as a

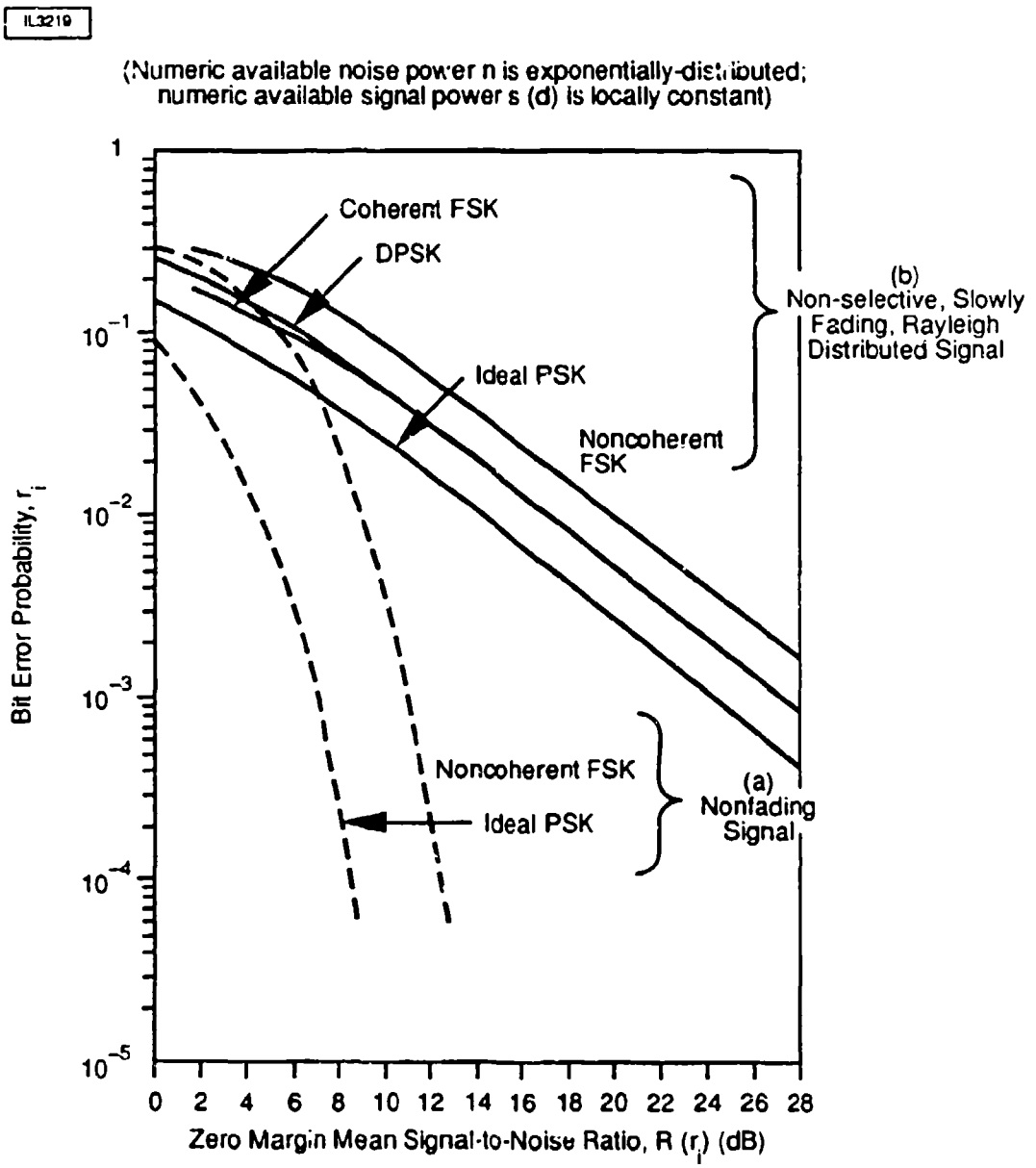

Figure 4-2. Zero-Margin Mean Signal-to-Noise Ratio Required for a Bit Error Probability r_i

a. Nonfading Signal
b. Raleigh Fading Signal

deterministic quantity. For a bit error probability $r_i = 0.1$ and noncoherent FSK, $R(r_i) \approx 5$dB and 9 dB for non-fading and fading signals, respectively. As a second example, consider r_i = probability of false alarm in a radar system with fading and non-fading signals. The required signal-to-noise ratio $R(r_i)$ may be constructed from Marcum [35] for a non-fluctuating target (signal) and by Swerling [37, 38] for a Swerling 1 non-fluctuating target (signal). The results are plotted in figure 4-3 which is reconstructed from figures 2.3 and 2.6 of reference 33 by arbitrarily assigning a system margin $\langle M \rangle = 0$ decibels to those values of signal-to-noise ratio that yield a probability of detection = 0.5. For a false alarm probability $r_i = 10^{-6}$, $R(r_i) \approx$ 11 dB and 13 dB for non-fading and fading signals, respectively.

Numerical values of $R(r_i)$ have also been tabulated for a few cases in which the numeric system margin $m(d, r_i)$ is log-normally distributed (locally and long term) for noise and signals that are both log-normally distributed [39]. For such cases, multiple lookup tables are required to specify $R(r_i)$.

Consider now a numeric system margin $m(d, r_i)$ that is log-normally distributed in the long-term and that locally, the numeric available signal power s(d) is constant and the numeric available noise power n is exponentially-distributed. Therefore, the long-term signal and/or noise power may be log-normally distributed. Let us assume that the detected information of quality r_i is a function of only the short-term (local) signal-to-noise ratio during a single-event detection time. The mean signal-to-noise ratio $R(r_i)$.required to detect information of quality r_i at zero dB system margin is then independent of the long-term system margin distribution. Figures 4-2 and 4-3 are therefore applicable to a numeric system margin that is log-normally distributed in the long-term but whose numeric available signal power s(d) is locally constant and whose numeric available noise power n is locally exponentially-distributed.

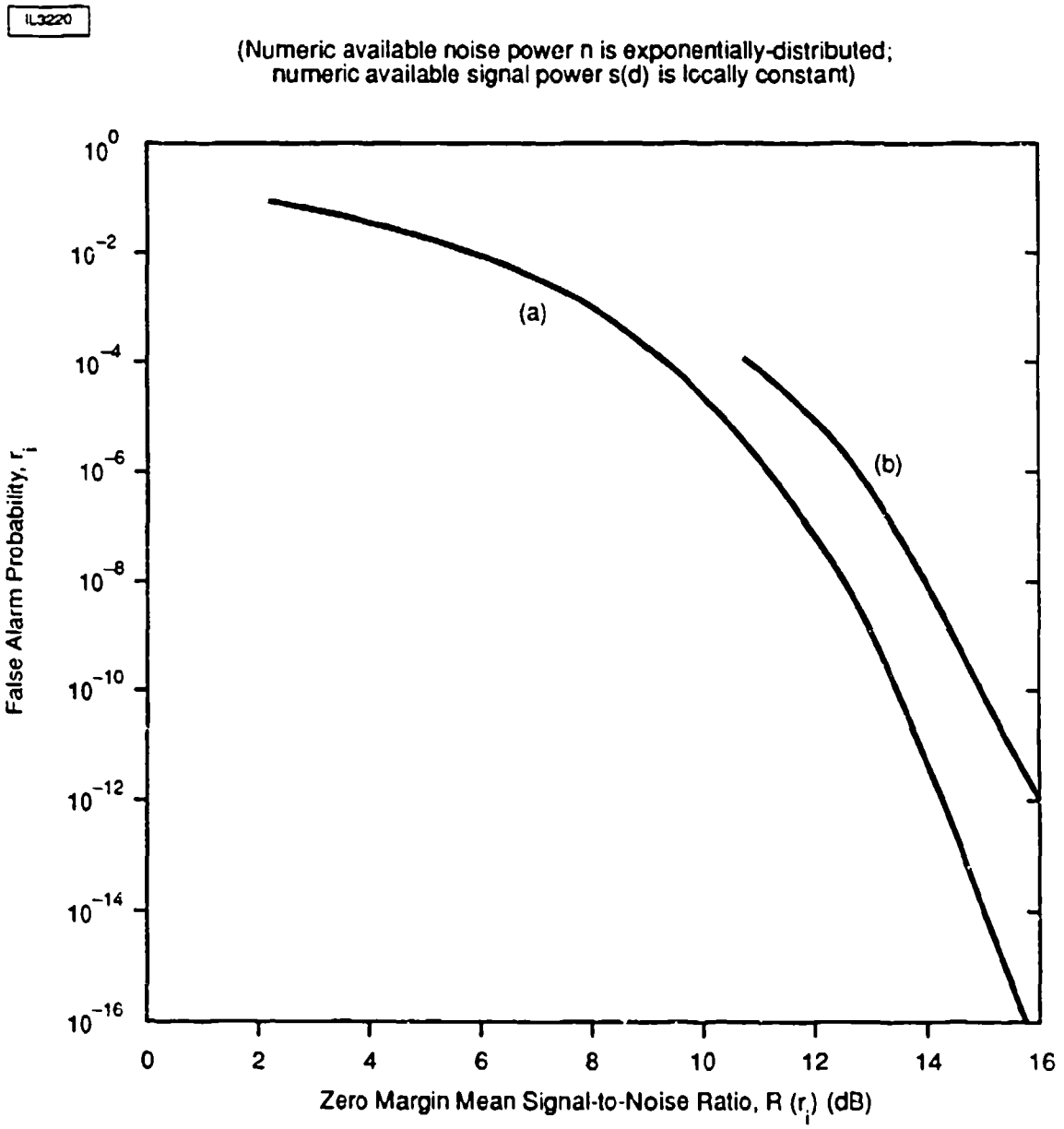

Figure 4-3. Zero-Margin Mean Signal-to-Noise Ratio Required for a False Alarm Probability r_i
a. Marcum Non-Fluctuating Target (Signal), Single Pulse, Linear Detection
b. Swerling Case 1 Fluctuating Target (Signal), Single Pulse, Square-Law Detector

4.5 MEAN SIGNAL-TO-NOISE RATIO REQUIRED TO ACHIEVE CHANNEL ADEQUACY

Channel adequacy is achieved when the probability of a non-negative system margin is greater than or equal to a required single-event detection probability p_T (see equation 4.7). The mean signal-to-noise ratio $(\langle S(d)\rangle - \langle N\rangle)|p_r$ in decibels required to achieve a single-event detection probability p_T is given by equation 4.8. In equation 4.8, the system margin standard deviation σ_M is given by equation 4.6 and the quantile $(\langle M\rangle / \sigma_M)|p_r$ is given by figure 5 for a normally-distributed system margin M in decibels. Examples of the signal-to-noise ratio $R(r_i)$ required to detect information of quality r_i at a system margin $\langle M\rangle = 0$ decibels are given in figures 4-2 and 4-3.

As an illustration of the mean signal-to-noise ratio required to achieve channel adequacy, consider a radar system with a single-pulse linear detector, locally non-fluctuating target, locally constant numeric available signal power s(d), and locally exponentially-distributed numeric available noise power n. To achieve channel adequacy the radar is required to have a single-event detection probability greater than or equal to p_T with a false alarm probability less than or equal to r_i. The mean signal-to-noise ratio $(\langle S(d)\rangle - \langle N\rangle)|p_r$ required to achieve channel adequacy for $r_i = 10^{-6}$ and $p_T = 0.1, 0.5, 0.9$ is summarized in table 4-1.

Using the subscript 1 to denote a numeric system margin **m** whose long-term distribution is characterized by a constant numeric available signal power s(d) and an exponentially-distributed numeric available noise power **n**, then $(\langle S(d)\rangle - \langle N\rangle)_1|p_r = 8.8$, 11.2, and 13.2 dB for $p_T = 0.1, 0.5, 0.9$, respectively (see figure 2.3 of reference 33 where the signal plus noise envelope is assumed to have a Rician distribution). The zero-margin required signal-to-noise ratio $R(10^{-6}) = 11.2$ dB corresponding to $p_T = 0.5$ [see figure 4-3, curve (a)]. Using the subscript 2 to denote a numeric system margin **m** that is long-term log-normally distributed, the quantile $(\langle M\rangle / \sigma_M)_2|p_r = -1.3, 0, 1.3$ for $p_T = 0.1, 0.5, 0.9$, respectively (see figure 4-1).

IL3231

Table 4-1. Mean Signal-to-Noise Ratio Required for a Detection Probability p_r with False-Alarm Probability r_i

Single-Pulse Linear Detector
Locally Non-Fluctuating Target
$r_i = 10^{-6}$
Signal Power is Locally Constant
Numeric Noise Power is Locally Exponentially-Distributed with $\sigma_n = \langle n \rangle$

Single-Event Detection Probability, p_r	$R(r_i)$ (dB) (Blake, 1990, $p_r = 0.5$)*	$(\langle M \rangle / \sigma_M) \mid p_r$ (Figure 4-1)	Mean Signal-to-Noise Ratio, $(\langle S(d) \rangle - \langle N \rangle) \mid p_r$ (dB)							
			Long-Term Distribution of Numeric System Margin m							
			Inverted-Gamma-1** (Blake, 1990)*	Log Normal						
				System Margin Standard Deviation σ_M (dB)						
				1.0	2.0	3.0	4.0	5.0	6.0	7.0
0.1	11.2	−1.3	8.8	9.9	8.6	7.3	6.0	4.7	3.4	2.1
0.5	11.2	0	11.2	11.2	11.2	11.2	11.2	11.2	11.2	11.2
0.9	11.2	1.3	13.2	12.5	13.8	15.1	16.4	17.7	19.0	20.3

* Blake, L.V., 1990, *Radar Handbook* (M. Skolnik, Editor), New York: McGraw-Hill, Second Edition, Chapter 2, Figure 2.3. $R(r_i) = D_o$ for $P_{f\cdot} = 10^{-6}$ and $p_r = 0.5$.

** An Inverted-Gamma-1 distributed numeric system margin corresponds to a constant signal power and exponentially-distributed numeric noise power.

The required signal-to-noise ratio $(\langle M\rangle / \sigma_M)_2|p_r$ relative to $(\langle M\rangle / \sigma_M)_1|p_r$ is given by

$$\frac{(\langle S(d)\rangle - \langle N\rangle)_2|p_r}{(\langle S(d)\rangle - \langle N\rangle)_1|p_r} = \begin{cases} < 1; & 0 \le p_r < 0.5, \sigma_M \ge 1.9 \text{ dB} \\ 0; & p_r = 0.5 \\ > 1; & 0.5 < p_r \le 1, \sigma_M \ge 1.5 \text{ dB} \end{cases} \tag{4.13}$$

In equation 4.13, the conditions on σ_M were obtained from equation 4.8 by setting $\left[(\langle S(d)\rangle - \langle N\rangle)_2|p_r = 0.1\right] = 8.8$ dB, $\left[(\langle S(d)\rangle - \langle N\rangle)_2|p_r = 0.9\right] = 13.2$ dB, $\left[(\langle M\rangle / \sigma_M)_2|p_r = 0.1\right]$ $= -1.3$, and $\left[(\langle M\rangle / \sigma_M)_2|p_r = 0.9\right] = 1.3$.

The required signal-to-noise ratio $\left[(\langle S(d)\rangle - \langle N\rangle)_2|p_r = 0.9\right]$ exceeds $\left[(\langle S(d)\rangle - \langle N\rangle)_1|p_r = 0.9\right]$ by 1.9, 3.2, 4.5, 6.8, and 7.1 dB for σ_M = 3, 4, 5, 6, 7 dB, respectively. These values of σ_M are typical for the scenarios of interest. In table 2-1, the standard deviation σ_{L_b} of basic transmission loss $L_b(d)$ varies from 0.1 dB to 8.0 dB. The system margin standard deviation σ_M for those scenarios will exceed σ_{L_b} by the amount given by equation 4.6.

Equation 4.13 demonstrates that the required signal-to-noise ratio $\langle S(d)\rangle - \langle N\rangle|p_r$ for $p_T = 0.5$ is independent of σ_M and independent of the distribution of the system margin M. For $0 \le p_T < 0.5$ and sufficiently large values of σ_M, the required signal-to-noise ratio $(\langle S(d)\rangle - \langle N\rangle)_2|p_r$ is less than $(\langle S(d)\rangle - \langle N\rangle)_1|p_r$. For $0.5 < p_T \le 1$ and sufficiently large values of σ_M, the required signal-to-noise ratio $(\langle S(d)\rangle - \langle N\rangle)_2|p_r$ is greater than $(\langle S(d)\rangle - \langle N\rangle)_1|p_r$.

SECTION 5

CONCLUSIONS

The Johnson-Gierhart tropospheric propagation program of the Institute for Telecommunications Sciences is a useful analytical tool for predicting tropospheric excess propagation loss (relative to free-space loss) for cases including SHF air-to-ground paths within or on the radio horizon. The principal loss (gain) mechanisms for these paths are atmospheric absorption, atmospheric refraction, surface multipath interference, smooth spherical Earth diffraction, and single knife-edge diffraction from irregular terrain and/or a site-specified obstacle. The program uses a semi-empirical database to statistically weigh the losses from these mechanisms. The excess propagation loss (expressed in dB) increases with increasing range.

This paper reports numerical results of excess propagation loss at frequencies of 2 to 15 GHz for an airborne antenna at altitudes of 22,000 ft to 66,000 ft, a ground-based antenna at altitudes of 10 ft and 20 ft, and paths over smooth and irregular terrain extending to the smooth Earth radio horizon. The excess propagation loss is either log-normally distributed or two-piecewise log-normally distributed.

Atmospheric attenuation by oxygen, water vapor, and precipitation causes an excess propagation loss that increases linearly in decibels with increasing range and can exceed an expected value of 3 dB at 10 GHz from water vapor alone for ranges as close as halfway to the radio horizon.

Atmospheric surface refractivity (which is largest in an equatorial climate and the least in a desert climate) causes an excess propagation loss in a desert climate that can be 30 dB more than that in an equatorial climate for ranges at or within the equatorial climate's smooth Earth radio horizon.

Surface multipath interference causes an excess propagation loss lobing pattern with peak losses that increase with increasing range. The peak losses exceed 30 dB for paths over smooth spherical Earth but are less than 2 dB for paths over slightly rough Earth (interdecile terrain roughness $\Delta h = 50$ ft).

Smooth spherical Earth diffraction reduces the depth of the multipath lobing pattern null on the radio horizon from an excess propagation loss of ∞ dB to approximately 10 dB to 20 dB [42].

Single knife-edge diffraction by a site-specified obstacle (50-ft tall at a distance of 0.6 nmi from the ground-based antenna) reduces the distance to the radio horizon by approximately 10 to 15 percent (30 nmi), whereas slightly rough terrain (interdecile terrain roughness $\Delta h = 50$ ft) has no such effect.

The magnitude and distribution of the resultant excess propagation loss from these mechanisms, at ranges as close as half-way to the radio horizon, yield probabilities of detection and mean signal-to-noise ratios that can be appreciably less that those obtained by assuming free-space propagation.

Since the excess propagation loss expressed in decibels is log-normally distributed or two-piecewise log-normally distributed for air-to-ground paths, within or on the radio horizon, care should be exercised in how one uses the quantiles of excess propagation loss in determining the required mean signal-to-noise ratio required to achieve a given probability of detection. The mean signal-to-noise ratio required to achieve probabilities of detection greater than 50 percent for a system whose numeric system margin **m** is log-normally distributed can be significantly greater than that for a system whose numeric system margin **m** is composed of deterministic signal power and exponentially-distributed noise power.

LIST OF REFERENCES

1. Rice, P. L., A. G. Longley, K. A. Norton, and A. P. Barsis, January 1967, "Transmission Loss Prediction for Tropospheric Communication Circuits," *NBS Tech. Note 101*, Vols. I and II (revised). Also available as Vol. I, NTIS, AD 687820; Vol. II, NTIS, AD 687821.

2. Longley, A. G., and P. L. Rice, 1968, "Prediction of Tropospheric Radio Transmission Loss Over Irregular Terrain: A Computer Method – 1968," ESSA Tech. Rep. ERL-79-ITS 67, U.S. Department of Commerce, Boulder, CO. Also available as NTIS, AD 676874.

3. Hufford, G. A., July 1979, *The Longley-Rice Model – An Implementation, 1979 Programmer's and User's Guide*, Institute for Telecommunication Sciences, Boulder, CO.

4. Hufford, G. A., A. G. Longley, and W. A. Kissick, April 1982, *A Guide to the Use of the ITS Irregular Terrain Model in the Area Prediction Mode*, NTIA Rep. 82-100, U.S. Department of Commerce, Boulder, CO.

5. Hufford, G. A., 30 January 1985, *Modifications to the Use of the ITS Irregular Terrain Model in the Point-to-Point Mode*, NTIA Memo, U.S. Department of Commerce, Boulder, CO.

6. Gierhart, G. D., and M. E. Johnson, September 1983, *The IF-77 Electromagnetic Wave Propagation Model*, Institute for Telecommunication Sciences, Report DOT/FAA/ES-83/3. Also available as NTIS, AD A134504.

7. Johnson, M. E., and G. D. Gierhart, March 1978, "Applications Guide, Propagation and Interference Analysis Computer Programs (0.1 to 20 GHz)," Institute for Telecommunication Sciences, Report FAA-RD-77-60. Also available as NTIS, AD A053242.

8. Gierhart, G. D., and M. E. Johnson, May 1978, "Propagation Model (0.1 to 20 GHz) Extensions for 1977 Computer Programs," Institute for Telecommunication Sciences, Report FAA-RD-77-120. Also available as NTIS, AD A055605.

9. Lustgarten, M. N., and J. A. Madison, August 1977, "An Empirical Propagation Model (EPM-73)," *IEEE Transactions Electromagnetic Compatibility*, Vol. EMC-19, No. 3, pp. 301-309.

10. Weissberger, M., R. Meidenbauer, H. Riggens, and S. Marcus, September 1982, *Radio Wave Propagation: A Handbook of Practical Techniques for Computing Basic Transmission Loss and Field Strength*, Electromagnetic Compatibility Analysis Center, Report ECAC-HDBK-82-049. Also available as NTIS, AD A122090.

11. Meeks, M. L., March 1982, "A Propagation Experiment Combining Reflection and Diffraction," *IEEE Transactions Antennas and Propagation*, Vol. AP-30, pp. 318-321.

LIST OF REFERENCES (CONTINUED)

12. Meeks, M. L., May 1983, "VHF Propagation Over Hilly, Forested Terrain," *IEEE Transactions Antennas and Propagation*, Vol. AP-31, pp. 483-489.

13. Ayasli, S., August 1986, "SEKE: A Computer Model for Low Altitude Radar Propagation Over Irregular Terrain," *IEEE Transactions Antennas and Propagation*, Vol. AP-34, No. 8, pp. 1013-1023.

14. Shatz, M. P., and G. H. Polychronopoulos, August 1990, "An Algorithm for the Evaluation of Radar Propagation in the Spherical Earth Diffraction Region," *IEEE Transactions Antennas and Propagation*, Vol. AP-38, No. 8, pp. 1249-1252.

Weiner, M. M., E. Jappe, and N. J. Johnson, October 1982, *Input Parameter Specification for the Longley-Rice and Johnson-Gierhart Tropospheric Radio Propagation Programs, 0.02–40 GHz*, ESD-TR-82-400, Electronic Systems Division, AFSC, Hanscom AFB, MA 01731-5000. Also available as NTIS, AD A122582.

16. Weiner, M. M., March 1986, "Use of the Longley-Rice and Johnson-Gierhart Tropospheric Radar Propagation Programs: 0.02–20 GHz," *IEEE Journal on Selected Areas in Communications*, Vol. SAC-4, No. 2, pp. 297-307.

17. Murray, J. P., August 1982, "An Atlas of Propagation Curves for Tactical E tronic Warfare Planning in Ground-to-Ground Scenarios," *Propagation Effects of ECM-Resistant Systems in Communication and Navigation*, 30th Symposium, Electromagnetic Wave Propagation Panel, Copenhagen, Denmark (24–28 May 1982), H. J. Albrecht, ed., AGARD Conference Proceedings, No. CP-331, NTIS AD A123251, pp. 16-1 -- 16-14.

18. CCIR, 1978, "The Concept of Transmission Loss in Studies of Radio Systems, Recommendation 341," Vol. 1, Annex 1, pp. 148, 14th Plenary Assembly, Kyoto, Japan (1978), International Radio Consultative Committee, International Telecommunications Union, Geneva, Switzerland.

19. Meeks, M. L., July 1981, "Radar Propagation at Low Altitudes: A Review and Bibliography," MIT Lincoln Lab., Technical Report 580, NTIS, AD A103773. Also available in book form (Dedham, MA: Artech House, 1982).

20. Beckman, P., and A. Spizzichino, 1963, *The Scattering of Electromagnetic Waves From Rough Surfaces*, New York: Pergamon Press, pp. 244-246.

21. Longley, A. G., R. L. Reasoner, and V. L. Fuller, 1971, "Measured and Predicted Long-term Distributions of Tropospheric Transmission Loss," Office of Telecommunication Research and Engineering, Report OT/TRER 16. Available from U.S. Government Printing Office, Washington, D.C., 20402.

LIST OF REFERENCES (CONTINUED)

22. Johnson, M. E., and G. D. Gierhart, August 1979, "Comparison of Measured Data with IF-77 Propagation Model Predictions," Report FAA-RD-79-9, National Telecommunications and Information Administration, Boulder, CO. Also available as NTIS, AD A076508.

23. Longley, A. G., and P. L. Rice, 1968, "Prediction of Tropospheric Radio Transmission Loss Over Irregular Terrain: A Computer Method – 1968," ESSA Technical Report ERL-79-ITS 67, U.S. Department of Commerce, Boulder, CO, pp. 2-1 through 2-42 (Annex 2) and pp. 3-4 (Annex 3), NTIS, AD676874.

24. Weiner, M. M., December 1981, *Terrain and Sea Surface Truth: Profile Distributions*, ESD-TR-81-387, Electronic Systems Division, AFSC, Hanscom AFB, MA 01731-5000. Also available as NTIS, AD A110219.

25. Jakes, W. C., 1974, *Microwave Mobile C unicatio* , New York: John Wiley, p. 85.

26. CCIR, 1975, "Propagation Data Required for Transhorizon Radio-Relay Systems," Report 238-2, 13th Plenary Assembly, Geneva (1974), International Radio Consultative Committee, International Telecommunications Union, Geneva, Switzerland.

27. Johnson, M. E., and G. D. Gierhart, March 1978, "Applications Guide, Propagation and Interference Analysis Computer Programs (0.1 to 20 GHz)," Institute for Telecommunication Sciences, Report FAA-RD-77-60, NTIS, AD A053242., pp. 75, 103, and 104.

28. Rice, P. L., A. G. Longley, K. A. Norton, and A. P. Barsis, January 1967, "Transmission Loss Prediction for Tropospheric Communication Circuits," *NBS Technical Note 101*, Vol. I, pp. 10-1 through 10-29; Vol. II, pp. III-44 through III-53.

29. Weiner, M. M., March 1988, "Noise Factor of Receiving System with Arbitrary Antenna Impedance Mismatch," *IEEE Transactions on Aerospace and Electronic Systems*, Vol. 24, No. 2, pp. 133-140.

30. Weiner, M. M., November 1991, "Noise Factor and Antenna Gains in the Signal/Noise Equation for Over-the-Horizon Radar," *IEEE Transactions on Aerospace and Electronic Systems*, Vol. 27, No. 6, pp. 886-890.

31. Hagn, G. H., September 1980, "VHF Radio System Performance Model for Predicting Communications Operational Ranges in Irregular Terrain," *IEEE Transactions on Communications*, Vol. COM-28, No. 9, pp. 1637-1644.

32. Abromowitz, M., and I. Stegun, 1972, *Handbook of Mathematical Functions*, New York: Dover Publications, equation 7.1.1 (definition), pp. 310-311 (tables).

LIST OF REFERENCES (CONCLUDED)

33. Blake, L. V., 1990, "Prediction of Radar Range," *Radar Handbook* (M. Skolnik, editor), New York: McGraw-Hill, second edition, chapter 2, pp. 2.3, 2.4, 2.20 through 2.24.

34. Schwartz, M., W. R. Bennett, and S. Stein, 1966, *Communication Systems and Techniques*, New York: McGraw-Hill, pp. 298, 407-408.

35. Marcum, J. I., April 1960, "A Statistical Theory of Detection by Pulsed Radar and Mathematical Appendix," *IRE Transactions Information Theory*, Vol. IT-6, pp. 59-267.

36. Raiffa, H. and R. Shlaifer, 1961, *Applied Statistical Decision Theory*, Boston, MA: Harvard University, Division of Research, p. 227, equation 7.54, $r = 1$.

37. Swerling, P., April 1960, "Probability of Detection for Fluctuating Targets," *IRE Transactions Information Theory*, Vol. IT-6, pp. 269-308.

38. Swerling, P., July 1966, "Detection of Radar Echoes in Noise Revisited," *IEEE Transactions Information Theory*, Vol. IT-12, pp. 348-361.

39. Kramer, J. D. R., R. M. O'Donnell, and P. F. Gleason, May 1972, *The Detection Problem for Log-Normally Distributed Signal and Noise*, Technical Paper MTP-136, The MITRE Corporation, Bedford, MA.

40. Weiner, M. M., May 1982, "A Comparison of the Longley-Rice Semi-Empirical Model with Theoretical Models for Coherent Scatter," ESD-TR-82-133, Electronic Systems Division, AFSC, Hanscom AFB, MA 01731-5000. Also available as NTIS, AD A114644.

41. CCIR, 1975, Report 233-3, 13th Plenary Assembly, Geneva, Switzerland (1974), Vol. V, Inter-national Radio Consultative Committee, International Telecommunications Union, Geneva, Switzerland.

42. ITT, 1983, *Reference Data for Radio Engineers*, New York: Howard W. Sams Co., sixth edition, p. 28-16.

43. Gierhart, G. D., and M. E. Johnson, September 1973, *Computer Programs for Air/Ground Propagation and Interference Analysis, 0.1 to 20 GHz*, Institute for Telecommunication Sciences, Report FAA-RD-73-103. Also available as NTIS, AD 770335.